A critical review of the current design guidelines for footbridges

With emphasis on the design for jogging forces.

CIV5000Z Thesis

Tessa Townshend

STCTES001

Prepared for: Prof. P. Moyo

Thesis submitted in partial fulfilment of the requirements for the degree of

Masters of Science in Engineering

Department of Civil Engineering, University of Cape Town

December 2013

(Key Words: Vibration, Serviceability, Footbridges, Jogging Loads)

Abstract

New materials and the modern trend of designing slender, lightweight footbridges with longer spans have resulted in bridges with lower inherent structural damping and natural frequency in the range of pedestrian-induced dynamic loading from activities such as walking, running and jogging. This has lead to a number of recent footbridges suffering from excessive vertical or lateral vibrations necessitating retrofitting, usually at high additional costs ((Butz, 2008; Sun and Yuan, 2008)).

One of the most important aspects of the design of modern footbridges for dynamic forces is the development of a reliable model of both the structure and the human induced loads applied to it. However, the current design codes and design procedures are either outdated or very limited with regards to the type of footbridge and pedestrian loading they consider. There is a "lack of commonly accepted models for walking, running and jumping" loads (Occhiuzzi *et al.*, 2008), and the majority of the research that has been done and human-induced loading models that are available only look at the vertical component of the walking load. Research done by Keller *et al.* (1996) found that slow jogging can cause vertical forces up to 1.6 times greater than those caused by walking at the same speed or running at higher speeds. However, of all the codes of practice reviewed in this thesis only the Sétra Guide gives an indication of how to model the vertical component of a person running using either the Semi-Sinusoidal method or the Fourier method. Occhiuzzi *et al.* (2008) proposed a third method, the Analytical method, for modelling the vertical component of the jogging load. This thesis extends these three jogging load models to include the lateral and longitudinal component of the jogging force and to account for multiple people.

The vertical forces obtained using these jogging load models were compared with those measured by a person running at various speeds on an instrumented treadmill. The comparison showed that for a contact period of 75 % of the running period all three jogging load models give a reasonable approximation of the actual vertical jogging forces.

Further verification of the developed jogging load models was done by comparing the accelerations obtained when applying them to a finite element model (FEM) of the Rhodes Memorial Bridge to the actual accelerations measured on the same bridge when groups of 1 to 7 people

jogged across it. The results showed that the FEM accelerations compared favourable with the root-mean-square (RMS) of actual accelerations measured for up to 4 people. For more than 4 people, the actual accelerations started to drop whereas the FEM accelerations continued to increase. The drop in the actual accelerations is most likely due to the pedestrians becoming unsynchronised once a certain number of pedestrians are jogging across a bridge. Further research and testing is required to improve the accuracy of the models, especially in the lateral and longitudinal directions, and to better predict the synchronisation behaviour of the pedestrians.

Acknowledgements

I would like to thank the following people for their assistance and guidance with this thesis. I am extremely grateful for all of their help:

- Dr Pilate Moyo, my supervisor in the Department of Civil Engineering, for his support, guidance and enthusiasm for this thesis.
- University of Sheffield for supplying me with their vertical ground reaction measurements of people running on an instrumented treadmill.
- Stephen Roux and Antonieta Rodrigues from the City of Cape Town for providing me with the record drawings of the Rhodes Memorial Bridge.
- Philip Keil for providing me with the measured accelerations taken while groups of 1 to 7 people jogged across the Rhodes Memorial Bridge. This was done as part of his undergraduate thesis.
- Aurecon for giving me a bursary which enabled me to do this thesis.
- My brother, Stefan Stoeckigt, for his help with Matlab programming and the COMSOL Multiphysics software.
- Finally I would like to thank my husband, David Townshend, for his support, encouragement and understanding throughout the period spent working on this thesis; for his help with formatting and proof reading the thesis, for his patience with my endless questions about programming.

Plagiarism Declaration

- I know the meaning of plagiarism and declare that all the work in the document, save for that which is properly acknowledged, is my own
- I have used the Harvard Convention for citation and referencing. Each significant contribution to and quotation in this report from the work or works of other people have been attributed and have been cited and referenced.

Signature: _____ Date:_____

Name: _____

Contents

Abstract i

Acknowledgements iii

Plagiarism Declaration iv

Contents v

List of Tables ix

List of Figures xi

Glossary of Terms xiv

Glossary of Abbreviations xvi

List of Symbols xvii

1 Introduction 1-1

2 Literature Review 2-1

2.1 Types of Bridges 2-1

2.2 Background to the Design for Vibration Serviceability 2-2

2.2.1 Source, Path and Receiver Approach 2-3

2.3 Human Induced Forces 2-4

2.3.1 Walking Forces 2-5

2.3.2 Jogging or Running Forces 2-12
2.3.3 Vandal Forces 2-16
2.3.4 Summary and Comparison 2-18
2.4 Modelling of Human-Induced Forces 2-19
2.4.1 Time-Domain Force Models 2-19
2.4.2 Frequency-Domain Force Models 2-34
2.5 Review of Current Design Codes and Guidelines 2-37
2.5.1 TMH7 2-37
2.5.2 Sétra Guide 2-39
2.5.3 The Old British Standard 2-43
2.5.4 Eurocode together with the UK Annex 2-44
2.5.5 ISO Guide 2-48
2.5.6 Other Codes 2-51
2.5.7 Summary 2-52
2.6 Running Load Models Found in Literature 2-53
2.6.1 Deterministic Models 2-53
2.6.2 Sétra Guide 2-54
2.6.3 Analytical Load Model by Occhiuzzi and Spizzuocco et al. 2-56
2.6.4 Summary 2-59
2.7 Summary and Conclusions 2-60

3 Development of a Jogging Load Model 3-1
3.1 Measured Jogging Forces 3-2
3.1.1 How the Jogging Loads are Measured 3-2
3.1.2 Typical Jogging Loads Measured 3-4
3.1.3 Comparison with Jogging Load Models 3-4
3.2 Developing the Jogging Load Model 3-7
3.2.1 Final Jogging Load Models 3-8

4 Methodology for Testing **4-1**

4.1 Simulations 4-1

4.2 Verification 4-1

5 Simulations Results **5-1**

5.1 Step 1 - Modelling of the Structure 5-1

5.2 Step 2 - Applying the Loads 5-3

5.3 Step 3 - Running the Simulation 5-4

5.4 Step 4 - Obtaining the Results 5-4

6 Verification Results **6-1**

6.1 Step 1 - Obtaining Data 6-1

6.2 Step 2 - Developing the FEM 6-2

6.3 Step 3 - Updating of the FEM 6-4

6.4 Step 4 - Applying the Jogging Load Models 6-4

6.5 Step 5 - Simplified Methods of Determining Accelerations 6-8

6.6 Step 6 - Summary of the Testing 6-9

6.7 Step 7 - Comparison of Results 6-12

6.7.1 Comparison of Accelerations 6-12

6.7.2 Review of relevant Codes of Practice 6-15

7 Discussion and Conclusions **7-1**

7.1 Accuracy of the jogging load models 7-5

7.2 Accuracy of the FEM 7-5

7.3 Conclusions 7-6

8 Recommendations **8-1**

A Jogging Models **A-1**

A.1 Introduction A-1

A.2 Comparison with Contact Period at Half Running Period A-1

A.3 Comparison with Longer Contact Period A-3

B Simulations Results **B-1**

B.1 Introduction B-1

B.2 Acceleration Results B-1

C Verification Results **C-1**

C.1 Introduction C-1

C.2 Rhodes Memorial Bridge Data C-1

C.2.1 Drawings C-1

C.2.2 Site Measurements C-4

C.3 COMSOL Multiphysics C-4

C.3.1 Input Data - Jogging Load Models Applied C-4

C.3.2 Output Data C-8

C.4 Calculated Accelerations using Simple Methods C-15

C.4.1 TMH7 - Simplified Method C-15

C.4.2 Eurocode - Method for Timber Footbridges C-16

C.4.3 Rainier et al's Method C-17

C.4.4 Allen and Murray's Method C-18

C.4.5 Grundmann et al's Method C-18

C.4.6 Young's Method C-19

C.4.7 Pimentel and Frenandes' Method C-19

D Measured Accelerations **D-1**

D.1 Introduction D-1

D.2 Vertical Time-History Responses D-1

D.3 Lateral Time-History Responses D-2

List of Tables

2.1 Types of Bridges. 2-2

2.2 Comparison of the Frequency Ranges for Human Induced Forces. 2-18

2.3 Dynamic load factors found in literature for walking and running. 2-22

2.4 Average step frequencies. 2-24

2.5 Average Walking and Jogging Parameters. (Barreira *et al.*, 2010) 2-26

2.6 Eriksson's design force model. 2-36

2.7 Estimated Frequency Range for Pedestrians from Sétra. 2-39

2.8 Classification of Footbridge Classes in Sétra. 2-40

2.9 Classification of Comfort Levels in Sétra. 2-40

2.10 Acceleration Ranged for the Different Comfort Levels in Sétra. 2-41

2.11 Frequency Range Classifications. 2-41

2.12 Load Cases Requiring Dynamic Load Calculations. 2-42

2.13 Directional Loads for Load Cases 1, 2 and 3. 2-42

2.14 Determination of the Effective Number of Pedestrians. 2-43

2.15 Maximum Allowable Acceleration for Pedestrian Bridges. 2-45

2.16 Frequency Ranges from Eurocode 1. 2-46

2.17 Fourier Coefficients According to ISO 101317 (ISO, 2004; Butz, 2008) 2-50

2.18 Comparison between the various codes of practice. 2-52

2.19 Coefficients of the Fourier Decomposition. 2-53

2.20 Walking, Running and Jumping Frequencies. 2-54

2.21 Typical Frequency Ranges for Walking and Running. 2-61

2.22 Acceleration response limits stated in various codes of practice. 2-62

2.23 Methods for Determining the Maximum Acceleration of a Footbridge. 2-62

3.1 Jogging data sets from University of Sheffield 3-4

3.2 Comparison of Vertical Jogging Forces 3-6

5.1 Maximum Accelerations of the Simple Beam Structure. 5-5

6.1 Maximum accelerations determined in COMSOL Multiphysics 6-8

6.2 Calculated accelerations for Simple Beam Structure 6-9

6.3 Accelerations Recording during Testing. (Keil, 2012) 6-10

6.4 Comparison of Vertical Accelerations 6-12

6.5 Comparison of Lateral and Longitudinal Accelerations 6-12

6.6 Accelerations Limits from the Codes of Practice for the Rhodes Memorial Bridge when subjected to Jogging Loads 6-17

List of Figures

1.1 London Millennium Bridge in UK. 1-2

1.2 EXPO 98 North Footbridge. 1-2

1.3 Passerelle Léopold-Sédar-Senghor Bridge in France. 1-3

2.1 Vertical and Horizontal Forcing Frequencies. 2-5

2.2 Path of Centre of Gravity for Human Walking. 2-6

2.3 Vertical Force from one person taking one step. 2-7

2.4 Periodic Walking Time History in the Vertical Direction. 2-7

2.5 Normal Distribution of Pacing Frequencies. 2-8

2.6 Periodic Walking Time History in the Horizontal Directions. 2-9

2.7 Flow chart of accidental pedestrian–structure synchronisation. 2-10

2.8 Typical running stride as a series of poses. 2-12

2.9 Vertical force patterns for different types of human activities. 2-13

2.10 Experimental results showing vertical ground force patterns. 2-13

2.11 Typical pattern of running and walking forces. 2-14

2.12 Vertical ground reactions for a running with shoes and barefoot. 2-15

2.13 The force function generating by jumping. 2-16

2.14 Vertical Forces due to jumping (a) and bouncing (b) at 2Hz. 2-17

2.15 Force time histories generating by jumping. 2-18

2.16 Dynamic Load Factors for the first four harmonics. 2-21

2.17 Dynamic Load Factors of walking force determined by Kerr. 2-23

2.18 Normal distribution of walking speed at around 1.8 Hz 2-25

2.19 Relationship between the step length and walking velocity. 2-26
2.20 Moving force model and forcing function for a pedestrian load. 2-27
2.21 Pedestrian modal force model. 2-29
2.22 ASD of a walking force produced by Eriksson. 2-34
2.23 Vertical coefficient of the fundamental natural frequency. 2-47
2.24 Horizontal coefficient of the fundamental natural frequency. 2-47
2.25 Vertical vibration base curve for acceleration. 2-49
2.26 Horizontal vibration base curve for acceleration. 2-49
2.27 Impact factor dependent on the relative period of contact. 2-55
2.28 Amplitude of the various harmonics. 2-55
2.29 Vertical Component of Running Loads. 2-56
2.30 Interaction forces between a runner and a footbridge. 2-57
2.31 Comparison of Running Load Models. 2-60

3.1 ADAL3D-F instrumented treadmill installed in the LSL. (Racic *et al.*, 2007) 3-2
3.2 Cross-section through an ADAL3D-F instrumented treadmill. (Racic *et al.*, 2007) 3-3
3.3 GRF measured using the ADAL3D-F (Racic *et al.*, 2007) 3-3
3.4 Comparison of Vertical Jogging Loads 3-5
3.5 Comparison of Vertical Jogging Forces with Longer Contact Period 3-5
3.6 Graphical Comparison of Vertical Jogging Forces 3-6
3.7 Final Vertical Jogging Load Models for 1 to 3 People 3-9
3.8 Final Lateral Jogging Load Model for 1 to 3 People 3-9
3.9 Final Longitudinal Jogging Load Model for 1 to 3 People 3-10

4.1 The location of the Rhodes Memorial Footbridge. (Google Maps, 2013) 4-2

5.1 Eigenfrequency plot for the Beam Structure in COMSOL Multiphysics. 5-1

5.2 Graphical Representation of Rayleigh Damping. (Faber, 2009) 5-2
5.3 Graphical representation of how the Jogging Loads were applied. 5-3
5.4 Locations of where the Loads will be Applied. 5-3
5.5 Vertical Load Plots for One Person 5-4
5.6 Semi-Sinusoidal Vertical Acceleration Plot at the Centre of the Beam 5-5

6.1 Rhodes Memorial Bridge 6-1
6.2 Modelled Cross Section through Footbridge 6-2
6.3 Actual support connection of the Rhodes Memorial Footbridge 6-3
6.4 Model of the Rhodes Memorial Bridge in COMSOL Multiphysics 6-3
6.5 Fundamental Natural Frequency of Modelled Bridge 6-4
6.6 Position of line upon which Jogging Loads will be applied. 6-5
6.7 Graphical representation of how the Jogging Loads were applied. 6-6
6.8 Semi-Sinusoidal Model Accelerations due to One Person - Normal Mesh 6-6
6.9 Final Mesh for the FEM of the Rhodes Memorial Bridge 6-7
6.10 Semi-Sinusoidal Model Accelerations due to One Person - Refined Mesh 6-7
6.11 Vertical Time-History Response due to 4 Joggers 6-11
6.12 Lateral Time-History Response due to 4 Joggers 6-11
6.13 Vertical Acceleration versus Number of People 6-13
6.14 Lateral Acceleration versus Number of People 6-14
6.15 Longitudinal Acceleration versus Number of People 6-14

7.1 Final Vertical Jogging Load Models for 1 to 3 People 7-3
7.2 Final Lateral Jogging Load Model for 1 to 3 People 7-3
7.3 Final Longitudinal Jogging Load Model for 1 to 3 People 7-4

Glossary of Terms

Accelerometer An electromechanical device that measures the acceleration of a structure.

Auto-Spectral Density Describes the average frequency content of a random process.

Damping The property of a structure or device that gradually reduces the amplitude of oscillations when is vibrates.

Dynamic Loading Loading that varies in both time and position.

Circular Frequency Normally denoted by ω, circular frequency is a scalar measure of the rate of rotation where one revolution is equal to 2π radians. It is related to ordinary frequency by: $\omega = 2\pi f$.

Gaussian probability distribution This is also referred to as a normal probability distribution.

Heel Strike The period when the heel of a person hits the ground when taking a step.

Frequency This is the number of times a recurring event is repeated per unit of time.

Lock-in Effect The interaction between pedestrians and a vibrating bridge deck, in which the pedestrians adapt and synchronise their step frequency with that of the vibrating bridge deck.

Modal Mass The mass of the structure participating in a particular mode of vibration.

Mode Shape A pattern of motion in which the structure moves when excited at a particular frequency.

Natural Frequency The frequency at which a system naturally vibrates once it has been set into motion.

Resonance The tendency of a structure to vibrate with larger amplitudes at some frequencies (natural frequencies) than others.

Static Loading Loading which does not vary in time or position.

Step Frequency The frequency at which a person moves from one leg to another when walking.

Traffic Level The number of people using a bridge at any one time.

Toe-off The period when the foot leaves the ground when a person takes a step.

Glossary of Abbreviations

ASD Auto-Spectral Density

DLF Dynamic Load Factor

DMF Dynamic Magnification Factor

DOF Degree of Freedom

FEM Finite Element Model

GRF Ground Reaction Force

IFMT Instrumented Force Measuring Treadmill

LSL Light Structures Laboratory

MDOF Multiple Degree of Freedom

PSD Power Spectral Density

RMS Root-Mean-Square

SDOF Single Degree of Freedom

SLS Serviceable Limit State

TMD Tuned Mass Damper

UCT University of Cape Town

ULS Ultimate Limit State

List of Symbols

$\alpha_{i,lat}$ Lateral dynamic load factors

$\alpha_{i,long}$ Longitudinal dynamic load factors

$\alpha_{i,vert}$ Vertical dynamic load factors

$F_{lat}(t)$ Lateral component of the ground force reaction

$F_{long}(t)$ Longitudinal component of the ground force reaction

$F_{vert}(t)$ Vertical component of the ground force reaction

f_m The running frequency

G_0 Weight of a runner in Newtons

m Factor to account for the synchronisation of a number of people crossing a bridge

n Number of people crossing a bridge

N Number of Fourier harmonics

k_p Impact factor

t Time

T_m The running step period

t_p Contact period

1. Introduction

Bridges do more than provide a safe and easy way of crossing a river or road, they form important landmarks in cities, with their own histories and identities (Feichtinger, 2008). They represent the political situation and the technical capability of the time in which they were designed and constructed. They are often named after important people in the history of a city or country, such as the Nelson Mandela Bridge in Johannesburg, South Africa. For this reason it is important to ensure that bridges fulfil their intended goals while still providing comfort to the end user.

Nowadays, a footbridge is often designed to be an "eye-catcher and transparent landmark" (Butz, 2008). This, together with the new materials available have lead to the design of footbridges with longer spans that are both slender and lightweight ((Butz, 2008; Sun and Yuan, 2008)). As a result, these bridges often have lower inherent structural damping and natural frequencies in the range of pedestrian-induced dynamic loading ((Butz, 2008; Sun and Yuan, 2008)). This has lead to a number of recently constructed footbridges to suffer from excessive vertical or lateral vibrations necessitating retrofitting, usually at high additional costs ((Butz, 2008; Sun and Yuan, 2008)). Some of the most famous footbridges with vibration problems in recent years include the London Millennium Bridge, the two EXPO 98 footbridges and the Passerelle Solférino.

The London Millennium Bridge shown in Figure 1.1 is a steel suspension bridge across the river Thames, linking St. Paul's Cathedral and the Tate Modern art gallery (Newland, 2002). The bridge is over 300 m long and consists of three spans. The longest span is the central one which is 144 m long (Newland, 2002). The bridge experienced severe pedestrian-induced lateral vibrations on the day it was opened (10 June 2000) and an immediate decision was made to limit the number of people on the bridge at any one time. However, this did not stop the lateral vibrations and the bridge was closed on the 12 June 2000 due to the risk to public safety (Newland, 2002). The original cost of the bridge was £18.2 million and it cost £5 million to retrofit the bridge with dampers before it was reopened $1\frac{1}{2}$ years later on the 22 February 2002 (Newland, 2002; A view on cities, 2014).

Figure 1.1.: *London Millennium Bridge in UK.*
(Project for Public Spaces)

The two EXPO 98 footbridges, shown in Figure 1.2, are three-dimensional steel truss bridges that connect the Orient Railway Station to the Vasco da Gama Shopping Centre at "Park of the Nations", the site of the 1998 World Exposition, in Lisbon, Portugal. These bridges suffer from both vertical and horizontal vibrations. The accelerations produced by the horizontal vibrations in either bridge can exceed the acceptable limit with only a few pedestrians walking across them. Due to safety concerns both of these bridges are closed to pedestrians (Adao da Fonseca, 2008).

Figure 1.2.: *EXPO 98 North Footbridge.*
(Adao da Fonseca, 2008)

The Passerelle Léopold-Sédar-Senghor in Paris, previously known as the Passerello Solférino, shown in Figure 1.3 is a double arch steel pedestrian bridge which crosses the river Seine with a span of 106 m and links the Musée d'Orsay and the Jardin des Tuileries (Tuileries Gardens). This bridge experienced pedestrian-induced lateral vibrations when it was opened in 1999.(Sun and Yuan, 2008; Sétra, 2006)

Figure 1.3.: *Passerelle Léopold-Sédar-Senghor Bridge in France. (Sun and Yuan, 2008)*

The vibration of footbridges is a serviceability problem that affects the comfort of the people using the bridge but rarely results in the collapse of the bridge. This means that vibration serviceability needs to be considered when designing footbridges. One of the most important aspects of the design of modern footbridges for dynamic forces is the development of a reliable model of both the structure and the human induced loads applied to it (Occhiuzzi *et al.*, 2008). The failures of the aforementioned footbridges have lead to an understanding that the current design codes are not adequate for the design of long slender pedestrian bridges and that there is a "lack of commonly accepted models for walking, running and jumping" loads (Occhiuzzi *et al.*, 2008). "Recent research into vibration serviceability of slender structures under human-induced dynamic loading suggests that improvements to the existing footbridge design guidelines are possible in the area of modelling human-induced excitation in the vertical direction." (Pimentel *et al.*, 2001)

In South Africa, TMH7 (1981) is probably the most commonly used code of practice for the design of footbridges and it is necessary to review TMH7 with reference to the codes of practice which are used elsewhere.

Reviewing the codes of practice only deals with the lesser of the two problems in the current design of footbridges. The other problem is that of modelling human induced forces. There is currently much research being conducted on the modelling of walking forces, but limited work has been done on the modelling of jogging forces.

This thesis will look at the various models available for jogging forces and will test how accurately they predict the actual behaviour of footbridges under jogging loads.

The main aim of this thesis is to develop a simplified method for the design of footbridges with respect to jogging forces. This will be done by meeting the following objectives:

1. A critical review of the applicable design codes currently available for footbridges, in respect to TMH7.
2. To investigate the current load models available for human induced forces, in particular those forces produced when jogging.
3. To determine the response of a footbridge to jogging forces and compare it to a finite element model of the same footbridge when subjected to the models available for jogging forces.

There are a number of limitations and assumptions which have been made throughout this thesis. These are:

- Acceleration limits given in the codes of practice were adopted for vibration limits of footbridges subject to jogging loads. No work was done to check whether these limits should be adjusted.
- Changes to the dynamic properties of a footbridge due to human-structure synchronisation is not taken into account.
- Since footbridges are generally classified as low-frequency structures the load models discussed and developed in this thesis are for low frequency structures.

This thesis has been written in eight chapters. This introductory chapter gives a brief background to the design of footbridges and the problems involved in modelling the human induced loads, and gives the objectives and limitations of the thesis. The body of the thesis consists of five chapters:

Chapter 2 is a literature review which gives a brief background to the various types of bridges and vibration serviceability. Thereafter, human induced forces and methods of modelling them are described. A comparison is made between several design codes with reference to the methods used for the design of footbridges.

Chapter 3 describes how the jogging load models tested in this thesis were developed.

Chapter 4 gives the methodology for testing these jogging load models.

Chapter 5 gives the results from the simulations done using the jogging load models.

Chapter 6 gives the results from the verifications done by comparing the accelerations measured on the Rhodes Memorial Bridge to those predicted by simplified methods given in codes of practice and from a finite element model of the bridge with the jogging load models applied to it.

Chapters 7 and 8 discuss the findings of the thesis and state the conclusions made from the research and tests conducted, and contains recommendations for future research in this field.

A complete list of references is given at the end of the thesis. This is followed by the appendices.

Appendix A gives the Matlab output for the jogging load models compared to the forces of a single person jogging on an instrumented treadmill.

Appendix B gives the COMSOL Multiphysics results from the simulations conducted using the jogging load models.

Appendix C gives the results from the verifications done on the Rhodes Memorial Bridge.

Appendix D gives the measured accelerations from the Rhodes Memorial Bridge that was obtained from Philip Keil's (2012) undergraduate thesis.

2. Literature Review

The purpose of this literature review is to study the current codes of practice for the design of pedestrian bridges in light of recent failures such as the London Millennium Bridge and to develop an understanding of how human induced forces are currently applied in the design of pedestrian bridges. The different types of human induced loading that could be applied to pedestrian bridges are investigated along with the current methods available for modelling them.

Before introducing the design procedures for footbridges a brief explanation is given of the different types of footbridges and the structural components of them. This is followed by some background to the study of vibration serviceability of footbridges. Thereafter the different types of human induced forces are described, followed by some procedures on how their forces can be modelled. Lastly, a number of the running load models that can be found in literature are outlined.

2.1. Types of Bridges

The classification of the different types of bridges are based on the basic structural system which enables the bridge to span between two points (Kubota and Kishimoto, 2008). The structural system may play an important role in the dynamic behaviour of a bridge and the way a bridge is modelled. For this reason it is important to understand the different structural systems and how they apply to the various types of bridges. There are three distinct structural systems which are used in all types of bridges (Kubota and Kishimoto, 2008):

- The Beam System
- The Arch System
- The Cable System

The beam system can be further subdivided into a full web system and a truss system (Kubota and Kishimoto, 2008). Table 2.1 gives an overview of the structural systems, listing the fundamental forces involved, the most common types of bridges using each one and the typical

spans. Bridges using the cable system are most often light and slender due to their long spans and are therefore most susceptible to vibrations from both wind and pedestrian loading (Keil, 2008).

Table 2.1.: *Types of Bridges.*
(Kubota and Kishimoto, 2008; Matsuo Bridge Co. Ltd, 1999)

Structural System	Fundamental Force	Types of Bridges	Typical Spans
Full Web System	Bending Moment	Girder / Beam Bridge	Between 10m and 200m
Truss System	Shearing Force	Truss Bridge	Between 40m and 500m
Arch System	Compression Force	Arch Bridge	Between 40m and 150m
Cable System	Tension Force	Cable Stayed Bridge	Between 110m and 480m
		Suspension / Stress Ribbon Bridge	Between 70m and 1000m

2.2. Background to the Design for Vibration Serviceability

In 1821 Stevenson wrote what is possibly one of the oldest reports of vibrations in footbridges. He reported that soldiers marching over a bridge in regiment could cause severe vibrations in the bridge (Stevenson, 1821). Ten years later pedestrian induced vibrations was discovered as a possible cause of failure in footbridges when a bridge in Broughton collapsed while soldiers marched across it (Butz, 2008). At this time investigations into human induced forces as a form of dynamic loading for bridges were already being carried out. These investigations showed that the cause of vibrations in footbridges were most relevant when the step frequencies of people crossing the bridge coincided with the natural frequencies of the bridge (Butz, 2008). This lead to the recommendation that bridges be designed in such a way that their natural frequency lies outside the range of common step frequencies for pedestrians (Butz, 2008).

In the 1970s researchers started investigating the effects of human induced forces. In particular they looked at “the response of bridges due to single pedestrians, groups and crowds and human tolerance to vibrations” (Butz, 2008). These investigations showed that “the human-induced forces scatter and that the correlation within a crowd is complex” (Butz, 2008) and that this correlation has an important affect on the response of the bridge. Equations 2.0a, 2.0b and 2.0c give the resulting load model which was developed based on the Fourier series (Butz, 2008).

$$F_{vert}(t) = G\sum_{i=0} \alpha_{i,vert} \cdot sin(2\pi \cdot i \cdot f_s \cdot t - \varphi_{i,vert}) \tag{2.0a}$$

$$F_{lat}(t) = G\sum_{i=1} \alpha_{i,lat} \cdot sin(\pi \cdot i \cdot f_s \cdot t - \varphi_{i,lat}) \tag{2.0b}$$

$$F_{long}(t) = G\sum_{i=1} \alpha_{i,long} \cdot sin(2\pi \cdot i \cdot f_s \cdot t - \varphi_{i,long}) \tag{2.0c}$$

F_{vert}, F_{lat} and F_{long} are the pedestrian induced forces in the vertical, lateral and longitudinal directions respectively, G is the body weight of the pedestrian, $\alpha_{i,vert}$, $\alpha_{i,lat}$ and $\alpha_{i,long}$ are the Fourier coefficients of the forces in the vertical, lateral and longitudinal directions, $\varphi_{i,vert}$, $\varphi_{i,lat}$ and $\varphi_{i,long}$ are the phase angles of the Fourier components, i is the i^{th} component of the Fourier series and f_s is the step frequency.

This model was adjusted for the effects of crowds by reducing the actual number of pedestrians by their square root as shown in Equation 2.1 (Butz, 2008).

$$n_{eff} = \sqrt{n} \tag{2.1}$$

where n is the actual number of pedestrians on the bridge and n_{eff} is the effective number of pedestrians on the bridge. A design could then be done using the harmonic force models for a single pedestrian of nominal weight and applying the Fourier coefficients in resonance with the natural frequencies (Butz, 2008). Since then the load models have been improved by taking into account the randomness of human induced loading, the interaction of the loading with the vibration of the bridge and the effects of crowd loading (Butz, 2008). These models are looked at in more detail in a Section 2.4.

2.2.1. Source, Path and Receiver Approach

Many design codes and studies done on the vibration serviceability of footbridges make use of the source, path and receiver approach. This approach breaks the problem into three basic elements; the source, the path and the receiver. Aspects of these basic elements are discussed in this section. (Pavic and Brownjohn, 2008)

The source component is the cause of vibrations in the structure. When considering the vibration of footbridges, the source is often humans, either individuals, groups or crowds crossing

the footbridge. The source also describes any coordination which may occur between the individual people crossing the bridge. This aspect of the design approach is looked at in more detail in Sections 2.3 and 2.4. (Pavic and Brownjohn, 2008)

In the case of footbridges, the path is the bridge itself since it transmits the vibrations from the source to the receiver. The path is characterised by the mass, stiffness and damping of the bridge, the possibility of any human-structure interaction and the presence of stationary people. The properties of the bridge, and therefore the path, result in the vibrations being modified from the source to the receiver. Nowadays this is done by finite element analysis. (Živanović *et al.*, 2005; Pavic and Brownjohn, 2008; ISO, 2004)

The main receivers of vibrations on footbridges are the people walking across the bridge. It should be noted that stationary people on the bridge will also feel the vibrations, although this is usually excluded when designing bridges. The reaction of people to vibrations is a very complex issue since people react differently to the same vibration. Furthermore, a person is likely to react differently when exposed to the same vibration on different days. However, since humans are highly perceptive to vibrations it is important that this is considered when designing bridges for vibration serviceability. Most of the studies conducted have used acceleration as the parameter to describe the problem because it is easy to measure. It is now generally accepted that moving pedestrians on footbridges have a higher tolerance to vibrations than people in buildings. Unfortunately, actual values for the vibrations which are acceptable on footbridges are scarce and further work is required in this area, especially with regards to horizontal vibrations. This thesis is concerned with jogging forces which fall under the first aspect of this approach and so the values given in the codes for the limits for acceleration will be used. (Živanović *et al.*, 2005)

2.3. Human Induced Forces

This section looks at the various human induced forces before proceeding, in the next section, to describe the load models available for these human induced forces. There are four main types of human induced forces which can result in vibrations when applied to a footbridge. These are walking, jogging, bouncing and jumping forces. According to Pavic and Brownjohn (2008) these forces are influenced by a number of factors, such as:

- Inter-Subject Factors such as the age, sex and weight of the pedestrian.
- Intra-Subject Factors such as the pacing rate and physical fitness level of the pedestrian.
- External Factors which include synchronisation cues, the slope of the bridge, the type

of surface of the bridge, the type of footwear the pedestrian is wearing, the foot landing position and the mood of the pedestrian.

2.3.1. Walking Forces

When a person walks across a bridge, forces are applied to the surface of the bridge deck in three directions, vertical, lateral and longitudinal, due to the acceleration and deceleration of the body mass of the person (Živanović *et al.*, 2005). These forces are dynamic and vary with time. They are also influenced by a number of parameters, including pacing frequency, walking speed and step length. (Hauksson, 2005).

It is generally agreed that human walking forces have an average frequency of $2\,Hz$ in the vertical and longitudinal directions and $1\,Hz$ in the lateral direction (Sun and Yuan, 2008; Sétra, 2006). However, the range of the frequencies can be as low as $1.4\,Hz$ in the vertical direction or $0.7\,Hz$ in the lateral direction. Figure 2.1 shows the range of walking frequencies in both the vertical and lateral direction.

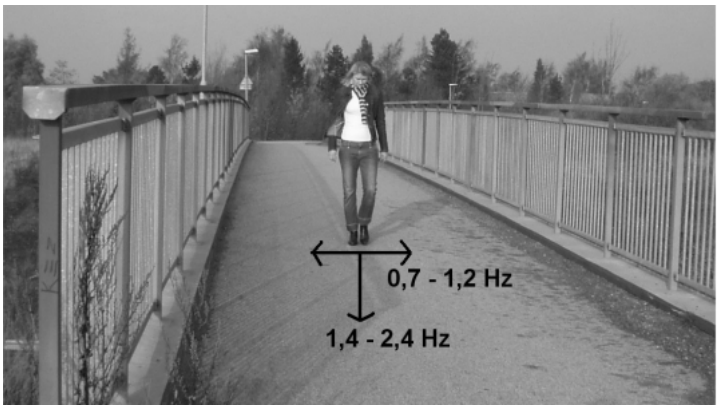

Figure 2.1.: *Vertical and Horizontal Forcing Frequencies. (Hauksson, 2005)*

The frequency in the lateral direction is approximately half the frequency in the vertical direction. This is because the frequency in the vertical direction is calculated by the length of time it takes for the weight of a person walking to be transferred from one foot to the next as shown in Figure 2.2(a) whereas the frequency in the lateral direction is calculated by the length of time it takes for the weight of a person walking to be transferred from one foot to the next and back to the first foot as shown in Figure 2.2(b).

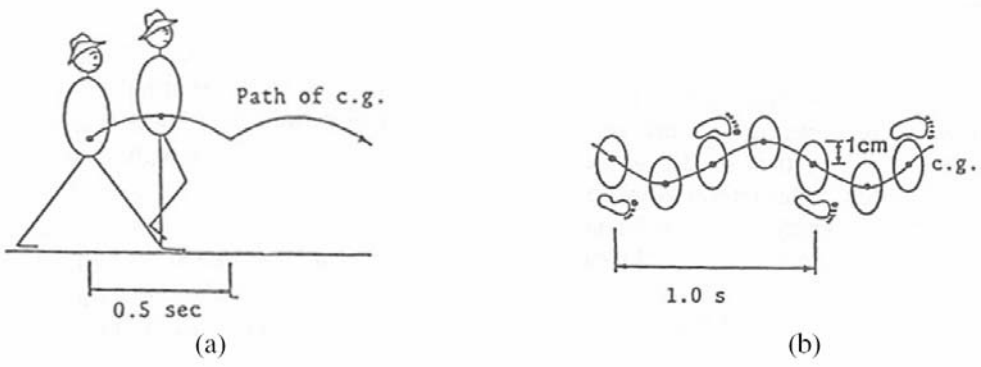

Figure 2.2.: *Path of Centre of Gravity for Human Walking. (Sun and Yuan, 2008)*

Numerous experiments have shown that if the speed at which a person walks is increased then their step length and the magnitude of the peak force also increases. Furthermore, an increase in speed also leads to an increase in the variability of the vertical and lateral forces. (Živanović *et al.*, 2005)

2.3.1.1. Vertical Loads

The effects of vertical forces induced by a single pedestrian have been known for some time and were included in some of the first codes on vibration serviceability of footbridges. These forces have been studied the most, and because they have a higher magnitude than those in other directions, they are often regarded as the most important (Živanović *et al.*, 2005). A typical vertical force for a single step measured on a force plate is shown in Figure 2.3(a) where the first peak represents the heel strike phase and the second peak represents the toe-off phase. (Racic *et al.*, 2009)

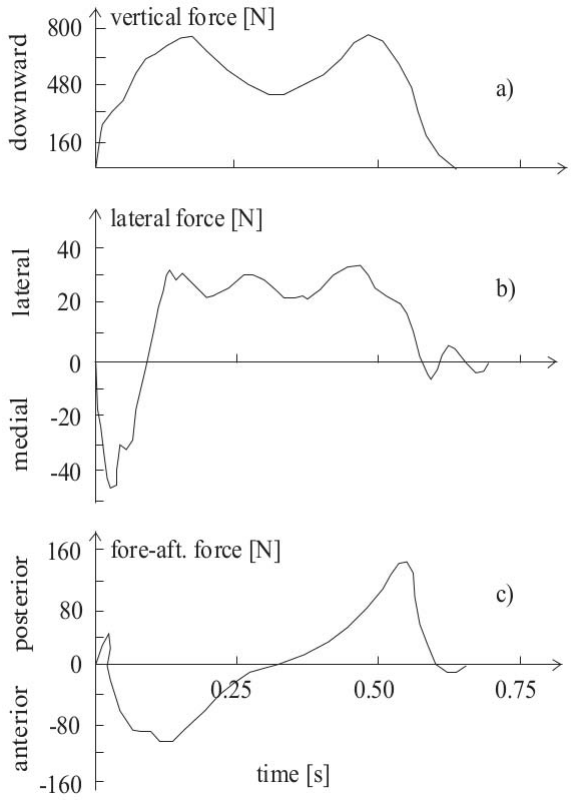

Figure 2.3.: *Vertical, Lateral and Longitudinal Forces from one person taking one step. (Živanović* et al.*, 2005; Andriacchi* et al.*, 1977)*

More complex experiments have been done in order to obtain measurements for continuous walking comprising a number of steps. Unfortunately, in most of these experiments only the vertical forces were recorded. Figure 2.4 shows an example of the time histories that were measured in one of these experiments. (Živanović *et al.*, 2005)

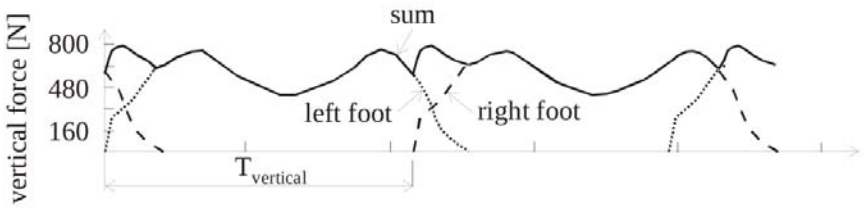

Figure 2.4.: *Periodic Walking Time History in the Vertical Direction. (Živanović* et al.*, 2005)*

Matsumoto *et al.* (1972) carried out an experiment in which the normal walking frequencies of 505 people were measured. The results of this experiment are illustrated in Figure 2.5 and

show that the measured frequencies can be represented by a normal distribution with a mean pacing rate of $2.0\,Hz$ and a standard deviation of $0.173\,Hz$. Further experiments conducted by other researchers have confirmed these results (Živanović *et al.*, 2005).

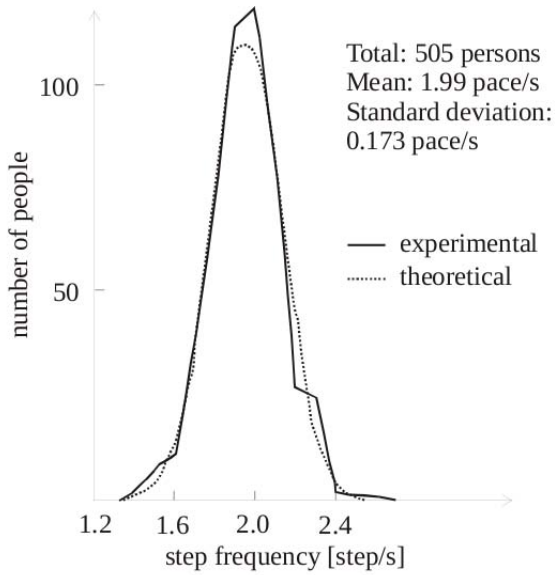

Figure 2.5.: *Normal Distribution of Pacing Frequencies.*
(Matsumoto et al.*, 1972)*

It is interesting to note that studies of people walking up and down a slope have shown that the slope affects the amplitude of the force parameters in Figure 2.3. When walking on a slope the magnitude of the first peak increases marginally while the magnitude of the second peak increases significantly. Furthermore, the horizontal forces also increase significantly when walking on a slope in comparison to walking on a level surface. (Racic *et al.*, 2009)

2.3.1.2. Horizontal Loads

Horizontal forces occur in two directions: laterally and longitudinally. Forces in the lateral direction are produced due to the lateral oscillation of the centre of gravity of the person as the weight is transferred from one foot to the other while walking as shown in Figure 2.2. The displacement amplitudes of these lateral oscillations are generally in the region of $1 - 2\,cm$ (Hauksson, 2005). Forces in the longitudinal direction are caused by the acceleration and deceleration of the mass of the person moving along the bridge (Živanović *et al.*, 2005). Movement in the longitudinal direction is generally not a problem in footbridges, but it is looked at in this section for completeness (Sétra, 2006).

Andriacchi *et al.* (1977) carried out an experiment to investigate the forces in all three directions when a person takes a step on a force plate. The resulting typical shapes of the lateral and longitudinal forces are shown in Figure 2.3(b) and Figure 2.3(c) respectively. (Živanović *et al.*, 2005)

Based on Andriacchi *et al*.'s (1977) measurements and assuming perfect periodicity and the fact that the frequency of the walking force in the lateral direction is half of that in the vertical and longitudinal directions, the general shapes for continuous walking forces in all three directions can be generated (Živanović *et al.*, 2005). These general shapes are shown in Figure 2.6.

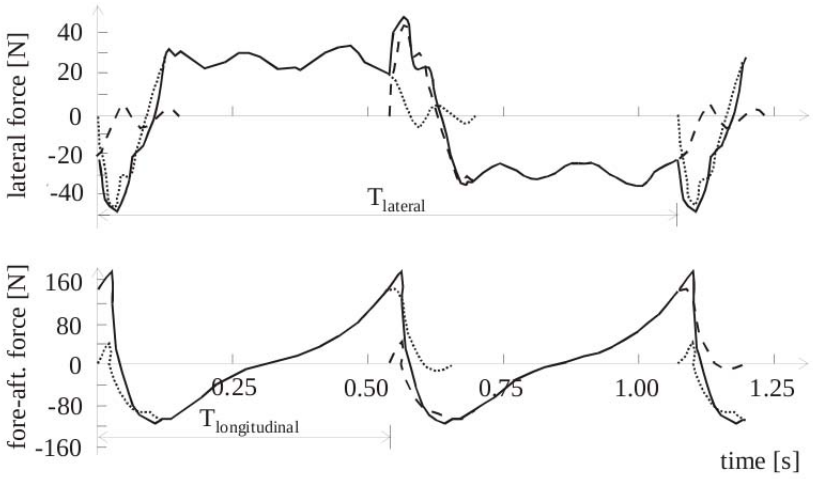

Figure 2.6.: *Periodic Walking Time History in the Horizontal Directions. (Živanović* et al.*, 2005)*

The measurements of walking forces in Figure 2.6 were obtained by experiments conducted on rigid surfaces. However, studies done by Pizzimenti and Ricciardelli (2005), and Ronnquist (2005) have shown that the magnitude of the horizontal walking force increases when the structure is vibrating at frequencies similar to the pacing rate of the person walking across it (Racic *et al.*, 2009). It is clear from the available research on horizontal walking forces that horizontal loading parameters are not as well quantified or understood as vertical loading parameters (Hauksson, 2005).

2.3.1.3. Crowd Loading and Synchronisation

Until recently, the majority of research has focused on the forces produced by a single pedestrian (Živanović *et al.*, 2005). However, since the much publicised serviceability failure of the London Millennium Bridge, more focus has been placed on understanding the effects of

groups of people and large crowds and the synchronisation of these crowds with the motion of the bridge. This synchronisation is often referred to as human-structure synchronisation and it occurs when pedestrians crossing a vibrating bridge change their step to coincide with the vibrations of the bridge (Hauksson, 2005).

It is generally understood that human-structure synchronisation can occur in two ways as shown in Figure 2.7, where δ_c is the critical crowd density at which there is an influence in the motion of the pedestrians in a group, x_c is the critical vibration amplitude at which the pedestrians become aware of the vibration of the structure and M_c is the critical mass of the pedestrians at which the inertial force will induce structural vibration with an amplitude equal to x_c (Racic *et al.*, 2009).

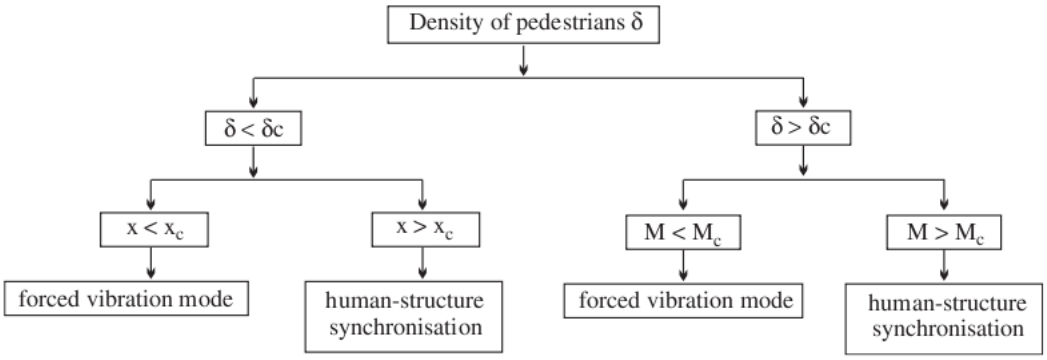

Figure 2.7.: *Flow chart of accidental pedestrian–structure synchronisation. Racic* et al. *(2009)*

When the density of the pedestrians, δ, is less than δ_c human-structure synchronisation will only occur if the amplitude of the structural vibrations is greater than the critical value, x_c. When the vibration amplitude is above x_c, pedestrians will instinctively change their step to coincide with the motion of the structure.

When the density of the pedestrians, δ, is greater than δ_c there is a dense crowd on the structure and therefore, it is more likely that the pedestrians in the crowd will walk in a synchronised manner because of the limited space. When this occurs the resultant force is equal to the sum of the forces exerted by each of the synchronised pedestrians. When the total mass of the synchronised pedestrians, M, is greater that M_c, the structural vibrations become unstable and the lock-in effect will occur. (Racic *et al.*, 2009)

There are two main factors which influence human-structure synchronisation. The first factor is related to the fact that the presence of pedestrians on a footbridge changes its dynamic properties such as damping and natural frequency. The second factor is related to how much

synchronisation is taking place between individual pedestrians as well as between the pedestrians and the structure. A large amount of research is currently being done in order to improve our understanding of both of these factors. (Živanović *et al.*, 2005)

The exact effect of moving people or crowds on the dynamic properties of a footbridge is not known. The majority of the research that has been done focuses on the effects of the vibrations in the vertical direction. For instance the pedestrian tests done on the London Millennium Bridge showed that the vertical damping of the bridge increased when a crowd walked across it. However, there is little information available on the effects of the dynamic properties in the horizontal direction. There is no accurate measure of the changes to the dynamic properties of the bridge and this is one aspect of human-structure synchronisation which needs to be investigated further. This does not form part of this thesis and additional studies need to be done to determine the effect of this. (Živanović *et al.*, 2005)

Human-structure synchronisation between individual pedestrians and between pedestrians and the structure can occur in both the vertical and the lateral directions (Živanović *et al.*, 2005). Synchronisation in the vertical direction is more difficult to achieve than synchronisation in the lateral direction. The reason for that is people can tolerate much higher vibrations in the vertical direction than in the horizontal direction before they will change their natural pace rate (Hauksson, 2005).

The lateral synchronisation of crowds on the other hand is now widely recognised as the main reason for severe lateral vibrations in footbridges (Sun and Yuan, 2008). People are sensitive to low frequency lateral vibrations in structures that they walk on and are more likely to adjust their steps to coincide with these vibrations (Hauksson, 2005). This is because when people walk their weight is constantly being shifted from one foot to another. Therefore, in order to maintain their balance on a surface which is moving in a lateral direction people will adjust their step to coincide with the frequency at which the surface is moving, and also will spread their legs further apart in order to improve their balance. This results in the movement of their upper body being more pronounced and thus increases the human-induced force on the structure. The synchronisation between the people and the bridge together with the increased force leads to an increase in the vibration of the bridge. This leads to more pedestrians changing their step to coincide with that of the bridge and so further increasing the lateral vibration. Luckily, when the vibrations become to high and uncomfortable it is human nature to stop walking which means that the vibrations slow and eventually stop. (Hauksson, 2005; Živanović *et al.*, 2005)

2.3.2. Jogging or Running Forces

As with walking, when a person jogs or runs across a bridge forces are induced onto the surface of the bridge deck in three directions, vertical, lateral and longitudinal. It is important to note that in literature running is characterised by a period of time when both feet are off the ground at the same time as shown in Figure 2.8.

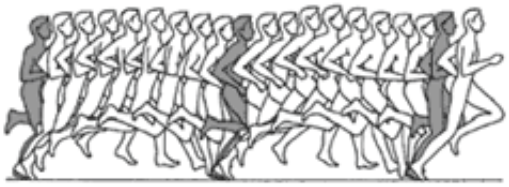

Figure 2.8.: *Typical running stride as a series of poses. (Romanov, 2006)*

Although jogging and running produces forces in three directions the available literature shows that researchers have mainly looked at the forces in the vertical direction. Comprehensive studies such as the one carried out by Matsumoto *et al.* (1972) to determine normal walking frequencies have not been done for jogging or running frequencies. However, several suggestions of typical vertical frequencies for running can be found in literature. This frequency range is generally defined to be between $1.9\,Hz$ and $3.5\,Hz$ (Occhiuzzi and Spizzuoco, 2008; Živanović *et al.*, 2005). It can logically be assumed that for running as with walking, the frequency range in the lateral direction is half of that in the vertical direction and is therefore between $0.95\,Hz$ and $1.75\,Hz$ (Sétra, 2006).

A number of experiments have been done to measure the changes in the vertical load from a person walking to a person running. Wheeler (1982) combined the work of many other researchers relating to the vertical forces for the different stages between a person walking slowly and a person running (Živanović *et al.*, 2005). His results are shown in Figure 2.9.

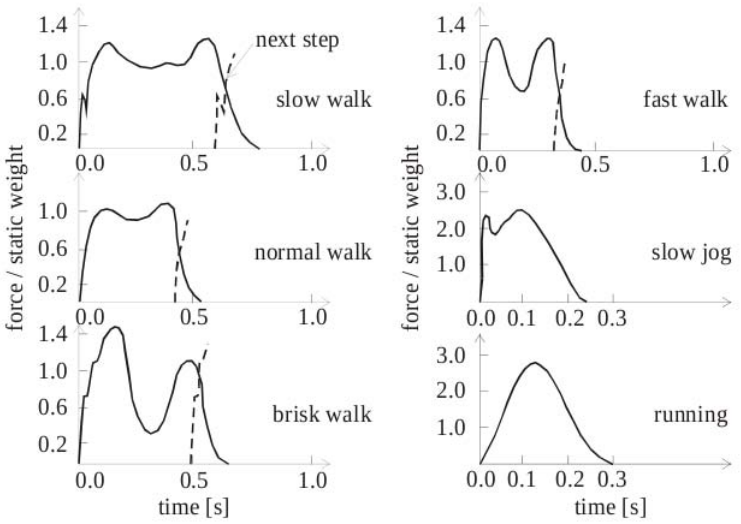

Figure 2.9.: *Vertical force patterns for different types of human activities. (Živanović* et al.*, 2005)*

As can be seen in Figure 2.9 the shape of the vertical force pattern for a person running is simpler than for a person walking. According to measurements done by Pirner and Urushadze (2008) the transition from walking to running occurs at a speed of 1.4 to 1.8 m/s.

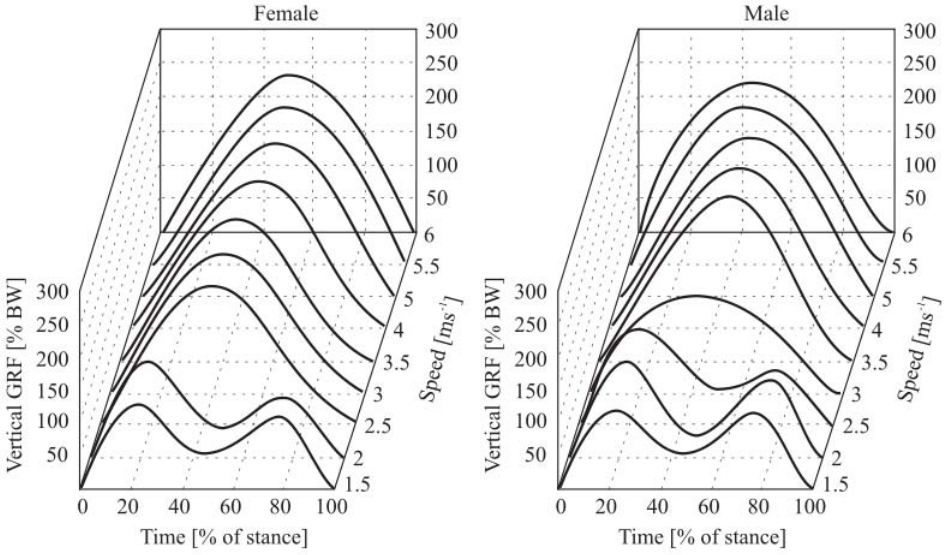

Figure 2.10.: *Experimental results showing vertical ground force patterns. (Racic* et al.*, 2009)*

Studies done by Keller *et al.* (1996) showed that the maximum vertical ground force increases linearly as the speed at which the person moves increases from 1.5 to 3.5 m/s, as shown in

Figure 2.10. At speeds higher than $3.5\,m/s$ they found that the maximum ground forces were constant. From these results they were able to derive two equations to determine the vertical force based on the speed, v, of the person (Racic *et al.*, 2009). These equations are:

$$\begin{aligned} F_z &= 0.614v + 0.208 \qquad (for\, 1.5 < v < 3.5) \\ &= 2.5 \times body weight \qquad (for\, v > 3.5) \end{aligned} \tag{2.2}$$

Keller *et al.* (1996) also found that slow jogging causes vertical forces which can be up to 1.6 times greater than those caused by walking at the same speed or running at higher speeds (Racic *et al.*, 2009). This means that it is important to consider the loading from jogging when designing footbridges.

Figure 2.11 shows the typical vertical force pattern for continuous walking and running which was achieved by Galbraith and Barton by combining the individual foot frequencies for walking and running. As can be seen in Figure 2.11, for the continuous walking force there are periods of time when both feet are on the ground which is represented by the walking time history of the left and the right leg overlapping. However, for continuous running there are periods of time when both feet are off the ground and the resulting vertical force is zero. (Živanović *et al.*, 2005)

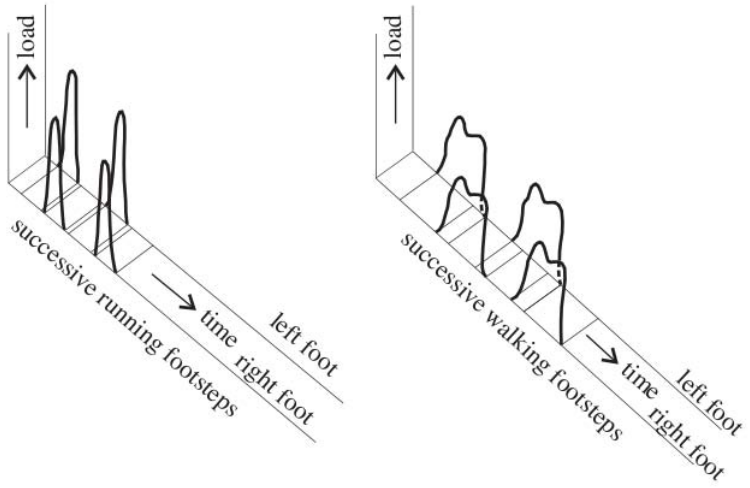

Figure 2.11.: *Typical pattern of running and walking forces. (Živanović* et al.*, 2005)*

Research has shown that there are a number of factors which influence the vertical force of a person jogging or running. These include the weight of the person, the step frequency and

the type of footwear (Racic *et al.*, 2009). An increase in the weight of a person results in higher vertical forces. An increase in the step frequency results in higher peak vertical force amplitudes, increased stride length and velocity, and decreased contact time with the ground. In addition there is a difference in the shape of the running force pattern depending on whether the person running is barefoot or wearing shoes, as shown in Figure 2.12. The difference is caused by the way in which the foot hits the ground. A person running with shoes on will generally land heel first, generating a small spike whereas a person running barefoot will generally land toe first and no spike occurs.

Studies done by McMahon and Greene (1979) showed that the stiffness of the surface on which someone is running affects the vertical ground force. They found that the vertical ground force decreases as the stiffness of the structure decreases and that it is actually easier to run on a flexible surface. (Racic *et al.*, 2009)

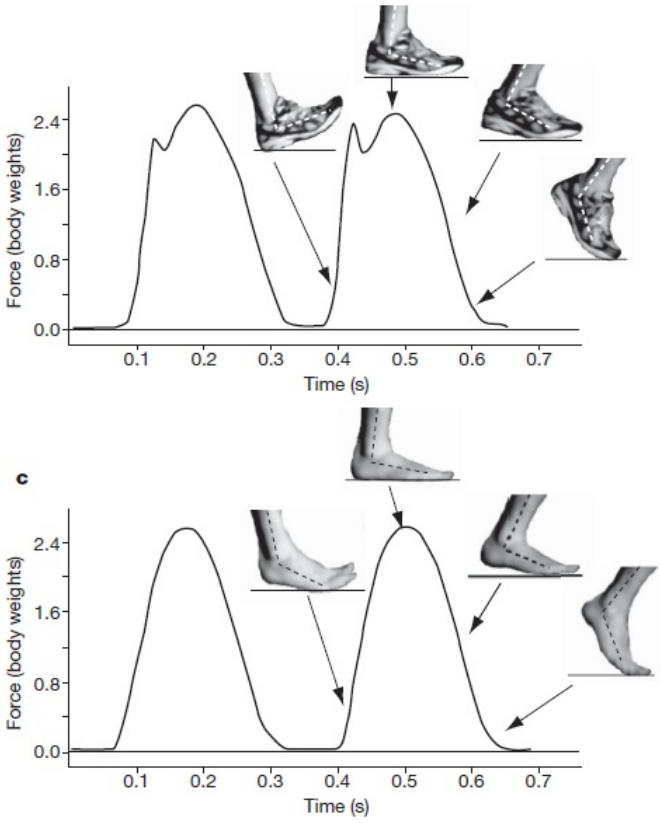

Figure 2.12.: *Vertical ground reactions for a person running with shoes and barefoot. (Switek, 2010)*

It should be noted that jogging and running is often seen as a recreational activity and is therefore often done in groups. The people in these groups will generally run at the same

speed in order to keep together and this could lead to a synchronised loading pattern on a footbridge. This loading phenomenon has not yet been studied in detail and is only briefly looked at in this thesis when developing a running model. (Occhiuzzi and Spizzuoco, 2008)

2.3.3. Vandal Forces

Jumping, bouncing and horizontal body swaying are often known as forms of deliberate vandal loading on footbridges (Živanović *et al.*, 2005). Jumping involves both feet leaving the ground for a short period of time whereas bouncing involves moving up and down without either foot leaving the ground. Horizontal body sway involves moving body weight from one foot to the other while standing in one spot. These forces are more crucial in grandstands and entertainment venues than on footbridges so this section only gives a brief overview of the forces involved.

Bachmann *et al.* (1995) have defined the typical frequency ranges for jumping, bouncing and horizontal body sway to be between 1.8 to 3.4 Hz, 1.5 to 3.0 Hz, and 0.4 to 0.7 Hz respectively (Živanović *et al.*, 2005).

It is well known that the vertical force of a single jump can be described as a harmonic force function as shown in Figure 2.13, where T_c represents the period of time when the person is in contact with the structure and T_s represents the period of time when both the person's feet are in the air (Faisca *et al.*, 2008).

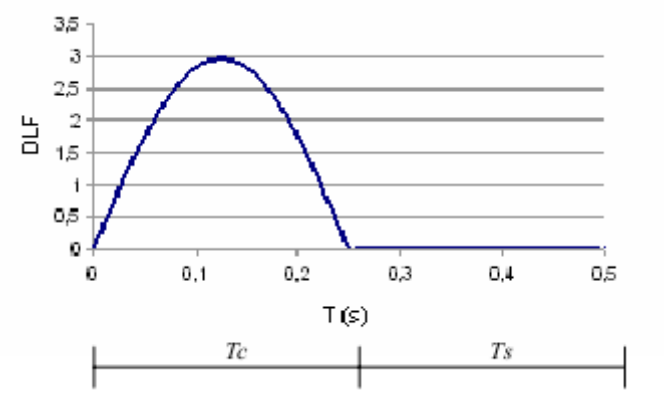

Figure 2.13.: *The force function generating by jumping. (Faisca* et al.*, 2008)*

The period force time history of a person jumping on one spot can be represented by a series of harmonics (Yao *et al.*, 2002). The force time history response of a person bouncing is similar

to that of a person jumping with the exception that there is not a time period represented by T_s as the person's feet are always in contact with the ground. Figure 2.14 shows a typical example of the force time history of a person jumping and bouncing at a constant frequency of $2\,Hz$.

It was recently shown by Pavic *et al.* (2005) that jumping causes forces in three directions; one in the vertical direction and two in the horizontal direction. Of the two forces in the horizontal direction the front-to-back horizontal force is higher than the lateral left-to-right force as shown in Figure 2.15.

Experiments done by Yao *et al.* (2006) on flexible structures showed that it is impossible to jump at a frequency close to the natural frequency of the structure. As the vibrations of the structure increase so the contact time between the person and the structure increases until the motion becomes bouncing instead of jumping. This study coincides with results obtained from biomechanical research which found that the vertical jumping force is higher on stiffer structures. (Racic *et al.*, 2009)

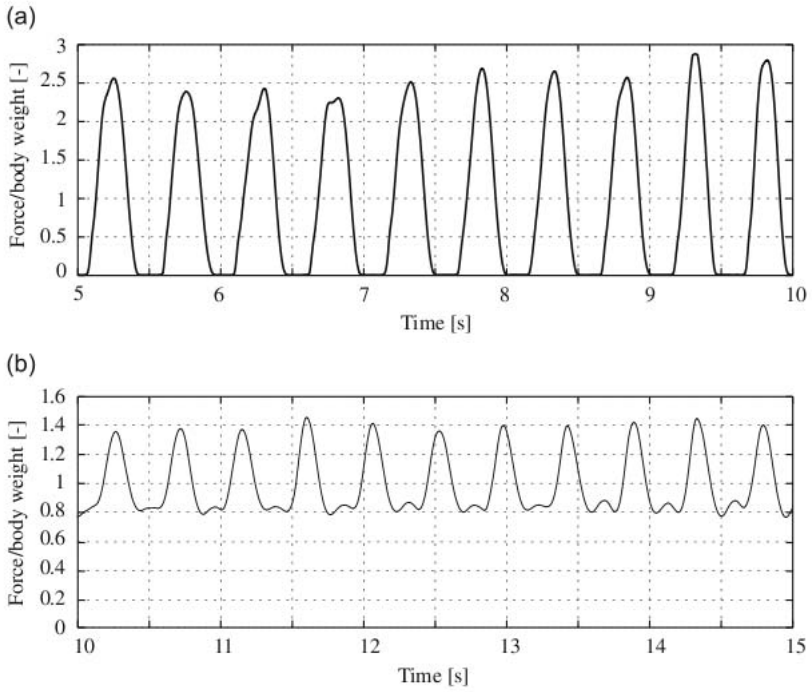

Figure 2.14.: *Vertical Forces due to jumping (a) and bouncing (b) at 2Hz. (Racic* et al.*, 2010)*

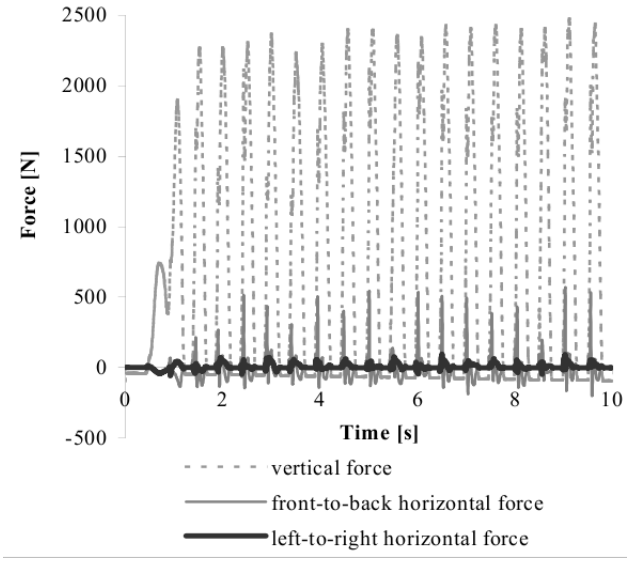

Figure 2.15.: *Force time histories generating by jumping. (Pavic* et al.*, 2005)*

2.3.4. Summary and Comparison

Table 2.2 gives a comparison of the typical frequency ranges for the various forces which could be applied to a footbridge.

Table 2.2.: *Comparison of the Frequency Ranges for Human Induced Forces.*

Forces	Frequency Range		
	Vertical	Lateral	Longitudinal
Walking	$1.4-2.4\,Hz$	$0.7-1.2\,Hz$	$1.4-2.4\,Hz$
Running	$1.9-3.5\,Hz$	$0.95-1.75\,Hz$	$1.9-3.5\,Hz$
Jumping	$1.8-3.4\,Hz$		
Bouncing	$1.5-3.0\,Hz$		
Body Sway		$0.4-0.7\,Hz$	

Of these forces, walking and running are applied most often during the life-cycle of a footbridge. Both these forces are within the natural frequency range of many of the more slender modern bridges and therefore it is important that the designer checks these forces when designing footbridges. Unfortunately, the majority of the design codes which are discussed in this thesis only take walking into account, and some do not even consider the lateral forces imposed onto the footbridge. The next section looks at the types of models available for modelling walking and running forces.

2.4. Modelling of Human-Induced Forces

This section discusses some of the models for human-induced loads described in the previous section. Literature shows that there are two main types of models for human-induced loads; time-domain and frequency-domain models (Racic *et al.*, 2009; Živanović *et al.*, 2005).

The mathematical modelling of human-induced dynamic forces is complicated. Živanović *et al.* (2005) give the following reasons for this:

1. The large variety of human-induced loads change in both time and position.
2. Human-induced loads are influenced by many parameters.
3. The single person dynamic force is a narrow-band process and is not well understood.
4. It is difficult to generalise the effects of a number of people and the amount of synchronisation in a group.
5. The manner in which people walk or run changes if they detect vibrations in the surface on which they are walking or running and therefore the forces involved also change.

Regardless of these complications, load models for human-induced forces do exist. This section looks at some of these models.

2.4.1. Time-Domain Force Models

Time-domain force models are probably the most common for walking and running forces (Racic *et al.*, 2009; Živanović *et al.*, 2005). They assume that the left and the right foot of a person produces the same force and that this force is periodic (Živanović *et al.*, 2005). There are two types of time-domain models which can be found in literature: deterministic and probabilistic.

Deterministic models do not take into account any variation in the way individuals perform an activity and therefore use a general force model for each activity. Probabilistic models take into account some of the parameters which influence human-induced forces such as body weight and frequency. These parameters are generally taken into account as probability density functions. (Racic *et al.*, 2009; Živanović *et al.*, 2005)

2.4.1.1. Deterministic Force Models

An important design parameter in determining the magnitude of the vibrations of a structure when acting under human-induced walking loads is the ratio between the pacing rate of the

pedestrian and the natural frequencies of a structure (Racic *et al.*, 2009). Years of research involving testing of structures under human-induced loads has revealed that a structure will either have a high-frequency response or a low-frequency response. The split between high-frequency and low-frequency responses generally occurs at about $10\,Hz$. (Racic *et al.*, 2009)

Resonant vibration occurs in low-frequency response structures when the natural frequency of the structure lies close to the normal pacing rate of between 1.4 and $2.4\,Hz$ or an integer multiple thereof. In high-frequency structures the natural frequencies are higher than the normal pacing rates and the vibrations generated are a transient impulsive response to each successive heel strike. This results in a transient response with decaying amplitudes following each heel strike. The difference in resonant and transient vibration responses has lead to the development of two different force models for low-frequency and high-frequency structures. Since footbridges are typically classified as low-frequency structures this section will look at these models only. (Racic *et al.*, 2009)

Based on the assumption that each step is identical and that the period between each step is T, then the vertical force, $F_p(t)$ can be represented as a Fourier series as shown in Equation 2.0a, 2.0b and 2.0c. (Racic *et al.*, 2009; Živanović *et al.*, 2005)

The dynamic load factors which form the basis of this load model have been reported in numerous publications and have often been incorporated into design guidelines. The results from measurements by a number researchers are shown in Table 2.3.

In 1977, Blanchard *et al.* (1977) proposed one of the first vertical dynamic load models for a single pedestrian walking on a footbridge with fundamental frequencies up to $4\,Hz$. They assumed a static body weight of $700\,N$ and determined that resonance due to the first harmonic would occur with the dynamic load factor equal to 0.257. Bachmann and Ammann (1987) went further and published the first five harmonics of the vertical and the horizontal walking forces. In the late 1980s Rainer *et al.* (1988) conducted a study in which the dynamic load factors for the first four harmonics were determined for a single person walking, running and jumping. The results of this study are shown in Figure 2.16 where (a) is for a person walking, (b) is for a person running and (c) is for a person jumping. It is clear that the dynamic load factors are dependent on the frequency of the activity. Unfortunately the study lacks statistical reliability as it only included three test subjects (Racic *et al.*, 2009; Živanović *et al.*, 2005).

Kerr (1998) conducted what is probably the most extensive study on walking forces in which he recorded approximately 1000 ground reaction forces from 40 individuals walking on a force plate. The resulting dynamic load factors from his study are shown in Figure 2.17. These results show a large scatter in the dynamic load factor values. Similar to the study by Rainer *et al.* (1988) the dynamic load factors for the first harmonic increases with increasing

pace frequency. The dynamic load factors for the higher harmonics had to be characterised statistically using a mean value and a coefficient of variation due to the large scatter which was measured (Racic *et al.*, 2009; Živanović *et al.*, 2005).

Young (2001) combined the work of Kerr (1998) and others and proposed the dynamic load factors for the first four harmonics as a function of the pacing frequency, f, which are shown in Table 2.3. In developing these functions he assumed that the pacing rate would be in the range of 1.0 to 2.8 Hz. This was probably the first attempt to take into account the stochastic nature of human induced loading (Racic *et al.*, 2009; Živanović *et al.*, 2005).

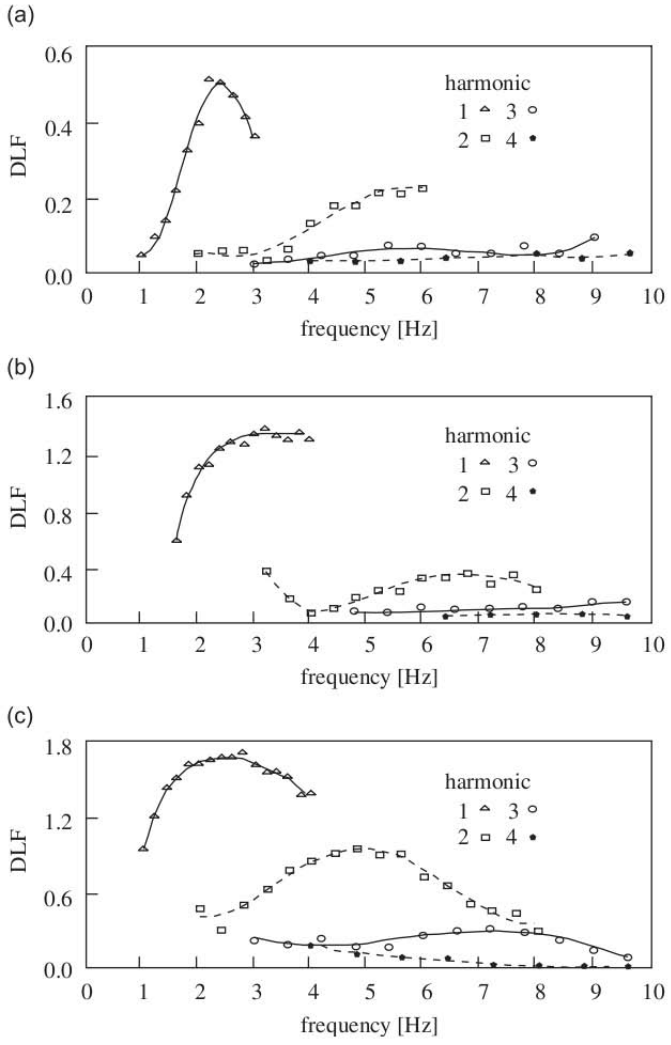

Figure 2.16.: *Dynamic Load Factors for the first four harmonics.*
Živanović et al. *(2005)*

Table 2.3.: *Dynamic load factors found in literature for walking and running.*
(Hauksson, 2005; Racic et al.*, 2009; Živanović* et al.*, 2005; Sun and Yuan, 2008)*

Author	Dynamic load factors					Direction	Stepping Frequency	Load Type
Blanchard *et al.* (1977)	$\alpha_1 = 0.257$					Vertical	$< 4\,Hz$	Walking
Bachmann and Ammann (1987)	$\alpha_1 = 0.4-0.5$	$\alpha_2 = 0.1$	$\alpha_3 = 0.1$			Vertical	$2-2.4\,Hz$	Walking
Schulze (after Bachmann and Ammann (1987))	$\alpha_1 = 0.37$ $\alpha_1 = 0.039$ $\alpha_{1/2} = 0.037$	$\alpha_2 = 0.10$ $\alpha_2 = 0.010$ $\alpha_2 = 0.204$	$\alpha_3 = 0.12$ $\alpha_3 = 0.043$ $\alpha_{3/2} = 0.026$	$\alpha_4 = 0.04$ $\alpha_4 = 0.012$ $\alpha_2 = 0.083$	$\alpha_5 = 0.08$ $\alpha_5 = 0.015$ $\alpha_{5/2} = 0.024$	Vertical Lateral Longitudinal	$2\,Hz$ $2\,Hz$ $2\,Hz$	Walking Walking Walking
Rainer *et al.* (1988)	Figure 2.16					Vertical		Walking, Running and Jumping
Allen and Murray (1993)	$\alpha_1 = 0.5$	$\alpha_2 = 0.2$	$\alpha_3 = 0.1$	$\alpha_4 = 0.05$		Vertical	$1.6-2.4\,Hz$	
Bachmann (1995)	$\alpha_1 = 0.4/0.5$ $\alpha_1 = 0.1$ $\alpha_1 = 0.1$	$\alpha_2 = 0.1$ $\alpha_1 = 0.2$	$\alpha_3 = 0.1$ $\alpha_3 = 0.1$ $\alpha_2 = 0.1$			Vertical Lateral Longitudinal	 $2\,Hz$	Walking Walking Walking
Kerr (1998)	$\alpha_1 = 1.6$ Figure 2.17	$\alpha_2 = 0.7$ $\alpha_2 = 0.07$	$\alpha_3 = 0.2$ $\alpha_3 = 0.06$			Vertical Vertical		Running Walking
Young (2001)	$\alpha_1 = 0.37\,(f-0.92)$	$\alpha_2 = 0.054 + 0.0044f$	$\alpha_3 = 0.026 + 0.0050f$	$\alpha_4 = 0.010 + 0.0051f$		Vertical	f=1-2.8 Hz	Walking
Sun and Yan (2004)	$\alpha_1 = 0.36$ $\alpha_1 = 0.033$	$\alpha_2 = 0.13$ $\alpha_2 = 0.009$				Vertical Lateral	$1.6-2.4\,Hz$ $1.6-2.4\,Hz$	

All of the aforementioned studies deal with a single pedestrian; similar studies for groups of people are uncommon. Ellis (2003) measured the structural response for groups of up to 32 people walking across a floor. He found that the dynamic load factors for a group decrease as the size of the group increases. Pernica (1990) published similar results for people walking, running and jumping in groups. Rainer *et al.* (1988) also reported that at higher harmonics there is a greater reduction in the dynamic load for groups of people, but that the dynamic load factors for the fundamental harmonic was roughly the same. These studies suggest that groups of people doing an activity are not perfectly synchronised and that the total dynamic load factor decreases.

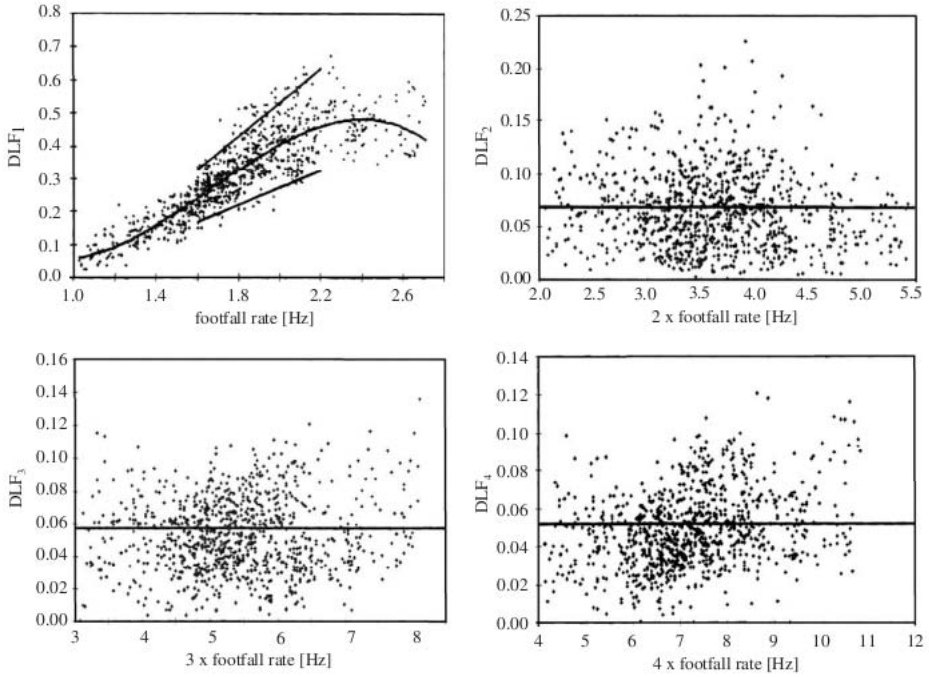

Figure 2.17.: *Dynamic Load Factors of walking force determined by Kerr. Živanović* et al. *(2005)*

It is important to note that all the dynamic load factors given above were determined by studies which measured the direct or indirect force on a rigid surface. As mentioned in Section 2.3 it has been found that the flexibility of the surface does affect the ground reaction forces and therefore affects the dynamic load factors due to human-structure interaction, as shown by Pimentel (1997) who found that the actual first and second resonant vertical harmonics measured on two footbridges were lower than those given in literature. (Živanović *et al.*, 2005)

2.4.1.2. Probabilistic Force Models

It is impossible for a person to produce two identical force-time history responses and therefore a probability approach to a walking or running force model would be more appropriate than a deterministic force model. If the loads are still assumed to be periodic then randomness can be taken into account by probability distributions of, for example, pacing rate, weight, and the time delay between people walking or running. In order to develop reliable probability distributions a large database of measurements for various human activities would be required. This section looks at the various probability distributions for step frequency, walking velocity and step length. (Racic *et al.*, 2009)

Step Frequency

Recently, Živanović *et al.* (2007) measured various time-distance parameters of 2000 people crossing the Podgorica footbridge in Montenegro. Their study found that the mean step frequency was $1.87\,Hz$ and the standard deviation was $0.186\,Hz$. Similar studies by other researchers have yielded varying results for the average walking step frequency, as summarised in Table 2.4. The differences in these statistics can be explained by the differences in the ethnic populations tested. It has been reported that the step frequency and velocity of walking may vary in different parts of the world and even depend on the location and environment (Racic *et al.*, 2009).

Table 2.4.: *Average step frequencies.*
Racic et al. *(2009)*

Author	Mean Step Frequency	Standard Deviation
Matsumoto *et al.* (1972)	$1.99\,Hz$	$0.173\,Hz$
Kerr (1998)	$1.9\,Hz$	
Pachi and Ji (2005)	$1.8\,Hz$	$0.13\,Hz$
Sahnaci and Kasperski (2005)	$1.82\,Hz$	
Živanović *et al.* (2007)	$1.87\,Hz$	$0.186\,Hz$

Walking Velocity

Pachi and Ji (2005) did a study in which they measured 100 men and 100 women walking across two footbridges and two shopping mall floors. They found that the people walked faster across the shopping floors than across the footbridges; the average velocities were $1.4\,m/s$ and $1.3\,m/s$ respectively. Furthermore, they found that there is a linear relationship between velocity and step frequency of a person. This relationship is given in Equation 2.3 where v is the velocity of the person, f is the step frequency and L_s is the average step length.

$$v = L_s f = \left\{ \begin{array}{cc} 0.75f & \text{for males} \\ 0.67f & \text{for females} \\ 0.71f & \text{for both} \end{array} \right\} \tag{2.3}$$

Based on the data collected by Pachi and Ji (2005), Živanović (2006) showed that at a specific frequency the walking velocities are normally distributed as illustrated in Figure 2.18.

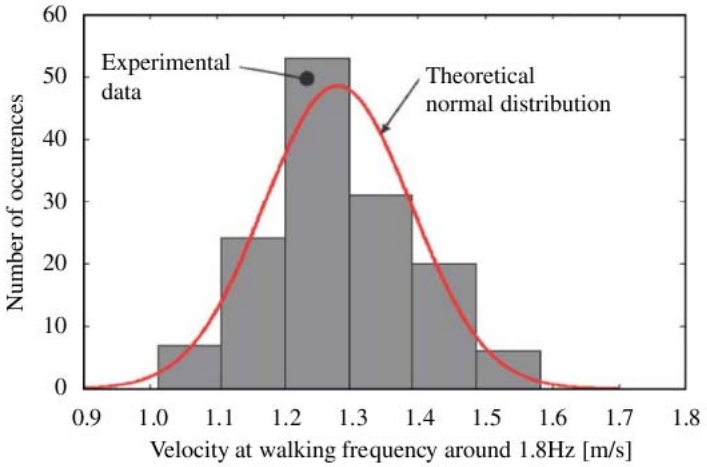

Figure 2.18.: *Normal distribution of walking speed at around 1.8 Hz. (Racic* et al.*, 2009)*

Step Length

The study done by Živanović *et al.* (2007) on the Podgorica footbridge also measured the step length of the people crossing the bridge. They found that the step length varied between $0.479\,m$ and $0.923\,m$ and that the mean value was $0.71\,m$ with a standard deviation of $0.071\,m$. Furthermore, they found that this data was normally distributed and that it was independent of the frequency at which the people were walking.

Barreira *et al.* (2010) did a study to determine the average heart rate, speed, stride length, and stride rate during moderate intensity walking and jogging in 115 healthy young adults. Table 2.5 gives a summary of their findings.

Table 2.5.: *Average Walking and Jogging Parameters.*
(Barreira et al.*, 2010)*

Activity	Heart Rate $beats/min$	Speed m/min	Stride Length $m/stride$	Stride Rate $strides/min$
Walking	107 ± 15	89.7 ± 10.3	0.78 ± 0.05	115 ± 12
Running	155 ± 16	183.7 ± 30.5	1.19 ± 0.21	157 ± 15

A biomechanical study done by Yamasaki *et al.* (1991) showed that the relationship between step length and walking velocity is not linear, as shown in Figure 2.19, and that this deviation from linearity becomes more pronounced at higher velocities. This deviation takes place at about $90\,m/min$. Furthermore, the study found that the relationship differs for males and females. Females have a shorter step length when walking and they increase their speed by increasing their step frequency. Males, on the other hand, increase their speed by increasing their step length.

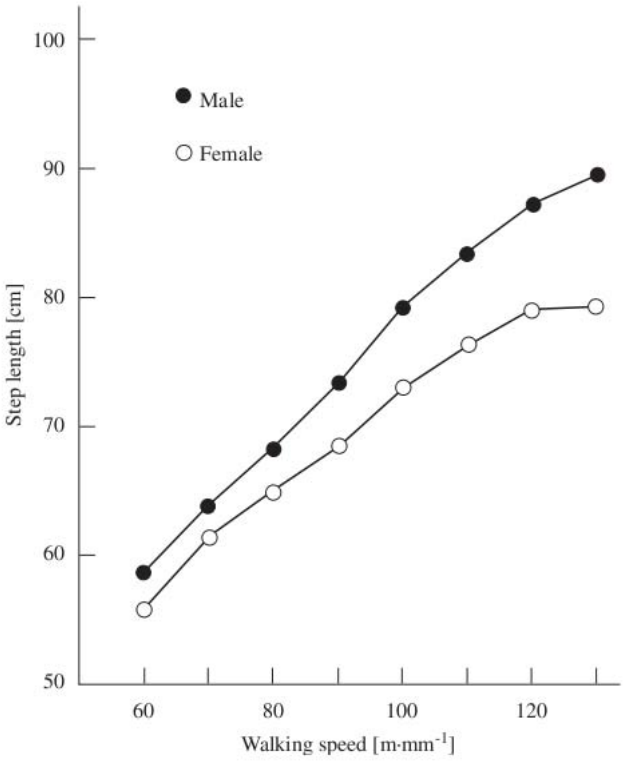

Figure 2.19.: *Relationship between the step length and walking velocity.*
(Racic et al.*, 2009)*

These probability density functions were used to develop a modelling procedure to estimate

the probability of occurrence of a particular walking loading scenario and therefore a certain level of vibration response. The probability that the vibration response will not exceed predefined limiting values could then be found (Racic *et al.*, 2009). Similar studies need to be done for running pedestrians and for groups of people in order to determine a probability-based model for running loads and multi-pedestrian loads.

2.4.1.3. Time-Domain Design Procedures

Time-domain design procedures assume that the human-induced forces are perfectly periodic and through Fourier decomposition (given in Equation 3.2) can be decomposed into harmonics. This means that only a single force resonant harmonic would need to be considered and that the structure can be represented as a single degree of freedom system in modal space. It is generally assumed that only the first three or four excitation harmonics could cause resonance on a footbridge. (Živanović *et al.*, 2005)

The majority of design procedures only consider the vertical forces. This is because the importance of the horizontal forces has only been realised in recent years with the design of more slender bridges and the recent lateral vibration failures of some of these bridges.

One of the first design procedures for vibration serviceability of footbridges was proposed by Blanchard *et al.* (1977). They advised that vibration serviceability due to human-induced loading need only be checked for footbridges with a fundamental natural frequency, f, up to $5\,Hz$. For footbridges with a fundamental natural frequency less than or equal to $5\,Hz$ they proposed that the maximum acceleration response in m/s^2 should not exceed $0.5\sqrt{f}$. The proposed moving force model for a walking force, illustrated in Figure 2.20(a) was a resonant sinusoid moving across the footbridge with a velocity of $v = 0.9f$. Figure 2.20(b) gives the forcing function for this pedestrian load. This is the procedure which was adopted in the old British standard (BS 5400) and TMH7, which are discussed in the next section. (Živanović *et al.*, 2005)

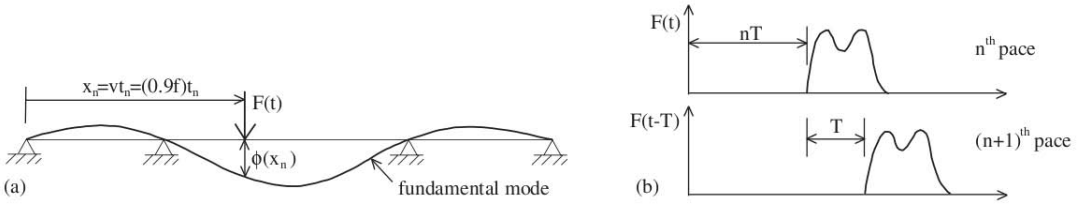

Figure 2.20.: *Moving force model and forcing function for a pedestrian load. (Živanović* et al.*, 2005)*

The modal force per modal mass for the fundamental vibration mode can be given as (Živanović *et al.*, 2005):

$$\frac{P_1(t)}{M_1} = \frac{P}{M_1}\phi(0.9ft)sin(2\pi ft) \tag{2.4}$$

where P is the force amplitude of $180\,N$, which corresponds to the dynamic load factor of 0.257 (as determined by Blanchard *et al.* (1977) and described in the Section 2.3), M_1 is the generalised mass for the fundamental mode and $\phi(0.9ft)$ is the location dependent ordinate of the first mode shape which is dependent on the position $x = 0.9ft$ of the pedestrian at time t after the start of walking. This procedure was simplified for bridges with one, two or three spans to a procedure which calculates the maximum acceleration response, a, directly using the formula (Živanović *et al.*, 2005):

$$a = \omega_1^2 y_s K \psi \tag{2.5}$$

where $\omega_1 = 2\pi f$ is the fundamental circular frequency of the bridge, y_s is the static deflection at midspan due to the weight of a pedestrian, K is a configuration factor which depends on the number of spans and ψ is the dynamic response factor which takes into account the span length and footbridge damping. The configuration factor and the dynamic response factor were derived by performing numerous simulations on footbridges with one, two or three spans under the general walking force shown in Figure 2.20(b). (Živanović *et al.*, 2005)

This model has several limitations:

- It only considers the vertical component of the walking load.
- The dynamic load factor of 0.257 does not represent the whole frequency range up to $5\,Hz$. This is because between $1.6\,Hz$ and $2.4\,Hz$, the walking frequency has a strong influence on the dynamic response factor for the first harmonic as shown in Figure 2.16. (Živanović *et al.*, 2005)
- There may be a mode other than the fundamental mode which has a frequency within the normal walking range, but this procedure only looks at the fundamental mode. (Živanović *et al.*, 2005)

The design procedure developed by Blanchard *et al.* (1977) was improved by Rainer *et al.* (1988) by taking into account the fact that the dynamic load factors for a walking or running force are dependent on the step frequency. In this procedure the moving force has a time duration which is limited by the length of the bridge. Figure 2.21 gives the SDOF model for

this procedure, where m is the modal mass, c is the damping and k is the stiffness. (Živanović *et al.*, 2005)

A dynamic amplification factor, Φ, was introduced to take into account the moving force and its limited time duration. This factor depends on the structural damping and the number of force cycles required to cross the bridge. Based on this, Rainer *et al.* (1988) proposed that the modal peak acceleration response could be calculated of shown in Equation 2.6.

$$a = \frac{\alpha P}{m}\Phi \tag{2.6}$$

where m is the modal mass, P is the pedestrian weight and α is the appropriate dynamic load factor. Although this procedure works very well and is verified with experimental measurements it is only applicable to single span footbridges. (Živanović *et al.*, 2005)

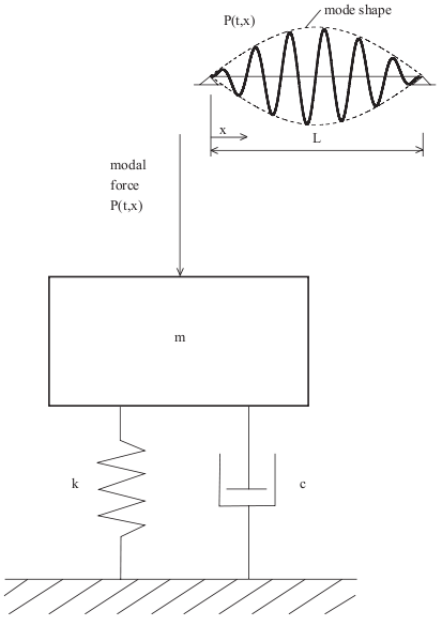

Figure 2.21.: *Pedestrian modal force model.*
(Živanović et al.*, 2005)*

A number of researchers tried to simplify or extend this procedure. One of the attempts to simplify the procedure was made by Allen and Murray (1993). They proposed replacing the moving walking force with a stationary sinusoid acting at midspan. The amplitude and frequency of this sinusoid changed in accordance with the harmonic which they were looking at. This resulted in a steady-state response. In order to take into account the actual nature of the force a reduction factor, R, was introduced. Thus the non-dimensional ratio between

the harmonic peak response and the gravity acceleration was determined as (Živanović *et al.*, 2005):

$$\frac{a}{g} = \frac{R\alpha_i P}{\beta W} cos(2\pi i f t) \tag{2.7}$$

where α_i is a dynamic load factor, P is the pedestrian weight, β is the damping ratio, W is the bridge total weight and R is a reduction factor which is 0.7 for footbridges (Živanović *et al.*, 2005). However, there are two main problems with this procedure. The first is that the reduction factor is constant and therefore cannot take into account the various span lengths and hence the different times required to cross the bridge. The second is that Allen and Murray (1993) took the maximum values for the dynamic load factors for each harmonic given in Figure 2.16 (i.e. $\alpha_1 = 0.5$, $\alpha_2 = 0.2$, $\alpha_3 = 0.1$ and $\alpha_4 = 0.05$) which would give overly conservative results. Taking into account the acceleration limits given in the ISO guide, Equation 2.7 can be modified to give the minimum natural frequency allowed for a footbridge as shown in Equation 2.8 (Živanović *et al.*, 2005).

$$f_0 \geq 2.86 ln \frac{K}{\beta W} \tag{2.8}$$

where K is a constant equal to $8\,kN$ and $\beta = 0.01$ is the recommended damping ratio (Živanović *et al.*, 2005).

Kerr (1998), derived the analytical form of Rainer *et al.*'s (1988) procedure by converting the dynamic load factors into a function of the step frequency as shown in Figure 2.17. Pimentel and Frenandes (2002) introduced a factor k_a in order to extend Rainer *et al.*'s (1988) procedure to include footbridges which have two spans. This resulted in the peak modal acceleration being determined by (Živanović *et al.*, 2005):

$$a_{max} = \omega_0^2 y_s \alpha_i \Omega_d k_a \tag{2.9}$$

where ω_0 is the fundamental circular bridge frequency, y_s is the static deflection due to the weight of a pedestrian, α_i is the dynamic load factor of the resonant i^{th} harmonic, Ω_d is the dynamic amplification factor and k_a is a numerically obtained factor which takes into account the differences between bridges with two spans and those with one span (Živanović *et al.*, 2005).

Grundmann *et al.* (1993) proposed calculating the resonant acceleration response of a footbridge due to a single pedestrian harmonic force by using the full theoretical expression in-

cluding the transient and steady-state parts and assuming that the initial conditions are zero, as follows (Živanović *et al.*, 2005):

$$a_{1rz} = 0.6\frac{0.4G}{M}\frac{\pi}{\delta}(1-e^{-n\delta}) \tag{2.10}$$

where the factor 0.4 is the dynamic load factor for the first harmonic, G is the weight of the pedestrian, M is the modal mass of the structure, δ is the logarithmic decrement and n is the number of steps required to cross the bridge. The factor 0.6 takes into account the variation of the amplitude of the mode shape in different sections of the walking path. Grundmann *et al.* (1993) also proposed a similar approach for determining the lateral acceleration response using a dynamic load factor which is a quarter of the vertical dynamic load factor (Živanović *et al.*, 2005).

The majority of these procedures are limited to girder footbridges with only one or two spans. This is not usually representative of the real world and does not take into account the latest trends in the design of slender and architectural footbridges. Furthermore, the majority of these procedures are only concerned with vertical loading from a single pedestrian (Živanović *et al.*, 2005). One attempt at solving these issues was made by Young (2001). He developed a design procedure which was independent of the type of footbridge. He used a harmonic force to represent the load applied to a footbridge and then determined the full theoretical expression for a steady-state acceleration response, a_n, in a single vibration mode, n (Živanović *et al.*, 2005).

$$a_n = \mu_i\mu_j(\frac{f}{f_n})^2\frac{P}{M}DMF \tag{2.11}$$

where μ_i and μ_j are the mode shape ordinates at the walking point and response point respectively, f and P are the frequency and amplitude of the harmonic force respectively, f_n and M are the natural frequency and modal mass of the vibration mode n respectively and DMF is the dynamic magnification factor. This dynamic magnification factor is calculated as shown in Equation 2.12 (Živanović *et al.*, 2005).

$$DMF = \frac{1}{1-(\frac{f}{f_n})^2+i(2\zeta_n(\frac{f}{f_n}))} \tag{2.12}$$

where ζ_n is the damping ratio for the vibration mode n. During resonance the DMF is simplified as only the imaginary part of Equation 2.12 would remain (Živanović *et al.*, 2005).

In order to take into account the limited duration of the pedestrian harmonic force and the fact

that it moves across the bridge (Young, 2001) proposed a reduction factor, r (Živanović *et al.*, 2005).

$$r = 1 - e^{-2\pi\zeta N} \tag{2.13}$$

where N depends on the number of cycles required for the n^{th} harmonic to cross the bridge and is calculated by (Živanović *et al.*, 2005):

$$N \approx 0.55n\frac{L}{l} \tag{2.14}$$

where L is the span of the bridge and l is the step length of the pedestrian (Živanović *et al.*, 2005).

In Chapter 6, the results from these simple models are compared with the actual accelerations measured on a bridge due to human induced jogging loads.

2.4.1.4. Modifications for Groups of People

The first attempt at modelling loads induced by a group of pedestrians was done by Matsumoto *et al.* (1978). They defined a factor m, shown in Equation 2.15, which is multiplied by the vibration amplitude calculated for one person to give the vibration amplitude for a group of people. In order to derive this factor they assumed that a Poisson distribution could be used to describe how the pedestrians would arrive at a bridge.

$$\begin{aligned} m &= \sqrt{\lambda T_0} \\ m &= \sqrt{n} \end{aligned} \tag{2.15}$$

where λ is the mean flow rate of pedestrians over the width of the deck measured in persons per second, T_0 is the time in seconds required to cross the bridge of length L, and n is the number of pedestrians on the bridge at any instant of time. This method does not take into account synchronisation of pedestrians in a crowd. If every person in a group of pedestrians were all synchronised with each other then $m = n$ (Hauksson, 2005; Živanović *et al.*, 2005). In fact, a real world situation would probably lie somewhere between these two extremes. Therefore, the increase in the load due to a crowd of people is not directly proportional to the number of people involved because perfect synchronisation is unlikely. Nor is the load only be the static weight of all the people in the crowd as there will be some synchronisation between some of

the people. The difficulty, then, is in determining the degree of synchronisation (Živanović *et al.*, 2005).

Studies done after Matsumoto *et al.*'s (1978) proposal showed that group loading is more important in bridges which have a natural frequency around the normal walking frequency range. However, it was only after the failure of the London Millennium Bridge that researchers really started considering the possibility of synchronisation between people in a dense crowd.

During the opening of the London Millennium Bridge the maximum crowd density was between 1.3 and 1.5 people per square meter (Živanović *et al.*, 2005). Similarly, the crowd density of the T-Bridge in Japan was between 1.0 and 1.5 people per square meter (Živanović *et al.*, 2005). At these densities both of these bridges experienced lateral movement. This shows that crowd density has an effect on the speed at which people will cross the bridge, the degree of synchronisation and therefore the intensity of loading on the bridge (Živanović *et al.*, 2005).

Three models representing the different possible configurations for pedestrians on a footbridge were proposed by Grundmann *et al.* (1993). Each of these models should be considered for every footbridge. These models are:

- A small group of people walking together across a footbridge would likely walk at the same speed but with different step frequencies and step lengths. In this situation some synchronisation between the people would be expected if the bridge frequency is within the normal walking frequency range (Živanović *et al.*, 2005).
- A light stream of pedestrians crossing a bridge where the people are able to move freely and at their own walking frequency. In this situation it is suggested that the maximum density would be 0.3 people per square meter Grundmann *et al.* (1993) This scenario was considered in the previously mentioned model proposed by Matsumoto *et al.* (1978).
- A crowd of pedestrians crossing a bridge where the people are unable to move freely and they are forced to adjust their step length and speed to that of the other pedestrians. This situation occurs with crowd densities in the region of 0.6 and 1.0 people per square meter and is the situation which occurred on the London Millennium Bridge and the T-Bridge. If the bridge deck is moving perceptively then synchronisation between the crowd and the structure is also possible (Živanović *et al.*, 2005).

When considering groups of people running across a bridge, the first and second of these models are possible, however, the third model is unlikely. The reasons for this are that in such a crowd, running would be difficult, and once the bridge started moving most people would slow down.

2.4.2. Frequency-Domain Force Models

In the early 1980s Ohlsson (1982) developed the basic concepts of using the frequency content of human-induced excitations to determine the vibration serviceability of structures. By treating the walking force as a transient signal where identical steps were repeated a couple of times the auto-spectral density (ASD) of that force was determined. Since Ohlsson was studying the behaviour of high-frequency floors only the high-frequency content of the ASD, between 6 and 50 Hz, was considered. Later, one of his students, Eriksson (1994), did a similar study for low-frequency floors and looked at an ASD frequency range below 6 Hz. Figure 2.22 shows the part of the spectrum below 6 Hz for a continuous walking force which lasts for approximately 100 seconds (Racic *et al.*, 2009; Živanović *et al.*, 2005).

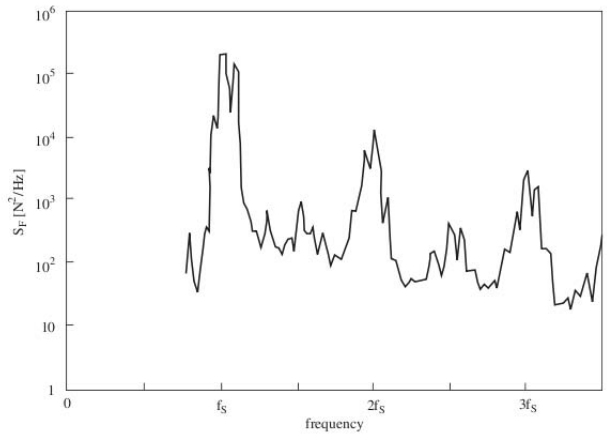

Figure 2.22.: *ASD of a walking force produced by Eriksson. (Živanović* et al.*, 2005)*

The reason for the width in the spectrum around each peak in the main harmonics is that human walking forces are not perfectly periodic, but instead a narrow-band random process. This means that it is not possible to accurately determine the dynamic load factors as required in the time-domain models (Racic *et al.*, 2009; Živanović *et al.*, 2005).

In order to determine a more realistic frequency-domain model for calculating the vertical response of a footbridge when a crowd of pedestrians walk across it, Brownjohn *et al.* (2004) measured the continuous vertical ground reaction force for three people walking on a instrumented treadmill. They found that by applying the Gaussian probability distribution of mean pacing rates (with mean value of 2 Hz and standard deviation of 0.2 Hz), the ASD of the response in a particular mode $S_x(f)$ in a degree of freedom (DOF) defined by the coordinate x can be calculated as shown in Equation 2.16 (Racic *et al.*, 2009).

$$S_x(f) = \psi_z^2 \mid H(f) \mid^2 S_{p,1}(f) \int_0^L \int_0^L \psi_{z_1} \psi_{z_2} coh(f, z_1, z_2) dz_1 dz_2 \tag{2.16}$$

where ψ_z is the ordinate of the mode shape at the same location, $H(f)$ is the frequency response function for acceleration response, $S_{p,1}(f)$ is the ASD of the pedestrian loads per unit length of the bridge span for the fundamental harmonic, ψ_{z_1} and ψ_{z_2} are the mode shape ordinates related to the location of each of the two pedestrians on the bridge at coordinates z_1 and z_2. Furthermore, the coherence function, $0 \leq coh(f, z_1, z_2) \leq 1$, takes account of any synchronisation between the pedestrians at different positions on the bridge. Unfortunately the form of this coherence function has not yet been determined as it will be based on the ongoing research into synchronisation among pedestrians and results from experiments on full-scale bridges (Racic *et al.*, 2009).

Differences in the step length and walking frequency of the right and left legs mean that humans do not walk in a symmetrical manner. This leads to energies between the bands of the main harmonics in the ASD plots as demonstrated by Sahnaci and Kasperski (2005). These energies are called subharmonics or intermediate harmonic load amplitudes and they could play an important role in determining the actual response of the structure. Because of this, Živanović *et al.* (2007) extended the force model proposed by Brownjohn *et al.* (2004) to incorporate the first five harmonics and related subharmonics without discontinuities. Using random phase shifts between spectral lines their model was transformed to the time-domain (Racic *et al.*, 2009).

2.4.2.1. Frequency-Domain Design Procedures

Ohlsson (1982) came up with the idea to use the theory of stationary random processes to assess the vibration serviceability of floors. Although this study investigated high-frequency floors, the design procedures used could form a basis for future design procedures for footbridges. The auto-spectral density (ASD) response for a stationary random process can be calculated as follows:

$$S_y(\omega) = \mid H(\omega) \mid^2 S_x(\omega) \tag{2.17}$$

where $H(\omega)$ is the frequency response function of the structure and $S_x(\omega)$ is the ASD of the force. By calculating the area under the spectral density curve of the response, the mean square value of the response, $E\left[y^2\right]$, can be determined by Equation 2.18. Hence the root-mean-square (RMS) value or peak acceleration can also be determined (Živanović *et al.*, 2005).

$$E\left[y^2\right] = \int_{-\infty}^{+\infty} S_y(\omega) d\omega \tag{2.18}$$

During the study by Eriksson (1994) on low-frequency floors, he measured the acceleration responses from a person walking, running and jumping on a floor as well as the acceleration response from a group of people walking across a floor. Based on the resulting measurements, and using Equation 2.17, he proposed a force mean square design model. This model has a constant mean square value for the first harmonic and thereafter the value is frequency dependent as shown in Table 2.6, where F_{rms} is the RMS function of the walking, running and jumping force, K_{np} is a multiplication factor for a single person RMS force as a function of the number of people in the group n_p, and f_0 is equal to $1\,Hz$. Mouring and Ellingwood (1994) came up with a different proposal in order to take crowd loading into account. They proposed multiplying the ASD of an individual force by the number people in the crowd (Živanović *et al.*, 2005).

Table 2.6.: *Eriksson's design force model. (Živanović* et al.*, 2005)*

Activity	Frequency interval (Hz)	F_{rms} (N)	K_{np} (n_p)
Walking	0 - 2.5	220	$n_p^{0.9}$ *
	2.5 - 10.0	$180\left(\frac{f_0}{f}\right)$	$n_p^{0.5}$
Running	0 - 3.0	690	$n_p^{0.9}$ †‡
	3.0 - 10.0	$4300\left(\frac{f_0}{f}\right)^2$	$n_p^{0.5}$ §
Jumping	0 - 3.5	1000	$n_p^{0.9}$
	3.5 - 10.0	$13000\left(\frac{f_0}{f}\right)^2$	$n_p^{0.5}$ ¶

* Factor for well correlated group. For normal traffic use $n_p^{0.5}$

† Factor for well correlated group. For normal traffic use $n_p^{0.5}$

‡ Factors given *inter-alia* in absence of sufficient data.

§ Factors given *inter-alia* in absence of sufficient data.

¶ Factors given *inter-alia* in absence of sufficient data.

In order to take into account the fact that people do not have perfectly periodic and repeatable walking patterns Brownjohn *et al.* (2004) proposed a model of the walking force for the first six harmonics based on direct measurements of three people walking on a treadmill. Based on this the ratio between the Fourier amplitudes for real and periodic forces, $G_n^{'}$, was given as a function of frequency f:

$$G_n'\left(\frac{f}{\bar{f}}\right) = A + Be^{-\left|\frac{f}{n\bar{f}}-1\right|^C/D} \tag{2.19}$$

where $\bar{f}$ is the fundamental frequency of the appropriate perfect periodic force, n is the order number of the harmonic while A, B, C and D are constants dependent on the harmonic considered (Živanović *et al.*, 2005). This is based on the ASD of the force harmonic $S_{F,n}(f)$:

$$S_{F,n}(f) = \left[WG_n\left(\bar{f}_i\right)\right]^2 S_{G_n'}\left(\frac{f}{\bar{f}}\right) \tag{2.20}$$

where W is the pedestrian weight, G_n is the dynamic load factor for the appropriate harmonic of the perfectly periodic walking force and $S_{G_n'}\left(\frac{f}{\bar{f}}\right)$ is the ASD of the function for G_n' given in Equation 2.19. The ASD should be obtained for a single pedestrian by using Equation 2.17 and for a group of people by using Equation 2.16 (Živanović *et al.*, 2005).

2.5. Review of Current Design Codes and Guidelines

The majority of the older design codes for footbridges consider a single person walking across the footbridge and the resulting vibration response (Zivanovic *et al.*, 2008). These codes are still used in a number of countries, although newer codes are now available. In South Africa TMH7 is the generally accepted code of practice for the design of footbridges. In this section TMH7 is compared with a number of other codes. The codes which are reviewed in this section are:

- TMH7
- Sétra Guide
- The old British Standard (BS 5400)
- Eurocode with the UK Annex
- ISO Guide

The emphasis during this review is placed on the vibration serviceability requirements of the various codes and the load models used for the human induced loading.

2.5.1. TMH7

TMH7 is the code of practice for the design of highway bridges and culverts in South Africa and is limited to the design of reinforced and prestressed concrete bridges with ordinary ag-

gregates. It was published in 1981 and is largely based on the old British Standard (BS 5400). It consists of two parts. Part 1 contains a general statement that explains the basic philosophy of design and defines various concepts and terms included in the code (CSIR, 1981). Part 2 specifies the design loads. (CSIR, 1981).

This code is based on the limit state design methodology; the design for vibrations falls under the serviceability limit state requirement. Appendix 2C of the code deals with the 'Vibration Serviceability Requirements for Pedestrian and Cycle Track Bridges' and is based on the research done by Blanchard *et al.* in the 1970's. (CSIR, 1981)

The initial step in the code's design procedure is to determine the fundamental natural frequency, n_o, of the unloaded bridge superstructure. If the frequency is greater than $5\,Hz$ then the vibration serviceability requirement for that particular bridge has been satisfied and no further checks are required. However, if the fundamental natural frequency is less than $5\,Hz$ then it is necessary to limit the vertical acceleration of any part of the superstructure to $0.5\sqrt{n_o}\ m/s^2$. (CSIR, 1981)

The code gives two methods for determining the maximum vertical acceleration of the superstructure.

- The Simplified Method is only applicable to bridges with a symmetrical superstructure and constant cross-section that are simply supported on bearings with up to three continuous spans (CSIR, 1981). In this method the maximum vertical acceleration can be calculated by using Equation 2.21.

$$a = 4\pi^2 n_o^2 Y_s K \psi \tag{2.21}$$

  where n_o is the fundamental natural frequency, Y_s is the static deflection, K is the configuration factor and ψ is the dynamic response factor.

- The General Method is applicable to all other bridges not covered by the simplified method. This method assumes "that the dynamic loading applied by a single pedestrian can be represented by a pulsation point load, F, moving across the main span of the superstructure at a constant speed V_t as follows:

$$F = 180 sin 2\pi n_o T \tag{2.22}$$

$$V_t = 0.9 n_o \tag{2.23}$$

  where T is the time" (CSIR, 1981).

To summarise, the design methodology for vibration serviceability is first to determine whether the bridge will be susceptible to vibrations by looking at the natural frequency of the bridge

and, if it is, then the maximum vertical acceleration of the bridge must be limited. In order to determine the maximum vertical acceleration the code considers a single pedestrian crossing the bridge and models the loading by means of a *sine* function. The code mentions the possibility of crowd loading and that in certain instances it would be important to take this into consideration, but no methodology is given on how this is to be done. The code does not cover vibrations in the lateral and longitudinal directions and no differentiation is made between walking and jogging.

2.5.2. Sétra Guide

The Sétra Guide is the French technical guideline for the assessment of the vibrational behaviour of footbridges under pedestrian loading and was published in 2006. It was developed based on the latest knowledge of the dynamic behaviour of footbridges under human induced loading at that time and provides a guide for the design of footbridges taking into account dynamic effects. This guide was developed from the results of tests performed on the Solférino footbridge and on an experimental platform. (Sétra, 2006)

The methodology in the guide requires that footbridges be classified by the number of people which are likely to use the bridge at the same time, referred to as the traffic level. Prior to the design, the required comfort level of the users must be decided. This generally means that a trade off needs to be made between comfort and aesthetics. (Sétra, 2006)

The guideline explains the varying effects of a person walking, a person running, several pedestrians, a crowd and the effect of 'lock-in' for a crowd of pedestrians. Table 2.7 below gives the frequency range for a person walking and running.

Table 2.7.: *Estimated Frequency Range for Pedestrians from Sétra. (Sétra, 2006)*

Designation	Specific Features	Frequency Range (Hz)
Walking	Continuous contact with the ground	1.6 to 2.4
Running	Discontinuous contact with the ground	2 to 3.5

The methodology given in the guideline for analysing the dynamic response of a footbridge is outlined below (Sétra, 2006):

2.5.2.1. Determine Footbridge Class

The first step is to determine the class of the footbridge, which gives an indication of the traffic level that can be expected. The classes are shown in Table 2.8. (Sétra, 2006)

Table 2.8.: *Classification of Footbridge Classes in Sétra. (Sétra, 2006; Butz, 2008)*

Class	Description
I	Urban footbridge linking high pedestrian areas, frequently used by dense crowds, very heavy traffic
II	Urban footbridge linking populated areas, heavy traffic, occasionally loaded with streams
III	Standard traffic, occasionally crossed by large groups but never by a stream
IV	Seldom used footbridge, link of sparsely populated areas, pedestrian bridges in motorway areas

2.5.2.2. Choose Comfort Level

The second step is to choose between possible comfort levels from Table 2.9. (Sétra, 2006)

Table 2.9.: *Classification of Comfort Levels in Sétra. (Sétra, 2006; Butz, 2008)*

Comfort Level	Description
Maximum	Structural accelerations are practically not perceived by the users
Average	Structural accelerations are merely perceived by the users
Minimum	Structural accelerations under seldom occurring loading configurations are perceived by the users but not assessed as intolerable.

2.5.2.3. Determine Acceleration Limits

Based on the comfort level, the guideline gives the associated acceptable acceleration ranges, which have been summarised in Table 2.10 (Sétra, 2006). It should be noted, however, that the horizontal acceleration range for all comfort levels is limited to $0.10\,m/s^2$ in order to prevent any 'lock-in' effect. (Sétra, 2006)

Table 2.10.: *Acceleration Ranged for the Different Comfort Levels in Sétra. (Sétra, 2006; Butz, 2008)*

Comfort Level	Vertical Acceleration Range (m/s^2)	Horizontal Acceleration Range (m/s^2)
Maximum	$0 < a_{crit} \leq 0.5$	$0 < a_{crit} \leq 0.15$
Average	$0.5 < a_{crit} \leq 1.0$	$0.15 < a_{crit} \leq 0.3$
Minimum	$1.0 < a_{crit} \leq 2.5$	$0.3 < a_{crit} \leq 0.8$
Discomfort	$a_{crit} > 2.5$	$a_{crit} > 0.8$

2.5.2.4. Determine the Natural Frequencies

The next step is to determine the natural frequencies of the footbridge and whether there is a need to perform dynamic load calculations. The natural frequencies need to be determined in three directions (vertical, lateral and longitudinal) for Class I to Class III footbridges with no additional loading, i.e. no pedestrians, and with an additional dead load of $0.7\,kN/m^2$ throughout the bridge deck, representing one pedestrian per square metre. Based on the obtained natural frequency it is possible to classify the bridge according to a frequency range as outlined in Table 2.11. (Sétra, 2006)

Table 2.11.: *Frequency Range Classifications. (Sétra, 2006)*

Classification	Natural Frequency Range (Hz)	
	Vertical and Longitudinal Vibrations	Lateral Vibrations
Range 1	$1.7 \leq n_o \leq 2.1$	$0.5 \leq n_o \leq 1.1$
Range 2	$1.0 \leq n_o \leq 1.7$ and $2.1 \leq n_o \leq 2.6$	$0.3 \leq n_o \leq 0.5$ and $1.1 \leq n_o \leq 1.3$
Range 3	$2.6 \leq n_o \leq 5.0$	$1.3 \leq n_o \leq 2.5$
Range 4	$n_o < 1.0$ and $n_o > 5.0$	$n_o < 0.3$ and $n_o > 2.5$

The frequency range, together with the bridge class, is then used to determined whether dynamic load calculations are required, and the required load cases for these calculations, as shown in Table 2.12. (Sétra, 2006)

Table 2.12.: *Load Cases Requiring Dynamic Load Calculations. (Sétra, 2006)*

Bridge Class	Natural Frequency Range			
	Range 1	Range 2	Range 3	Range 4
I	Case 2	Case 2	Case 3	Not required
II	Case 1	Case 1	Case 3	Not required
III	Case 1	Not required	Not required	Not required
IV	Not required	Not required	Not required	Not required

Case 1 represents a sparse to dense crowed, Case 2 represents a very dense crowd and Case 3 represents crowd complement. (Sétra, 2006)

2.5.2.5. Perform Dynamic Load Calculations

The next step is to perform the dynamic load calculations where required. The calculations vary for each load case. Table 2.13 gives the vertical, longitudinal and lateral loads which need to be applied to the bridge in order to determine the vibration in the vertical, longitudinal and lateral directions respectively. (Sétra, 2006)

Table 2.13.: *Directional Loads for Load Cases 1, 2 and 3. (Sétra, 2006; Butz, 2008)*

Direction	Load per unit area	
	Load Case 1 and 2	Load Case 3
Vertical	$p_{vert}(t) = \frac{280 \cdot n_{eff}}{A} \cos(2\Pi \cdot f_{vert} \cdot t) \cdot \psi_{vert}$	$p_{vert}(t) = \frac{70 \cdot n_{eff}}{A} \cos(2\Pi \cdot f_{vert} \cdot t) \cdot \psi_{vert}$
Longitudinal	$p_{long}(t) = \frac{140 \cdot n_{eff}}{A} \cos(2\Pi \cdot f_{long} \cdot t) \cdot \psi_{long}$	$p_{long}(t) = \frac{35 \cdot n_{eff}}{A} \cos(2\Pi \cdot f_{long} \cdot t) \cdot \psi_{long}$
Lateral	$p_{lat}(t) = \frac{35 \cdot n_{eff}}{A} \cos(2\Pi \cdot f_{lat} \cdot t) \cdot \psi_{lat}$	$p_{lat}(t) = \frac{7 \cdot n_{eff}}{A} \cos(2\Pi \cdot f_{lat} \cdot t) \cdot \psi_{lat}$

In this table, p_{vert}, p_{long} *and* p_{lat} are the loads per unit area in the vertical, longitudinal and lateral directions, n_{eff} is the effective number of pedestrians calculated as shown in Table 2.14, f_{vert}, f_{long} *and* f_{lat} are the frequencies in the vertical, longitudinal and lateral directions, t is the time in seconds and ψ_{vert}, ψ_{long} *and* ψ_{lat} are the second minus factors according to the natural frequency of the mode. (Sétra, 2006)

Table 2.14.: *Determination of the Effective Number of Pedestrians. (Sétra, 2006)*

Load Case	Bridge Class	Density of Crowd	Effective Number of Pedestrians
Case 1	Class II	0.8	$n_{eff} = 10.8\sqrt{(\xi \cdot n)}$
Case 1	Class III	0.5	$n_{eff} = 10.8\sqrt{(\xi \cdot n)}$
Case 2	Class I	1.0	$n_{eff} = 1.85\sqrt{(n)}$
Case 3	Class I	1.0	$n_{eff} = 1.85\sqrt{(n)}$
Case 3	Class II	0.8	$n_{eff} = 10.8\sqrt{(\xi \cdot n)}$

ξ is the critical damping ratio and n is the number of pedestrians derived from the crowd density and footbridge area. (Sétra, 2006)

2.5.2.6. Modify the Footbridge

The next step is to modify the footbridge if the dynamic calculations show that the bridge does not meet the required accelerations. This can be done by:

- Modifying the natural frequencies by increasing the stiffness of the footbridge.
- Reducing the accelerations by increasing the mass of the bridge deck or by using products that increase the damping.
- Installing dampers.
  (Sétra, 2006)

2.5.2.7. Perform Structural Checks

The final step is to perform structural checks under the applied dynamic loads. These include checking displacements and the strength of the footbridge (Sétra, 2006).

Even though the guide mentions the potential effects of running on a footbridge, these effects are not specifically dealt with. However, Appendix 2 in the guide does give a model of pedestrian loads, including running loads. This model is discussed in Section 2.6.

2.5.3. The Old British Standard

The old British Standard for steel, concrete and composite bridges, BS 5400, is based on the old walking model proposed by Blanchard *et al.* (1977) in which the first mode of the

vibration of a footbridge is assumed to be synchronised with a sinusoidal force. Later studies have shown that this model does not appropriately represent the forces produced when single or multiple pedestrians cross a bridge (Racic *et al.*, 2009).

This standard is no longer the applicable design standard in Britain. As of the 31 March 2010 (The Concrete Centre, 2004) it has been replaced by the Eurocode together with the UK Annex, which is described in Section 2.5.4. However, since TMH7 was based on the original BS 5400 this section gives a brief overview of BS 5400.

The standard consists of eleven parts of which Part 2 deals with the specification of loads for bridges and Annex B deals with the vibration serviceability requirements for footbridges and cycle track bridges. (Standards Policy and Strategy Committee, 2006)

As with TMH7, the first step is to determine the fundamental natural frequency, f_o, of the unloaded bridge. If the natural frequency is greater than $5\,Hz$ in the vertical direction and $1.5\,Hz$ in the horizontal direction then no further checks are required. However, if the fundamental natural frequency in the vertical direction is less than or equal to $5\,Hz$ then it is necessary to limit the vertical acceleration of any part of the superstructure to $0.5\sqrt{f_o}\ m/s^2$. Furthermore, if the fundamental natural frequency in the horizontal direction is less than or equal to $1.5\,Hz$ then the code states that "special consideration shall be given to the possibility of excitation by pedestrians of lateral movements of unacceptable magnitude"(Standards Policy and Strategy Committee, 2006). No limit is given for the maximum horizontal acceleration of the superstructure although the code states that the method for deriving this acceleration would need to be determined with the relevant authority.

BS 5400 gives the same two methods for determining the maximum vertical acceleration of the superstructure as TMH7.

2.5.4. Eurocode together with the UK Annex

The Eurocode is the new design code for civil engineers in Europe. It consists of ten codes each of which consists of a number of parts. These codes are shown below. Part 2 in Eurocodes 1, 2, 3, 4, 5 and 8 are for bridges. (The Institution of Structural Engineers, 2007)

- EN 1990 - Eurocode 0: Basis of structural design
- EN 1991 - Eurocode 1: Actions on structures
- EN 1992 - Eurocode 2: Design of concrete structures
- EN 1993 - Eurocode 3: Design of steel structures

- EN 1994 - Eurocode 4: Design of composite steel and concrete structures
- EN 1995 - Eurocode 5: Design of timber structures
- EN 1996 - Eurocode 6: Design of masonry structures
- EN 1997 - Eurocode 7: Geotechnical design
- EN 1998 - Eurocode 8: Design of structures for earthquake resistance
- EN 1999 - Eurocode 9: Design of aluminium structures

Of these, Eurocodes 0 and 1 apply to all footbridges covered in Eurocodes 2, 3, and 5. The relevant parts in these two codes are discussed at in detail below.

In Eurocode 0 maximum acceleration is used to define the pedestrian comfort criteria as shown in Table 2.15.

Table 2.15.: *Maximum Allowable Acceleration for Pedestrian Bridges. (Hauksson, 2005)*

Direction of Vibrations	Maximum Acceleration
Vertical Vibrations	$0.7\,m/s^2$
Horizontal Vibrations, Normal Use	$0.2\,m/s^2$
Horizontal Vibrations, Crowd Conditions	$0.4\,m/s^2$

In Part 2 of Eurocode 1, the imposed loads for the design of road, railway and footbridges, including the dynamic effects are defined (The Institution of Structural Engineers, 2007; Hauksson, 2005). Section 5, in particular, deals with the actions on footways, cycle tracks and footbridges and Chapter 5.7 deals with dynamic models of pedestrian loads. It states that the natural frequencies resulting in the vertical, horizontal and torsional vibrations of the main structure of the bridge deck should be determined from an appropriate structural model which takes the dynamic characteristics of the structure into account. Furthermore, it states that pedestrian induced forces with a frequency close to that of the natural frequency of the structure could lead to resonance and therefore need to be taken into account when verifying the limit state in terms of vibrations. Finally, it states that appropriate comfort criteria and dynamic load models for the pedestrian loads need to defined (BSI, 2010). It should be noted that the method for modelling the dynamic loads of a pedestrian is left to the designer. (Hauksson, 2005), although the Eurocode does go on to give the various frequency ranges which may be used to account for a pedestrian walking, or a group of people jogging across a bridge. These frequency ranges are summarised in Table 2.16.

Table 2.16.: *Frequency Ranges from Eurocode 1.*

Activity	Direction	Frequency Range
Walking	Vertical	$1-3\,Hz$
Walking	Horizontal	$0.5-1.5\,Hz$
Group of joggers		$3\,Hz$

Part 2 of Eurocodes 2, 3 and 4 do not give any additional information on designing footbridges for vibration serviceability, however Part 2 of Eurocode 5 contains information for the design of timber bridges under pedestrian loads. It requires the calculation of the vertical and horizontal acceleration responses of a timber bridge due to small groups and streams of pedestrians. It uses the same maximum accelerations for pedestrian comfort as given in Eurocode 0, namely $0.7\,m/s^2$ vertically and $0.2\,m/s^2$ horizontally. Annex B gives a simplified method for determining the vertical and horizontal vibrations caused by pedestrians when crossing a timber bridge which has simply supported beams or a truss system. In this method the accelerations caused by a single pedestrian walking across the bridge can be determined in the vertical and horizontal directions by Equation 2.24 and Equation 2.25 respectively.

$$a_{vert,1} = \begin{cases} \frac{200}{M\zeta} & \text{for } f_{vert} \leq 2.5Hz \\ \frac{100}{M\zeta} & \text{for } 2.5Hz < f_{vert} \leq 5.0Hz \end{cases} \tag{2.24}$$

$$a_{hor,1} = \frac{50}{M\zeta} \quad \text{for } 0.5Hz < f_{hor} \leq 2.5Hz \tag{2.25}$$

Where M is the total mass of the bridge in kg, ζ is the damping ratio, f_{vert} and f_{hor} are the fundamental natural frequencies for the vertical and horizontal deformations of the bridge respectively. (BSI, 2010; Hauksson, 2005)

If there are several people crossing the bridge then the vertical and horizontal accelerations can be determined by Equation 2.27 and Equation 2.27 respectively.

$$a_{vert} = 0.23\,a_{vert,1}\,n\,k_{vert} \tag{2.26}$$

$$a_{hor} = 0.18\,a_{hor,1}\,n\,k_{hor} \tag{2.27}$$

n is the number of pedestrians and should be taken as 13 for a distinct group of pedestrians or $0.6A$ for a continuous stream of pedestrians, A is the plan area of the bridge deck in m^2,

and k_{vert} and k_{hor} are coefficients which are determined from the graphs in Figure 2.23 and Figure 2.24 respectively. (BSI, 2010; Hauksson, 2005; Butz, 2008)

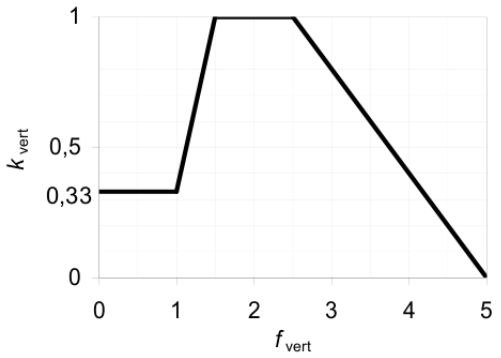

Figure 2.23.: *Vertical coefficient of the fundamental natural frequency. (BSI, 2010)*

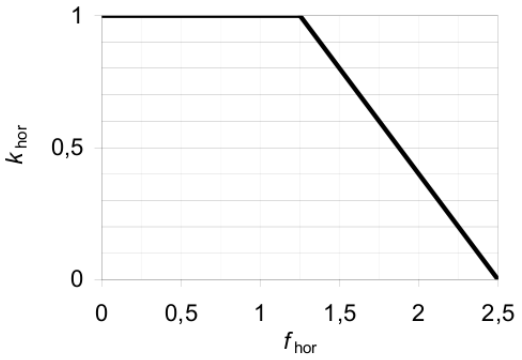

Figure 2.24.: *Horizontal coefficient of the fundamental natural frequency. (BSI, 2010)*

The factor 0.23 in Equation 2.26 accounts for the synchronisation probability of the group of pedestrians crossing the bridge, and the factor 0.18 in Equation 2.27 accounts for the horizontal lock-in probability for the group of pedestrians crossing the bridge. The coefficients k_{vert} and k_{hor} account for the probability that the step frequencies coincide with the natural frequencies. (Butz, 2008)

Finally, for a single person running across the bridge the vertical acceleration can be determined as shown in Equation 2.28. (BSI, 2010; Hauksson, 2005)

$$a_{vert} = \frac{600}{M\zeta} \quad \text{for } 2.5Hz < f_{vert} \leq 3.5Hz \tag{2.28}$$

According to Butz (2008) these formulae given in the Eurocode are based on the following assumptions:

- The weight of the pedestrian is $700\,N$
- The Fourier coefficients for walking are $\alpha_{vert,1} = 0.4$, $\alpha_{vert,2} = 0.2$, $\alpha_{lat,1} = \alpha_{lat,2} = 0.1$ and for running $\alpha_{vert,1} = 1.2$.
- A reduction factor of 0.7 takes into account the reduction due to the pedestrian's movement in space.

For more complex bridge structures there is no method or guidelines given for determining the acceleration (Hauksson, 2005). Similar methods are not available for concrete, steel or composite bridges.

2.5.5. ISO Guide

The ISO 101317 guideline was published by the International Organisation for Standardization and is the guideline for the vibration serviceability design of buildings and pedestrian walkways. This guideline uses the vibration source, path and receiver approach to deal with the vibration serviceability of any structure. This approach is described briefly in Section 2.2.1. (Hauksson, 2005; ISO, 2004)

Section 7.7.7 of ISO 10137 states that "pedestrian bridges shall be designed so that the vibration amplitude from the applicable vibration sources do not alarm potential users" (ISO, 2004). Annex C then goes on to give some proposed scenarios to consider when looking at the vibration serviceability of a pedestrian bridge. These are:

- One person walking across the bridge.
- An average pedestrian flow for groups of between 8 and 15 people.
- Streams of pedestrians for groups of significantly more than 15 people.
- The occasional festive or choreographic event if relevant. (ISO, 2004; Hauksson, 2005; Butz, 2008)

In addition, Annex C gives some examples of the vibration criteria for pedestrian bridges. It suggests the use of base curves for vibrations in both the vertical and horizontal directions and multiplying them by a factor of 60 in general and 30 in the case where there are one or more stationary people on the bridge. These base curves are shown in Figures 2.25 and 2.26. (ISO, 2004; Hauksson, 2005)

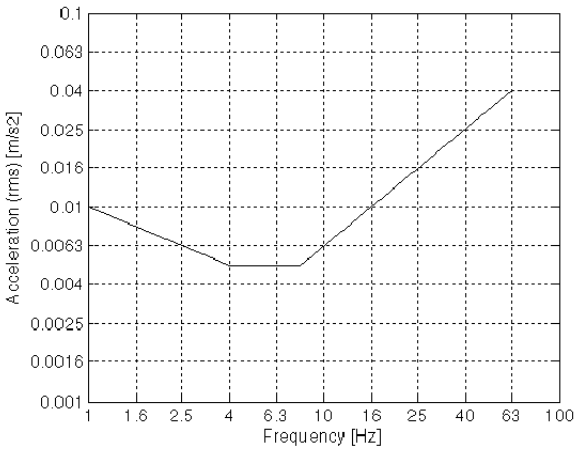

Figure 2.25.: *Vertical vibration base curve for acceleration. (Hauksson, 2005)*

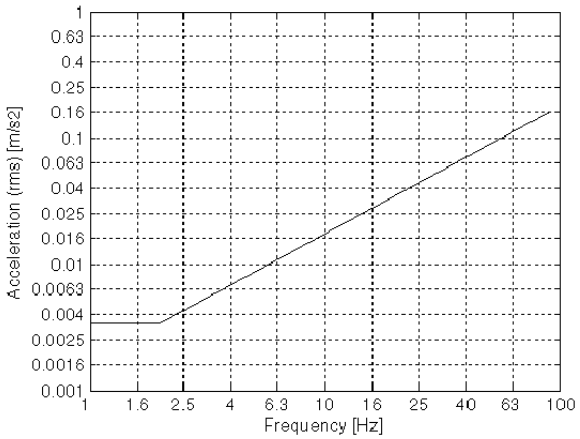

Figure 2.26.: *Horizontal vibration base curve for acceleration. (Hauksson, 2005)*

ISO 10137 describes the dynamic actions of one or more people by use of force-time histories which vary with time and position as people move across the structure. Annex A expresses the dynamic force produced by a person crossing a bridge, $F(t)$, in the frequency domain as a Fourier series in the vertical and horizontal directions as shown in Equation 2.29 and 2.30 respectively. (ISO, 2004; Hauksson, 2005)

$$F_v(t) = Q\left(1 + \sum_{n=1}^{k} \alpha_{n,v} \sin(2\Pi n f t + \phi_{n,v})\right) \tag{2.29}$$

$$F_h(t) = Q\left(1 + \sum_{n=1}^{k} \alpha_{n,h} \sin(2\Pi n f t + \phi_{n,h})\right) \tag{2.30}$$

where $\alpha_{n,v}$ and $\alpha_{n,h}$ are the numerical coefficients corresponding to the n^{th} harmonic in the vertical and horizontal directions respectively, Q is the static load of the participating person, f is the frequency component of the repetitive loading, $\phi_{n,v}$ and $\phi_{n,h}$ are the phase angles of the n^{th} harmonic in the vertical and horizontal directions respectively, n is the integer designating harmonics of the fundamental and k is the number of harmonics that characterise the forcing function in the frequency range of interest. Examples of the numerical coefficient α_n given in Annex A of ISO 101317 are summarised in Table 2.17. (ISO, 2004; Hauksson, 2005)

Activity	Forcing Frequency Range	Fourier Coefficient	
		Vertical	Horizontal
Walking	1.2-2.4	$\alpha_1 = 0.37(f_s - 1.0)$	$\alpha_1 = 0.1$
	2.4-4.8	$\alpha_2 = 0.1$	
	3.6-7.2	$\alpha_3 = 0.06$	
	4.8-9.6	$\alpha_4 = 0.06$	
	6.0-12.0	$\alpha_5 = 0.06$	
Running	2.0-4.0	$\alpha_1 = 1.4$	$\alpha_1 = 0.2$
	4.0-8.0	$\alpha_2 = 0.4$	
	6.0-12.0	$\alpha_3 = 0.1$	

Table 2.17.: *Fourier Coefficients According to ISO 101317 (ISO, 2004; Butz, 2008)*

In order to take into account the dynamic actions of groups of pedestrians, Annex A of ISO 10137 states that this "depends primarily on the weight of the participants, the maximum density of persons per unit floor area and on the degree of coordination of the participants" (ISO, 2004) and that the coordination can be taken into account by applying a coordination factor, $C(N)$, to the forcing function as shown in Equation 2.31. (ISO, 2004; Hauksson, 2005)

$$F(t)_N = F(t) \cdot C(N) \tag{2.31}$$

In the case of pedestrian bridges the movements of a group of people are most likely to be uncoordinated and the coordination factor can be represented as shown in Equation 2.32, where N is the number of participants. (ISO, 2004; Hauksson, 2005)

$$C(N) = \frac{\sqrt{N}}{N} \tag{2.32}$$

2.5.6. Other Codes

There are a number of other design codes which are worth mentioning. The details of these are briefly given in this section.

2.5.6.1. The Hong Kong Structures Design Manual for Highways and Railways

This design manual limits the vertical acceleration response of a footbridge to a single pedestrian as in BS 5400 and limits the lateral acceleration to $0.15\,m/s^2$. In addition, the design manual requires that the acceleration response as a result of a stream of pedestrians is checked by assuming a continuous load moving at a velocity of $3\,m/s$ over a simple beam. However, details on how to carry out the load simulation are not given. (Živanović *et al.*, 2005)

2.5.6.2. Swiss Standard SIA 160

This standard takes a slightly different approach in which the natural frequencies of the bridge are checked to ensure that they are not in the ranges of 1.6 to $2.4\,Hz$ for the first walking harmonic, 3.5 to $4.5\,Hz$ for the second walking harmonic and 2.4 to $3.5\,Hz$ if runners or joggers are likely to cross the bridge. If the natural frequency is within one of these ranges the vibration response of the structure needs to be checked. (Živanović *et al.*, 2005)

2.5.6.3. The American Guide Specification

This guide is similar to the Swiss Standard in that it also suggests that certain vertical fundamental frequencies for footbridges should be avoided. In the case of the American Guide Specification these frequencies are anything below $3\,Hz$ in general, but if the bridge is likely to have pedestrians running or jumping on it then any frequency below $5\,Hz$ would need to be avoided. No lower limits are given for the fundamental frequencies, which the guide recommends avoiding. The guide goes further to say that if these frequencies are not met, then in order to satisfy the serviceability requirements of the footbridge the minimum natural frequency given by Allen and Murray and shown in Equation 2.33 should apply. (Živanović *et al.*, 2005)

$$f_0 = 2.86 \ln \frac{K}{\beta W} \tag{2.33}$$

where K is a constant equal to $8\,kN$, the recommended damping ratio, β, is equal to 0.01 and W is the total weight of the bridge. The guide also suggests the installation of vibration absorbers and dampers as a possible means of improving the dynamic performance of a bridge. (Živanović *et al.*, 2005)

2.5.7. Summary

It can be seen that there are two main approaches in the guidelines for footbridge vibration serviceability design. The first approach requires the calculation of the actual dynamic response of the bridge in order to check whether it is within the acceptable limits for people using the bridge. The second approach recommends that the typical frequencies for human-induced loads are avoided for the natural frequency of a footbridge. (Živanović *et al.*, 2005)

Table 2.18 below compares the serviceability criteria for the five main codes discussed.

Table 2.18.: *Comparison between the various codes of practice for a single pedestrian.*

Code of Practice	Weight of Pedestrian	Vertical Acceleration	Horizontal Acceleration
TMH7	$0.7\,kN$	$a_{max} \leq 0.5\sqrt{n_o}\,m/s^2$	No Requirement
Sétra Guide	$0.7\,kN$	$a_{max} \leq 0.5\,m/s^2$	$a_{max} \leq 0.15\,m/s^2$
British Standard	$0.7\,kN$	$a_{max} \leq 0.5\sqrt{f_o}\,m/s^2$	To be determined with relevant authority. No requirement given.
Eurocode	$0.7\,kN$	$a_{max} \leq 0.7\,m/s^2$	$a_{max} \leq \begin{cases} 0.2\,m/s^2 & \text{generally} \\ 0.4\,m/2^2 & \text{in crowd conditions} \end{cases}$
ISO Guide		60 times base curve, Figure 2.25	60 times base curve, Figure 2.26

Some of the codes recommend avoiding the typical resonant frequency range for the first and second harmonics while others give a design procedure to calculate the response of the bridge to human-induced loading and then check whether it is acceptable. However, none of the codes cover all the aspects of vibrations induced by pedestrians (Živanović *et al.*, 2005). In addition the older codes, such as TMH7, are now outdated and should be revised.

2.6. Running Load Models Found in Literature

Jogging and running are recreational activities which are often done in groups, in which individuals synchronise with each other to keep to the same speed. This results in synchronised load patterns which could cause a significant level of vibration on a footbridge. However, as can be seen only the Sétra Guide gives a load model for running forces. This section looks at the deterministic models that are used for running loads, the section of the Sétra Guide which deals with running forces as well as a few other load models found in literature.

2.6.1. Deterministic Models

As described in Section 2.3, when someone walks or runs across a structure the resultant load induced on the structure consists of a lateral, longitudinal and vertical force. The vertical force is often modelled as the sum of the static and dynamic components of that force as shown in Equation 2.34.

$$F(t) = G\left[1 + \sum_{i=1}^{n} A_i \cdot \sin(2i \cdot \Pi \cdot f_s \cdot t - \varphi_i)\right] \tag{2.34}$$

where f_s is the fundamental walking or running frequency, G is the body weight, A_i and φ_i are the amplitude and the phase angle of the i^{th} harmonic respectively. Tables 2.19 and 2.20 below show the first three dynamic load factors, A_i, the phase angles, φ_i, and the typical pacing frequencies for walking, running and jumping which are often used in conjunction with Equation 2.34. (Živanović *et al.*, 2005; Occhiuzzi *et al.*, 2008)

Table 2.19.: *Coefficients of the Fourier Decomposition. (Occhiuzzi* et al.*, 2008)*

Activity	A_1	φ_1 (rad)	A_2	φ_2 (rad)	A_3	φ_3 (rad)
Walking	0.4	0	0.1	1.57	0.1	1.57
Running	1.6	0	0.7	0	0.2	0
Jumping	1.7	0	1.1	1.73	0.5	1.73

Table 2.20.: *Walking, Running and Jumping Frequencies. (Occhiuzzi* et al.*, 2008)*

Activity	Total Range	Slow	Normal	Fast
Walking	$1.4-2.4\,Hz$	$1.4-1.7\,Hz$	$1.7-2.2\,Hz$	$2.2-2.4\,Hz$
Running	$1.9-3.3\,Hz$	$1.9-2.2\,Hz$	$2.2-2.7\,Hz$	$2.7-3.3\,Hz$
Jumping	$1.3-3.4\,Hz$	$1.3-1.9\,Hz$	$1.9-3.0\,Hz$	$3.0-3.4\,Hz$

This load model is widely adopted for both walking and running forces on footbridges. However, although this load model is acceptable for the modelling of vertical walking loads where the force is continuous it is not acceptable for vertical running loads. This is because Equation 2.34 is continuous and contains negative values, while the actual force applied when a person runs is discontinuous and always positive. (Occhiuzzi *et al.*, 2008)

2.6.2. Sétra Guide

Appendix 2.1 in the Sétra Guide describes modelling a running load. It describes modelling the vertical component of the running load in two different manners: using a semi-sinusoidal approximation and using a Fourier transform. (Sétra, 2006)

The semi-sinusoidal approach approximates the vertical component of the running load as a series of semi-sinusoids as shown in Equation 2.35

$$\begin{array}{cc} F(t) = k_p G_0 \sin\left(\frac{\Pi t}{t_p}\right) & (j-1)T_m \leq t \leq (j-1)T_m + t_p \\ F(t) = 0 & (j-1)T_m + t_p < t \leq jT_m \end{array} \tag{2.35}$$

where k_p is the impact factor which is equal to the maximum load divided by the weight of the pedestrian G_0, j is the step number, t_p is the period of contact and T_m is the period which is equal to the reciprocal of the running frequency, which is generally between 2 and 3.5 Hz. The model given in the Sétra Guide assumes that the period of contact t_p is equal to the half-period T_m. This means that Equation 2.35 can be rewritten as Equation 2.36. The impact factor k_p can be determined using Figure 2.27 where T_m is represented by T_p.

$$\begin{array}{cc} F(t) = k_p G_0 \sin(2\Pi f_m t) & (j-1)T_m \leq t \leq (j-\frac{1}{2})T_m \\ F(t) = 0 & (j-\frac{1}{2})T_m < t \leq jT_m \end{array} \tag{2.36}$$

The assumptions made in determining the period of contact and hence the impact factor mean that the semi-sinusoidal approximation for running loads is a conservative approach. (Sétra,

2006)

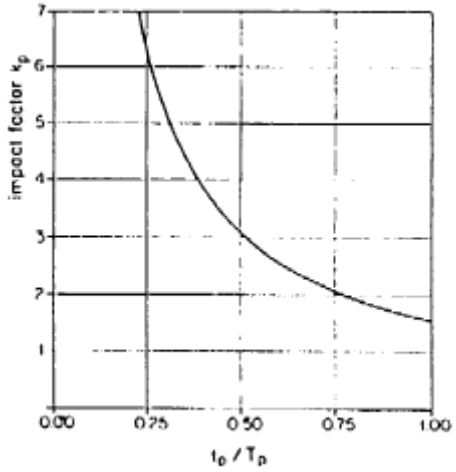

Figure 2.27.: *Impact factor dependent on the relative period of contact. (Sétra, 2006)*

The second method given in the Sétra Guide uses a Fourier transform to approximate the vertical part of the running load. Due to the discontinuous contact between the person running and the surface they are running across only the positive part of the Fourier transform is used as shown in Equation 2.37. (Sétra, 2006)

$$\begin{array}{cc} F(t) = G_0 + \sum_{i=1}^{n} G_i \sin(2\Pi i f_m t) & (j-1)T_m \leq t \leq (j-\frac{1}{2})T_m \\ F(t) = 0 & (j-\frac{1}{2})T_m < t \leq jT_m \end{array} \tag{2.37}$$

This equation assumes that any phase shifts are negligible and that if the contact period is half the period, the amplitudes of the first three harmonics are $G_1 = 1.6G_0$, $G_2 = 0.7G_0$ and $G_3 \approx 0.2G_0$ as shown in Figure 2.28. (Sétra, 2006)

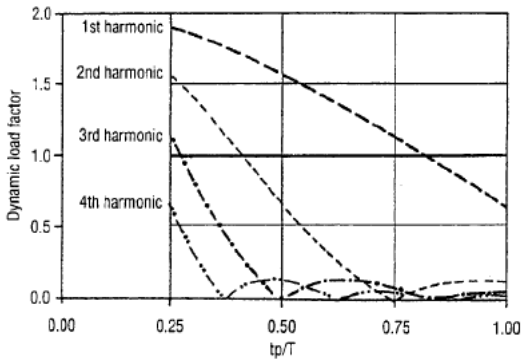

Figure 2.28.: *Amplitude of the various harmonics. (Sétra, 2006)*

The main advantage of the Fourier transform method is that it is not necessary to determine the impact factor. However, both methods give a similar approximation for the vertical component of the running load. For example, if a pedestrian weighing $700\,N$ runs at a frequency of $3\,Hz$ then the semi-sinusoidal approximation and the first three harmonics of the Fourier transform for the running load are as shown in Figure 2.29 below. (Sétra, 2006)

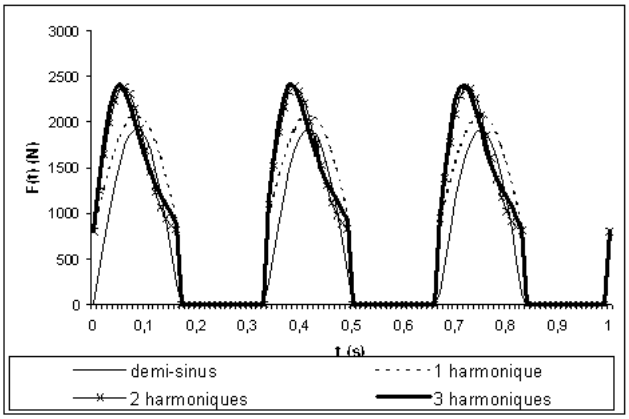

Figure 2.29.: *Vertical Component of Running Loads. (Sétra, 2006)*

The Sétra Guide then briefly discusses the possible horizontal components of the running load. It states that it is likely that the transverse component would have a lower amplitude than the vertical component, whereas the longitudinal component would have a higher amplitude. Furthermore, the frequency of the transverse component would be half that of the vertical component as with walking. However, no actual load model is given for the horizontal components.

2.6.3. Analytical Load Model by Occhiuzzi and Spizzuocco *et al.*

Occhiuzzi *et al.* (2008) proposed a loading model for running pedestrians which takes into account the discontinuity of the force applied for running by combining two concepts.

The first concept uses time histories involving a large contact force which is applied for a limited time known as the contact phase followed by a zero force which is applied during the stance phase. This type of time history can be described analytically by use of a Fourier series where the coefficients depend on the ratio of the contact time to the fundamental period of the load which is dependent on the fundamental frequency of the activity. The second concept involves the use of energy concepts to model walking and running activities. This is based on the continuous change between kinetic and potential energy which takes place when walking

or running and requires finding the path of the centre of mass of the person which results in the lowest dissipation of energy. (Occhiuzzi *et al.*, 2008)

By analysing the movement of a person running for a period of one step and using the two concepts above, Occhiuzzi *et al.* (2008) developed the following analytical model for running. Firstly, each step period, T, consists of a contact period, $\triangle t_c$, and a period of no contact, $\triangle t_{nc}$. For normal running the contact period and the period of no contact can both be assumed to be equal to half the step period as shown in Equation 2.38. (Occhiuzzi *et al.*, 2008)

$$\triangle t_c = \triangle t_{nc} = \frac{T}{2} \tag{2.38}$$

However, in the case where this is not true, and the contact period can be expressed by Equation 2.39, with $k < 1$, then the period of no contact is expressed as shown in Equation 2.40. (Occhiuzzi *et al.*, 2008)

$$\triangle t_c = k \cdot T \tag{2.39}$$

$$\triangle t_{nc} = (1-k) \cdot T \tag{2.40}$$

When a person runs across a footbridge, loading occurs during the contact period. This load consists of an increasing force in the initial stance phase and a decreasing force in the final toe-off phase, as illustrated in Figure 2.30. (Occhiuzzi *et al.*, 2008)

Figure 2.30.: *Interaction forces between a runner and a footbridge. (Occhiuzzi* et al.*, 2008)*

By using the principle of conservation of energy and the impulse theorem a mathematical model for the vertical component of the running force can be derived as shown in Equation 2.40a and 2.40b. (Occhiuzzi *et al.*, 2008)

$$\frac{1}{2}m \cdot v_n^2 = m \cdot g \cdot \triangle h \tag{2.40a}$$

$$\int_0^{\triangle t_c} [F(t) - mg]\, dt = 2 \cdot m \cdot v_n \tag{2.40b}$$

where m is the mass of the runner, g is the acceleration due to gravity, h is the height of the centre of mass, v_n is its vertical velocity at the final toe-off phase, and $h + \triangle h$ is the maximum height reached by the centre of mass during the period of no contact. Rearranging Equation 2.40a for vertical velocity gives Equation 2.41. (Occhiuzzi *et al.*, 2008)

$$v_n = \sqrt{2 \cdot g \cdot \triangle h} \tag{2.41}$$

Since the acceleration during the period of no contact is uniform, Equation 2.42 can be obtained. (Occhiuzzi *et al.*, 2008)

$$\triangle h = \frac{1}{2} g \left(\frac{\triangle t_{nc}}{2} \right)^2 \tag{2.42}$$

Substituting Equation 2.42 into Equation 2.41 gives Equation 2.43:

$$v_n = g \frac{\triangle t_{nc}}{2} \tag{2.43}$$

Thus, by assuming that the vertical component of the running force during the contact period can be represented by half a *sine* wave, Equation 2.44 is derived. (Occhiuzzi *et al.*, 2008)

$$\begin{array}{cc} F(t) = A \cdot m \cdot g \cdot \sin\left(\frac{\pi f}{k} \cdot t\right) & i \cdot T < t \leq (i+k) \cdot T \\ F(t) = 0 & (i+k) \cdot T < t \leq (i+1) \cdot T \end{array} \tag{2.44}$$

Where i is the number of the step and A is an amplification factor which determines the force amplitude as shown in Equation 2.45. A is also the dynamic load factor used in Equation 2.34. (Occhiuzzi *et al.*, 2008)

$$F_0 = A \cdot m \cdot g \tag{2.45}$$

The amplification factor can be derived from the impulse theorem given in Equation 2.40b as shown in Equation 2.46. Therefore, the amplification factor is π when $k = \frac{1}{2}$ for the case of

normal running given in Equation 2.38. This means that the amplification factor is dependent on the ratio of contact period to period of no contact. (Occhiuzzi *et al.*, 2008)

$$A = \frac{\pi}{2k} \tag{2.46}$$

This load model has been validated by comparing the results of numerical calculations with full-scale measurements taken on a cable-stayed footbridge. The results showed that the predicted values agreed reasonably well with the measured response. (Occhiuzzi *et al.*, 2008)

2.6.4. Summary

All of the running load models discussed look at the vertical component of the load only. Although the Sétra Guide does mention the horizontal components of the load no guidance is given on how to model them. Furthermore, the deterministic model is not appropriate for modelling the vertical running load owing to the fact that it does not take the discontinuity of the force into account. However, this can be rectified if this model is rewritten in a similar manner to the other models as shown in Equation 2.47.

$$\begin{array}{cc} F(t) = G\left[1 + \sum\limits_{i=1} A_i \cdot \sin\left(2i \cdot \Pi \cdot f_s \cdot t - \varphi_i\right)\right] & (j-1)T_m \leq t \leq (j-1)T_m + t_p \\ F(t) = 0 & (j-1)T_m + t_p < t \leq jT_m \end{array} \tag{2.47}$$

Since the phase angles for running in this model are zero for each phase (as shown in Table 2.19) and the values for A_1, A_2 and A_3 are the same as those used to determine G_1, G_2 and G_3, the above model will yield the same result as the Fourier Transform Model.

Figure 2.31 gives a comparison of the four running load models discussed in this section, assuming a pedestrian weighing $700\,N$ runs across a bridge at a frequency of $3\,Hz$.

As can be seen the four models give relatively similar results although they have slightly different force amplitudes. The Deterministic and Fourier Transform load model shown in Figure 2.31 give exactly the same results. For the rest of this thesis only the Fourier Transform model is used since no adjustments are required to this model.

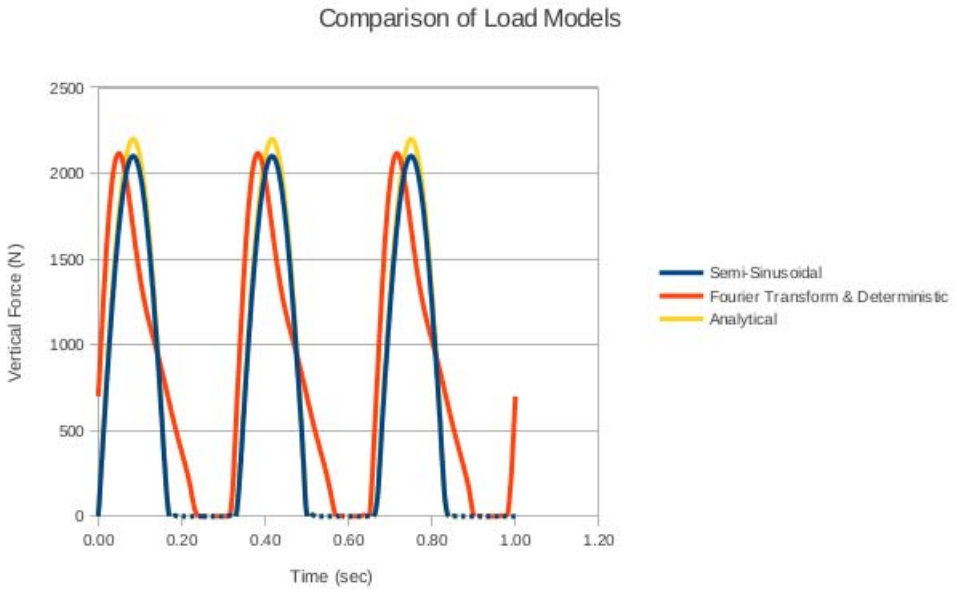

Figure 2.31.: *Comparison of Running Load Models.*

2.7. Summary and Conclusions

The problem of vibration serviceability in footbridges is not a new issue. There is a modern trend of designing slender, lightweight footbridges with longer spans which has lead to a number of these modern bridges having a natural frequency within the normal range of frequencies for human activities such as walking, running and jogging. This has recently resulted in several vibration serviceability failures and highlights the need to accurately model these human-induced loads when designing new bridges.

Human-induced forces are influenced by a number of factors ranging from a person's age, weight and gender to the type of footwear a person is wearing and their mood. In addition, the number of people crossing a bridge and whether or not any synchronisation occurs plays an important role in modelling these forces.

In general when a person walks, runs or jogs across a bridge, forces are applied to the surface of the bridge deck in three directions: vertical, lateral and longitudinal. The typical frequencies of these forces differ as shown in Table 2.21.

Table 2.21.: *Typical Frequency Ranges for Walking and Running. (Occhiuzzi and Spizzuoco, 2008)*

Force	Frequency Range		
	Vertical	Lateral	Longitudinal
Walking	$1.4-2.4\,Hz$	$0.7-1.2\,Hz$	$1.4-2.4\,Hz$
Running	$1.9-3.5\,Hz$	$0.95-1.75\,Hz$	$1.9-3.5\,Hz$

There are two main approaches to the modelling of human-induced forces: time-domain force models, either deterministic force models or probabilistic force models, and frequency domain force models. Time-domain force models make up the largest proportion of the models available for human-induced forces. Deterministic force models make use of a general force model for an activity and do not take into account any variations in terms of how individuals perform. Conversely, probabilistic force models take into account some of the factors that influence the way individuals perform an activity by using probability density functions. The weakness of both these time-domain models is that they rely on dynamic load factors which cannot be accurately determined. Frequency response models treat the human-induced forces as transient signals by determining the auto-spectral density of the forces. The majority of the design procedures for footbridges are based on time-domain models and only consider the vertical component of the walking force for a single pedestrian. They are often limited to girder footbridges with only one or two spans.

The majority of the current codes of practice in use are based on deterministic force models. Some of the older codes that are still in use only consider a single pedestrian walking across a bridge. There are two main approaches which are adopted by codes of practice for determining the vibration serviceability of a footbridge. The first approach checks whether the actual dynamic response of a footbridge falls within acceptable limits. The second approach recommends that the typical frequencies for human-induced forces should be avoided for the natural frequency of the bridge.

The codes that are based on the second approach often also give a limit for the dynamic response of the footbridge should the natural frequency of the bridge fall within the typical frequencies for human-induced forces. The limits for the dynamic responses from a selection of codes are given in Table 2.22.

Table 2.22.: *Acceleration response limits stated in various codes of practice.*

Code of Practice	Vertical Acceleration	Horizontal Acceleration
TMH7	$a_{max} \leq 0.5\sqrt{n_o}\, m/s^2$	No requirement given
Sétra Guide	$a_{max} \leq 0.5\, m/s^2$	$a_{max} \leq 0.15\, m/s^2$
British Standard	$a_{max} \leq 0.5\sqrt{f_o}\, m/s^2$	No requirement given.
Eurocode	$a_{max} \leq 0.7\, m/s^2$	$a_{max} \leq 0.2\, m/s^2$
ISO Guide	60 times base curve, Figure 2.25	60 times base curve, Figure 2.26

In addition, some of the codes of practice give a simplified method for determining the maximum acceleration that could occur on a footbridge due to pedestrian loading. These methods, and other simple methods which can be found in literature, have been summarised in Table 2.23. The majority of these simplified methods are applicable only for single span simply supported footbridges and they only look at the vertical acceleration due to a single pedestrian walking across the footbridge. For any more complex situation a complete dynamic analysis would need to be done.

Table 2.23.: *Methods for Determining the Maximum Acceleration of a Footbridge.*

Name	Maximum Acceleration
TMH7	$a = \omega_1^2 y_s K \psi$
Eurocode	$a_{vert,walk} = \begin{cases} 0.23\left(\frac{200}{M\zeta}\right) nk_{vert} & \text{for } f_{vert} \leq 2.5Hz \\ 0.23\left(\frac{100}{M\zeta}\right) nk_{vert} & \text{for } 2.5Hz < f_{vert} \leq 5.0Hz \end{cases}$ $a_{hor,walk} = 0.18\left(\frac{50}{M\zeta}\right) nk_{hor}$ for $0.5Hz < f_{hor} \leq 2.5Hz$ $a_{vert,run} = \frac{600}{M\zeta}$ for $2.5Hz < f_{vert} \leq 3.5Hz$
Rainer *et al.* (1988)	$a = \frac{\alpha P}{m}\Phi$
Allen and Murray (1993)	$\frac{a}{g} = \frac{R\alpha_i P}{\beta W}\cos(2\pi i f t)$
Grundmann *et al.* (1993)	$a_{vert,1rz} = 0.6\frac{0.4G}{M}\frac{\pi}{\delta}(1-e^{-n\delta})$ $a_{lat,1rz} = 0.6\frac{0.1G}{M}\frac{\pi}{\delta}(1-e^{-n\delta})$
Young (2001)	$a_n = \mu_i\mu_j\left(\frac{f}{f_n}\right)^2\frac{P}{M}DMF$
Pimentel and Frenandes (2002)	$a_{max} = \omega_0^2 y_s \alpha_i \Omega_d k_a$

None of the codes of practice reviewed cover both vertical and horizontal vibrations for all combinations of individuals, groups or crowds of people walking, jogging or running across

a bridge. In fact there are very few jogging or running load models to be found in literature. The deterministic force model is sometimes used for running loads, however this model is not very accurate because it produces a continuous force whereas the actual force generated by a person running is discontinuous.

The Sétra Guide gives two options for modelling the vertical component of a person running, both of which take into account the discontinuous nature of the force. The first makes use of a semi-sinusoidal approximation and the second a Fourier transform. Another load model for running forces was developed by Occhiuzzi *et al.* (2008) and is called an analytical load model. In this model, the concept of conservation of energy in conjunction with a Fourier series is used to describe analytically the period of time when a person's feet are in contact with the ground. All three of these load models approximate the vertical component of the running force fairly well but none of them model the horizontal forces.

This research and the recent serviceability failures of footbridges show that current codes of practice are out of date and do not cover all aspect of human-induced vibrations on footbridges. Many of them, in particular the older ones, do not even consider the horizontal component of the walking force, nor do they give much information on crowd loading and synchronisation. Only the Sétra Guide gives any indication of how to model running loads and it only looks at the vertical component of these loads. Since the failure of London's Millennium Bridge a lot of research has been done on crowd loading and the horizontal components of the walking force. This research has now been incorporated into some of the new codes, but a lot of work still needs to done on modelling running loads, in particular how to model the horizontal components of these loads and the effects of a group of people running together over a bridge.

3. Development of a Jogging Load Model

The Literature Review describes and compares four jogging load models, namely the deterministic model, the semi-sinusoidal model (Equation 3.1), the Fourier transform model (Equation 3.2) and the analytical method (Equation 3.3). The original deterministic model is inaccurate because it does not account for the discontinuous nature of the running force and it is therefore excluded. A comparison of the remaining three models showed that they produce similar results in terms of the half sine curve shape of the jogging force, the discontinuous nature of the force and the frequency of the force, however they have different force amplitudes. The three models have been rewritten in Equations 3.1, 3.2 and 3.3 to use the same symbols.

$$\begin{array}{cc} F_{vert}(t) = k_p \cdot G_0 \cdot \sin\left(\frac{\pi t}{t_p}\right) & (j-1)T_m \leq t \leq (j-1)T_m + t_p \\ F_{vert}(t) = 0 & (j-1)T_m + t_p < t \leq jT_m \end{array} \tag{3.1}$$

$$\begin{array}{cc} F_{vert}(t) = G_0 + \sum_{i=1}^{N} G_0 \cdot \alpha_{i,vert} \cdot \sin(2 \cdot \pi \cdot i \cdot f_m \cdot t) & (j-1)T_m \leq t \leq (j-1)T_m + t_p \\ F_{vert}(t) = 0 & (j-1)T_m + t_p < t \leq jT_m \end{array} \tag{3.2}$$

$$\begin{array}{cc} F_{vert}(t) = \left(\frac{\pi}{2 \cdot t_p}\right) \cdot G_0 \cdot \sin\left(\frac{\pi}{t_p} \cdot t\right) & (j-1)T_m \leq t \leq (j-1)T_m + t_p \\ F_{vert}(t) = 0 & (j-1)T_m + t_p < t \leq jT_m \end{array} \tag{3.3}$$

$F_{vert}(t)$ is the vertical jogging force, G_0 is the weight of the runner, k_p is the impact factor, t_p is the period of contact, t is the time, f_m is the running frequency, T_m is the running step period and $\alpha_{i,vert}$ are the vertical dynamic load factors. As can be seen the only difference between the semi-sinusoidal and analytical jogging models is the first part of the equation which affects the amplitude of the jogging force.

One additional method for determining the jogging forces described in the literature review was proposed by Keller *et al.* (1996). This method can only be used to predict the maximum vertical force and does not take into account the varying nature of the force. It is shown in Equation 3.4, where v is the speed at which a person is jogging.

$$\begin{aligned} F_{vert} &= 0.614v + 0.208 \qquad (for\, 1.5 < v < 3.5) \\ &= 2.5 \times body\,weight \qquad (for\, v > 3.5) \end{aligned} \tag{3.4}$$

In this chapter the jogging load models are compared with the loads obtained from a person running on an instrumented treadmill in order to illustrate how accurately these models predict the loading of a running person. From this it is possible to develop a running load model which can be used to predict the response of a footbridge to jogging forces.

3.1. Measured Jogging Forces

The Vibration Engineering Section in the Department of Civil and Structural Engineering at the University of Sheffield has done a lot of research into vibration serviceability, structural health monitoring and active vibration control. As part of this research they have collected data from people running on an instrumented treadmill. Their data is used in this section.

3.1.1. How the Jogging Loads are Measured

The University of Sheffield makes use of an instrumented force measuring treadmill (IFMT) to collect ground reaction forces (GRFs) of people walking and running. The dynamometric treadmill ADAL3D-F, shown in Figure 3.1, is designed to continuously measure the GRF in three directions while walking or running slowly at speeds ranging between 0.1 and 10 km/h (Racic *et al.*, 2007). This treadmill is installed in the Light Structures Laboratory (LSL) of the University of Sheffield (Racic *et al.*, 2007).

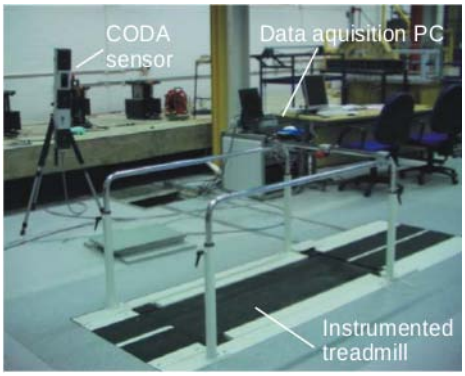

Figure 3.1.: *ADAL3D-F instrumented treadmill installed in the LSL. (Racic* et al.*, 2007)*

The double belt design of the ADAL3D-F shown in Figure 3.2 allows for the separate measurement of the forces under each foot. Each belt has a multiple Kistler 9077B force transducer which measures six analog channels of forces. These forces can be up to 3000 N in the vertical direction and 500 N in the longitudinal and lateral directions. The measured forces are digitised using an analog to digital converter at sampling rates between 100 and 1000 Hz. (Racic *et al.*, 2007)

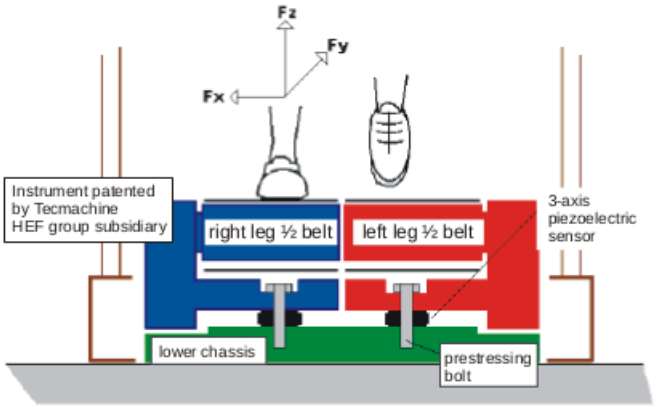

Figure 3.2.: *Cross-section through an ADAL3D-F instrumented treadmill.*
(Racic et al.*, 2007)*

A typical resulting GRF generated by a person walking on the ADAL3D-F is shown in Figure 3.3, where the image on the left shows the GRF in the vertical direction, the middle image shows the GRF in the lateral direction and the image on the right shows the GRF in the longitudinal direction. (Racic *et al.*, 2007)

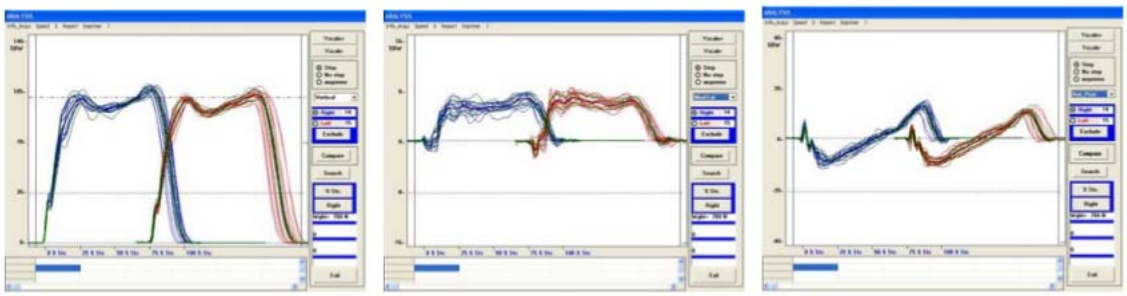

Figure 3.3.: *GRF measured using the ADAL3D-F*
(Racic et al.*, 2007)*

3.1.2. Typical Jogging Loads Measured

The vertical jogging forces obtained from the University of Sheffield were generated by a single person jogging at speeds ranging from $1.7603\,m/s$ to $2.6942\,m/s$. A total of 9 data sets were obtained, one for each of the jogging speeds measured. The general information regarding the weight of the person, sampling time step and jogging speed is summarised in Table 3.1. The sampling time step of $0.005\,s$ corresponds to a sampling rate of $200\,Hz$.

Table 3.1.: *Jogging data sets from University of Sheffield*

Reference	Body Weight, W (N)	Sampling Time Step, dt (s)	Jogging Speed (m/s)
J0001	761	0.0050	1.7603
J0002	761	0.0050	1.8948
J0003	766	0.0050	2.0258
J0004	766	0.0050	2.1543
J0005	766	0.0050	2.1620
J0006	766	0.0050	2.2967
J0007	766	0.0050	2.4321
J0008	766	0.0050	2.5674
J0009	766	0.0050	2.6942

3.1.3. Comparison with Jogging Load Models

Each of the jogging load models described in the literature review makes the assumption that the period of contact is equal to half the total period. Using this assumption and applying the data in Table 3.1 to the jogging load models, the jogging forces can be determined for each speed in Table 3.1 and compared with the actual measured jogging forces. The forces for running at $1.7603\,m/s$ are shown in Figure 3.4. Similar plots were produced for each of the other speeds and can be found in Appendix A.

From this plot it is clear that the predicted forces are significantly higher than the measured forces. The most likely reason for this is that the assumption that the contact period is 50 % of the total period is incorrect. This plot indicates that the contact period is closer to 75% of the total period. If the models are adjusted for the increased contact period then the predicted forces are much closer to the recorded running forces as shown in Figure 3.5. The comparison for each of the other speeds produces similar plots and can be found in Appendix A.

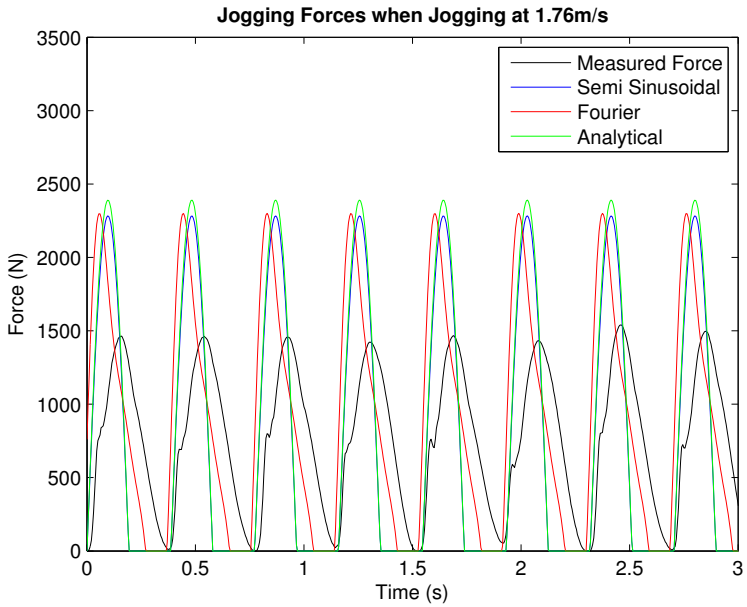

Figure 3.4.: *Comparison of Vertical Jogging Loads*

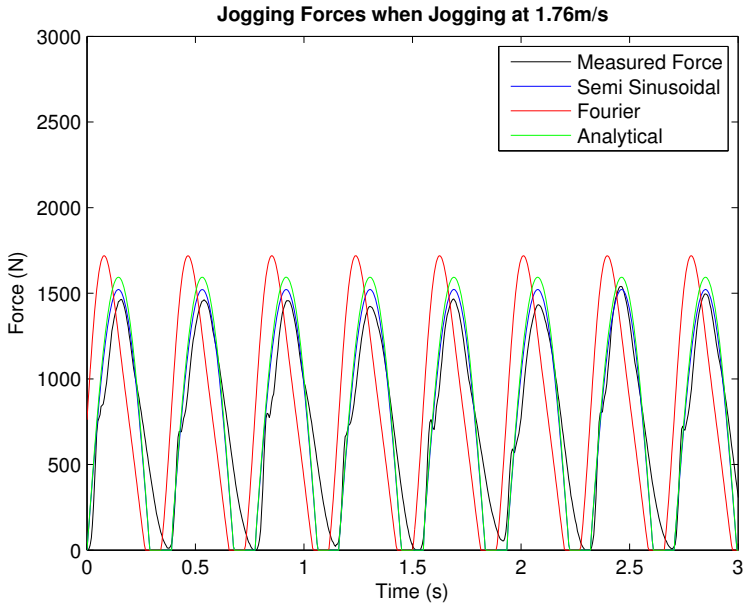

Figure 3.5.: *Comparison of Vertical Jogging Forces with Longer Contact Period*

The method proposed by Keller *et al.* (1996) to determine the maximum vertical force is based solely on the speed at which the person is jogging for speeds between $1.5\,m/s$ and $3.5\,m/s$ and the person's body weight for speeds above $3.5\,m/s$, as shown in Equation 3.4. Using this method the maximum vertical jogging force can be predicted for each of the jogging speeds

measured by the University of Sheffield. Table 3.2 and Figure 3.6 compares the calculated maximum vertical force with those measured by the University of Sheffield.

Speed (m/s)	Actual Measured Vertical Force (kN)	Calculated Vertical Force (kN) (Keller *et al.*, 1996)
1.7603	1.622	1.289
1.8948	1.605	1.371
2.0258	1.607	1.452
2.1543	1.663	1.531
2.1620	1.636	1.535
2.2967	1.670	1.618
2.4321	1.654	1.701
2.5674	1.677	1.784
2.6942	1.676	1.862

Table 3.2.: *Comparison of Vertical Jogging Forces*

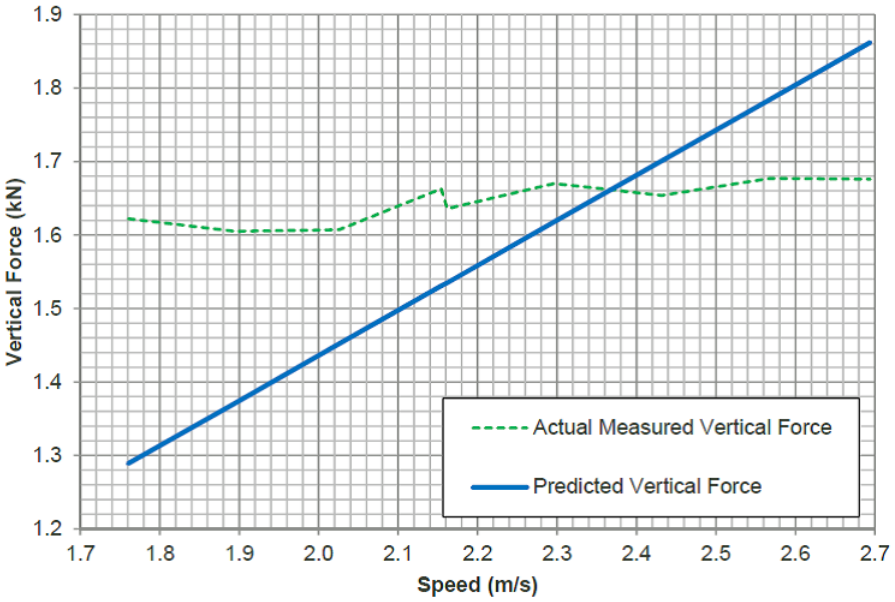

Figure 3.6.: *Graphical Comparison of Vertical Jogging Forces*

As expected, the calculated forces increase linearly with speed. However, the measured forces have a gradient which is much closer to zero. Therefore, for this limited sample, the linear relationship given by Keller *et al.* (1996) does not hold true.

3.2. Developing the Jogging Load Model

One of the problems with the running load models currently available is that they only consider the vertical component of the jogging force. However, as shown in Section 2.2, the Fourier series can be used to determine the forces in the lateral and vertical directions as well using Equations 2.0b and 2.0c. The difficulty with applying these equations is in determining the dynamic load factors and phase angles for the Fourier components in the lateral and longitudinal directions as they are not easily found in literature. By making a similar assumption to that made in the Sétra Guide (i.e. that any phase shifts for running forces are negligible) the phase angles in the lateral and longitudinal directions are equal to zero. Furthermore, the discontinuous nature of running forces can be taken into account in a similar manner to the force in the vertical direction. Therefore, the lateral and longitudinal running forces can be determined as shown in Equations 3.5 and 3.6 respectively.

$$\begin{array}{cc} F_{lat}(t) = \sum_{i=1}^{N} G_0 \cdot \alpha_{i,lat} \cdot \sin(\pi \cdot i \cdot f_m \cdot t) & (j-1)T_m \leq t \leq (j-1)T_m + t_p \\ F_{lat}(t) = 0 & (j-1)T_m + t_p < t \leq jT_m \end{array} \tag{3.5}$$

$$\begin{array}{cc} F_{long}(t) = \sum_{i=1}^{N} G_0 \cdot \alpha_{i,long} \cdot \sin(2 \cdot \pi \cdot i \cdot f_m \cdot t) & (j-1)T_m \leq t \leq (j-1)T_m + t_p \\ F_{long}(t) = 0 & (j-1)T_m + t_p < t \leq jT_m \end{array} \tag{3.6}$$

Unfortunately, the dynamic load factors in the lateral and longitudinal directions for running are not readily available and not much research has been done to obtain them. However, ISO 101317 provides a horizontal dynamic load factor, $\alpha_1 = 0.2$, for running at a running frequency range of between 2.0 and 4.0 Hz. Further research is required to determine the accuracy of this dynamic load factor as well as factors for the other harmonics.

Another problem with the available running load models is that they do not take into account multiple people running. Many of the walking load models described in the literature review used a simple method to take multiple people into account by multiplying the force by a factor m, where $m = \sqrt{n}$ for unsynchronised people crossing the bridge and $m = n$ for synchronised people. For this thesis it is assumed that this method can also be applied to the running load models.

3.2.1. Final Jogging Load Models

By consolidating the methods and models described so far in this Chapter, three load models can be obtained, tested and compared with loading on a real bridge. These models are given in Equations 3.7, 3.8 to 3.10 and 3.11 and include consideration for multiple people. The Fourier Model additionally considers the components of the running force in all three directions; vertical, lateral and longitudinal.

The first model is the Semi-Sinusoidal Model given by Equation 3.7.

$$\begin{array}{cc} F_{vert}(t) = m \cdot k_p \cdot G_0 \cdot \sin\left(\frac{\pi t}{t_p}\right) & (j-1)T_m \leq t \leq (j-1)T_m + t_p \\ F_{vert}(t) = 0 & (j-1)T_m + t_p < t \leq jT_m \end{array} \tag{3.7}$$

The second model is the Fourier Transform Model which is given by Equations 3.8, 3.9 and 3.10 and gives the force in the vertical, lateral and longitudinal directions.

$$\begin{array}{cc} F_{vert}(t) = m \cdot G_0 + \sum_{i=1}^{N} m \cdot G_0 \cdot \alpha_{i,vert} \cdot \sin(2 \cdot \pi \cdot i \cdot f_m \cdot t) & (j-1)T_m \leq t \leq (j-1)T_m + t_p \\ F_{vert}(t) = 0 & (j-1)T_m + t_p < t \leq jT_m \end{array} \tag{3.8}$$

$$\begin{array}{cc} F_{lat}(t) = \sum_{i=1}^{N} m \cdot G_0 \cdot \alpha_{i,lat} \cdot \sin(\pi \cdot i \cdot f_m \cdot t) & (j-1)T_m \leq t \leq (j-1)T_m + t_p \\ F_{lat}(t) = 0 & (j-1)T_m + t_p < t \leq jT_m \end{array} \tag{3.9}$$

$$\begin{array}{cc} F_{long}(t) = \sum_{i=1}^{N} m \cdot G_0 \cdot \alpha_{i,long} \cdot \sin(2 \cdot \pi \cdot i \cdot f_m \cdot t) & (j-1)T_m \leq t \leq (j-1)T_m + t_p \\ F_{long}(t) = 0 & (j-1)T_m + t_p < t \leq jT_m \end{array} \tag{3.10}$$

The third model is the analytical model which is given by Equation 3.11.

$$\begin{array}{cc} F_{vert}(t) = m \cdot \left(\frac{\pi}{2 \cdot t_p}\right) \cdot G_0 \cdot \sin\left(\frac{\pi}{t_p} \cdot t\right) & (j-1)T_m \leq t \leq (j-1)T_m + t_p \\ F_{vert}(t) = 0 & (j-1)T_m + t_p < t \leq jT_m \end{array} \tag{3.11}$$

Figures 3.7, 3.8 and 3.9 give a graphical representation of these jogging load models using a contact period of 75% of the total period and assuming 1 to 3 pedestrians, each weighing $700\,N$ and running in synchronisation at a frequency of $3\,Hz$. For the Fourier model three harmonics were used in the vertical direction and one in the horizontal directions.

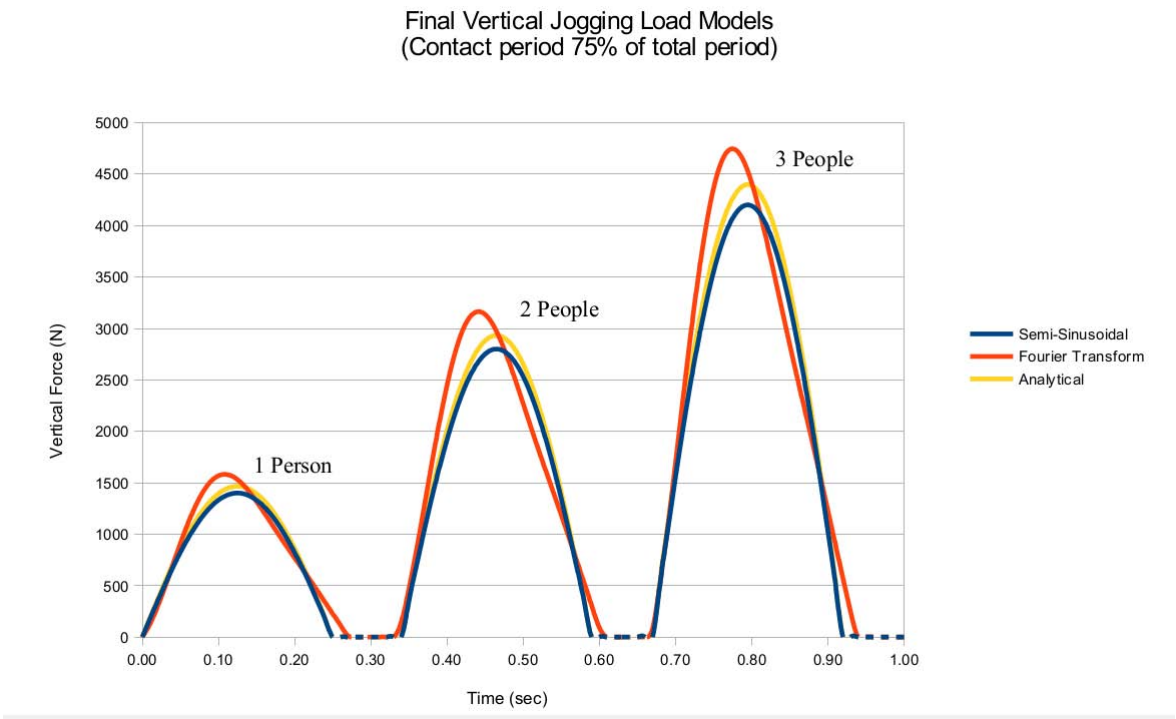

Figure 3.7.: *Final Vertical Jogging Load Models for 1 to 3 People*

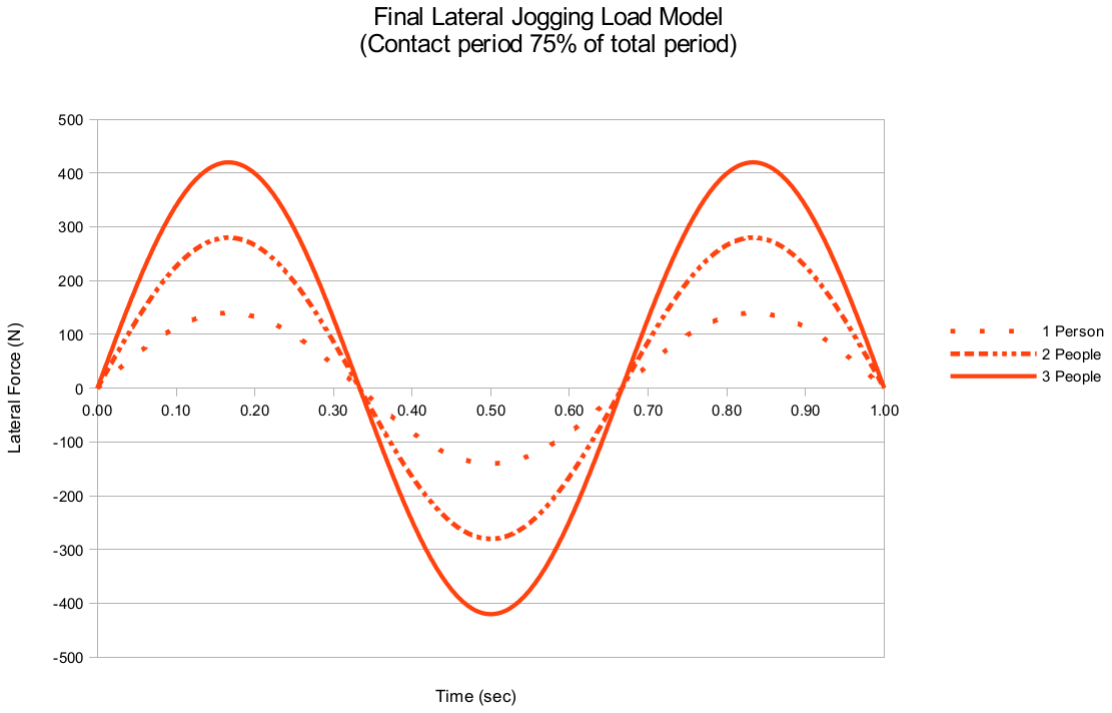

Figure 3.8.: *Final Lateral Jogging Load Model for 1 to 3 People*

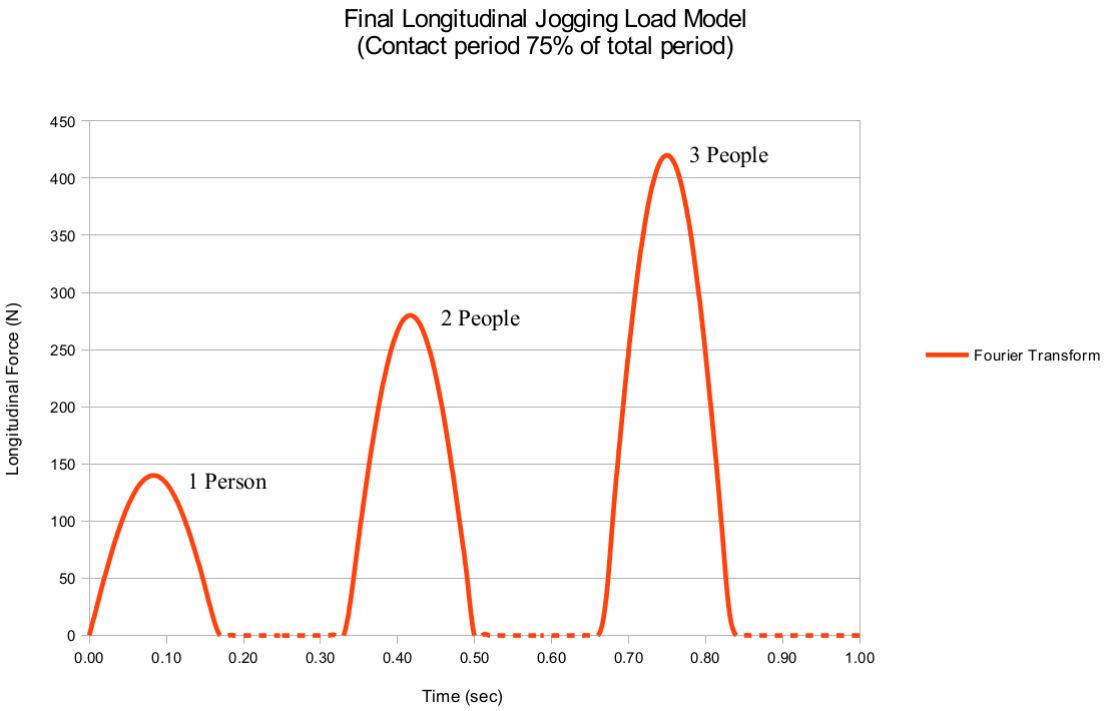

Figure 3.9.: *Final Longitudinal Jogging Load Model for 1 to 3 People*

4. Methodology for Testing

The models presented in Chapter 3 are tested in two ways. The first is using simulations and the second is via verification. These are outlined in more detail in this Chapter.

4.1. Simulations

Simulations were done for each of the jogging load models to determine the ease with which they can be used. This was done by applying the verified jogging load models from Chapter 3 to a simply supported beam. The aim of these simulations was to determine the method to use to extract the accelerations from a simple model. This section describes how the simulations were done. The computer program, COMSOL Multiphysics, was used to do the simulations.

The following methodology describes the procedure used to conduct the simulations:

1. The simply supported beam structure was modelled.
2. The vertical jogging loads models were applied to the model of the beam structure.
3. Simulations were run using the jogging load models.
4. The acceleration results from the simulations were obtained.

4.2. Verification

After the simulations, the models were applied to a simple finite element model (FEM) of an existing bridge in order to compare the approximated accelerations with those measured on the real bridge.

The University of Cape Town (UCT) has done a number of tests on the Rhodes Memorial Footbridge which crosses the M3 highway near UCT and Mostert's Mill. Figure 4.1 shows the location of the footbridge as a red line on the map. This bridge is well documented to have vibration serviceability problems and due to its location between the upper and middle

campuses of the university it is readily accessible. For this reason it was decided to use this bridge to test the jogging load models developed as part of this thesis.

Figure 4.1.: *The location of the Rhodes Memorial Footbridge. (Google Maps, 2013)*

The Rhodes Memorial Bridge is a simply supported concrete bridge with a span of approximately $30\,m$ and a natural frequency for the first mode of vibration of $2.89\,Hz$ (Keil, 2012).

The following methodology describes the procedure that was used to verify the jogging load models developed in this thesis:

1. Geometric data for the bridge was obtained, including as-built drawings and on site measurements.
2. The FEM for the Rhodes Memorial Bridge was developed using COMSOL Multiphysics software.
3. The FEM for the bridge was updated to ensure that the natural frequencies matched the actual natural frequencies of the Rhodes Memorial Bridge.
4. The running load models were applied to the updated FEM for groups of 1 to 7 people jogging across the bridge at a jogging footfall frequency equal to the natural frequency of the bridge and the accelerations due to these loads were obtained.
5. The possible accelerations for the bridge were calculated using the simple methods found in various codes of practice and other sources described in Chapter 2.
6. The testing procedure and the results of the testing of the Rhodes Memorial Bridge were summarised. This testing was done by Philip Keil as part of his undergraduate

thesis for the University of Cape Town; “Evaluation of the Vibration Serviceability of Footbridges with regards to Jogging”. A summary of the results he obtained are given in Appendix D.

7. The predicted accelerations from simplified methods and the FEM were compared with the measured accelerations of the real bridge when subjected the same loads.

5. Simulations Results

5.1. Step 1 - Modelling of the Structure

A simply supported beam with the following properties was modelled in COMSOL Multiphysics using a solid element:

- The length of the beam was $15\,m$,
- The thickness of the beam was $250\,mm$,
- The damping ratio was $\zeta = 1\%$,
- The structural material for the beam was concrete with a density of $2400\,kg/m^3$ and a Young's modulus of $25\,GPa$.

The beam dimensions and support types were chosen to ensure that the fundamental natural frequency of the beam corresponded with the jogging load frequency which would be applied to the beam. A jogging speed of $1.7603\,m/s$ was used, which corresponds to the speed of the first measured jogging forces obtained from the University of Sheffield for reference number J0001 (see Table 3.1). With a jogging step length of $1\,m$, the load is applied at a frequency of $1.7603\,Hz$. Figure 5.1 shows the natural frequency of $1.7603\,Hz$ for the first mode of vibration for this beam.

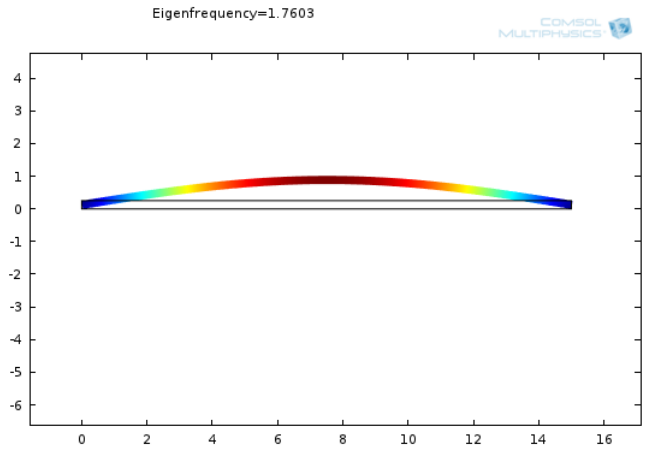

Figure 5.1.: *Eigenfrequency plot for the Beam Structure in COMSOL Multiphysics.*

COMSOL Multiphysics makes use of the Rayleigh Damping Model to define the damping parameter as shown in Equation 5.1, where α_{dM} is the mass damping parameter and β_{dK} is the stiffness damping parameter (COMSOL, 1998-2013).

$$c = \alpha_{dM} m + \beta_{dK} k \tag{5.1}$$

Figure 5.2 gives a graphical representation for Rayleigh Damping. As can be seen, in this situation for natural frequencies greater than $1\,Hz$ the stiffness damping parameter dominates. For this reason the COMSOL documentation states that for most applications it is sufficient to assume that the mass damping parameter is zero, and that Equation 5.2 can therefore be used to define the damping using only the stiffness damping parameter (COMSOL, 1998-2013). By making this assumption, the stiffness damping parameter for the modelled beam was calculated to be 0.0012.

$$\beta_{dK} = \frac{\zeta}{\pi f_0} \tag{5.2}$$

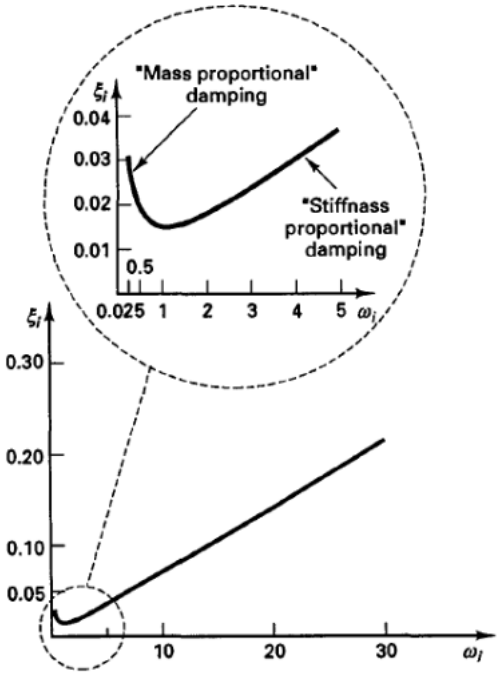

Figure 5.2.: *Graphical Representation of Rayleigh Damping. (Faber, 2009)*

A normal mesh was used for this simulation. COMSOL Multiphysics automatically generates the optimum meshing based on the geometric properties. Since the aim of the simulations was

to determine the method to use to extract the accelerations from a simple model no further refinement of the meshing was required.

5.2. Step 2 - Applying the Loads

The simplest method of applying the jogging loads to the two dimensional beam structure was as a series of loads applied over a distance of 0.1 *m* at the position of each of the jogger's steps. For the purpose of the simulations it was assumed that the step length of a person running across the beam was 1 *m*. This is illustrated in Figure 6.7.

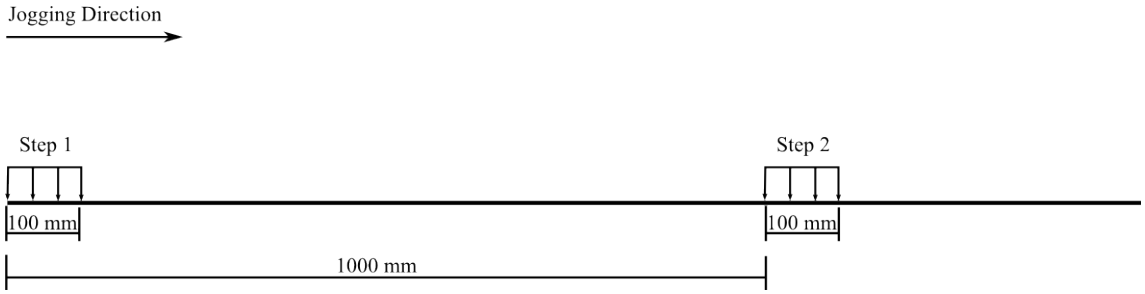

Figure 5.3.: *Graphical representation of how the Jogging Loads were applied.*

Figure 5.4 shows the positions at which the loads occur along the entire length of the beam.

Figure 5.4.: *Locations of where the Loads will be Applied.*

Vertical jogging loads for each of the jogging load models described in the Section 3.2.1 were modelled. One period of the vertical load plots for one person for each model is given in Figure 5.5. These loads were applied to each position at a time equal to the period it would take the persons foot to land on that specific position on the beam. Based on the findings in

Chapter 4 the contact period used for the loading is 75% of the total period, as can be seen on the plot in Figure 5.5.

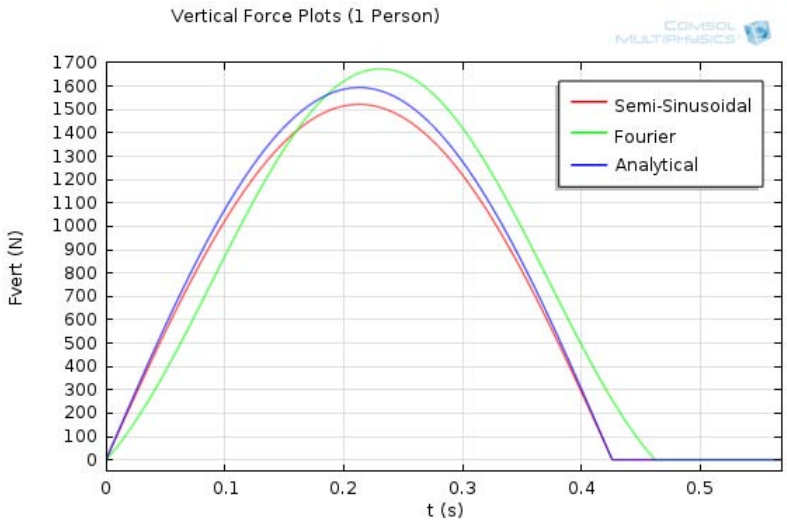

Figure 5.5.: *Vertical Load Plots for One Person*

The lateral and longitudinal loads are not shown for the simulations since no measured data for these were obtained from the University of Sheffield. However, when doing the verification of the Rhodes Memorial Bridge the lateral and longitudinal load models were also considered.

5.3. Step 3 - Running the Simulation

In order to run the simulation a time dependent study was conducted in COMSOL Multiphysics. The following time steps were used in the study:

- Start time = 0 s
- Time steps = 0.01 s
- End time = 60 s

5.4. Step 4 - Obtaining the Results

The main aim of this exercise was to determine the ease with which one can obtain the accelerations of a structure under a jogging load. The accelerations for the structural model in COMSOL were determined by obtaining the accelerations at the centre of the beam for each

time step. Figure 5.6 gives the resulting vertical acceleration at the centre of the beam due to the semi-sinusoidal jogging model. Refer to Appendix B for the vertical acceleration results for each jogging load model.

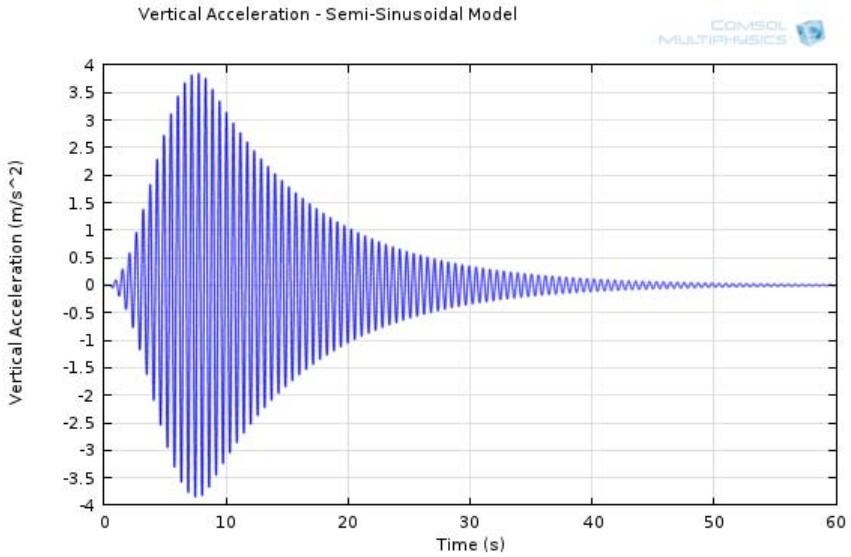

Figure 5.6.: *Semi-Sinusoidal Vertical Acceleration Plot at the Centre of the Beam*

Using this data the maximum acceleration over all the time steps was found. Table 5.1 gives a summary of the maximum vertical accelerations for each of the jogging load models.

Table 5.1.: *Maximum Accelerations of the Simple Beam Structure.*

Load Model	Max Vertical Acceleration
Semi-Sinusoidal	3.85
Fourier	4.11
Analytical	4.04

As can be seen the 3 jogging load models give similar vertical accelerations ranging from $3.85\,m/s^2$ to $4.11\,m/s^2$. The Fourier model results in the highest acceleration and the Semi-Sinusoidal model results in the lowest acceleration. This agrees with the differences in the amplitudes of the applied forces for each model shown in Figure 5.5.

Based on these simulations it can be seen that it is a simple process to obtain the accelerations of a structure due to the loading from the jogging load models. The next step was to apply the jogging load models to a FEM of an actual bridge and compare the accelerations to those measured in real life.

6. Verification Results

6.1. Step 1 - Obtaining Data

The structural material properties and the geometric data of the Rhodes Memorial Bridge were obtained from two sources. The first involved obtaining the structural drawings of the bridge from the City of Cape Town and the second involved site measurements to confirm the information on the drawings.

Two drawings of the Rhodes Memorial Bridge were obtained from the City of Cape Town. These drawings were compiled in 1961 and copies of them can be found in Appendix C. Based on these drawings the geometric properties of the bridge were easily determined. However, in order to confirm that the as-built dimensions were the same as the drawings it was necessary to conduct a site visit to verify these measurements. The site measurement can be found in Appendix C.

The site visit took place on the 23 July 2013. Figure 6.1 is a photo that was taken during the site visit and shows the Rhodes Memorial Bridge

Figure 6.1.: *Rhodes Memorial Bridge*

Based on the site measurements it is clear that the bridge deck is narrower than shown on the drawings. All the other dimensions, however, are reasonably represented on the drawings. Therefore, it was decided to use the dimensions given on the drawings for the FEM with the exception of the bridge deck width, for which the measured dimension was used. Figure 6.2 shows a cross section through the FEM of the bridge deck showing the modelled dimensions.

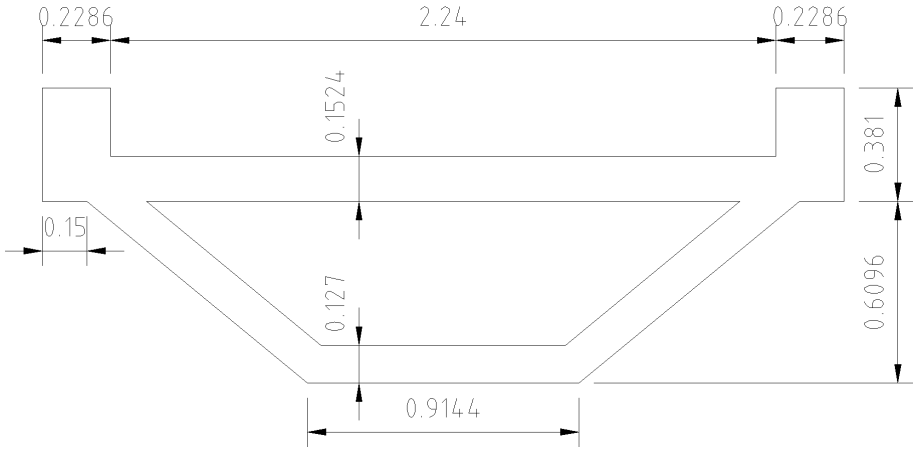

Figure 6.2.: *Modelled Cross Section through Footbridge*

6.2. Step 2 - Developing the FEM

The bridge was modelled in COMSOL Multiphysics using a solid element with a constant cross section as illustrated in Figure 6.2. The remaining bridge dimensions and properties that were applied to the model are as follows:

- The span of the bridge is $27.7\,m$
- The rise of the bridge across it's length to form the arc is $695\,mm$
- The structural material for the bridge was concrete with the following properties:
  - A concrete density of $2400\,kg/m^3$
  - A Young's modulus of $25\,GPa$.
  - A Poisson's ratio of 0.3
- From previous measurements and studies done on the bridge the damping ratio for the bridge is known to be $\zeta = 4.5\%$ (Keil, 2012). Hence, by assuming that the mass damping parameter for Rayleigh Damping is zero as discussed in the previous chapter, the stiffness damping parameter was determined using Equation 5.2 to be 0.0050.

- The bridge is fixed to the bridge piers on either side by means of a bearing connection as shown in Figure 6.3. This was modelled in COMSOL Multiphysics by means of a pinned connection on one end and a spring connection on the other end on the bottom edge of the bridge.

Figure 6.3.: *Actual support connection of the Rhodes Memorial Footbridge*

The FEM for the Rhodes Memorial Bridge was developed in COMSOL Multiphysics using these properties. Figure 6.4 shows a plot of the bridge model.

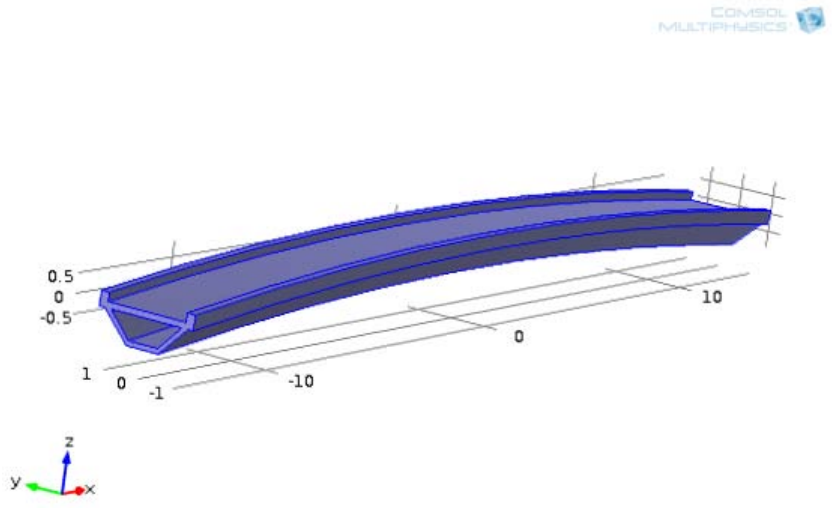

Figure 6.4.: *Model of the Rhodes Memorial Bridge in COMSOL Multiphysics*

6.3. Step 3 - Updating of the FEM

It has been well documented in previous studies that the fundamental natural frequency for the Rhodes Memorial Bridge is $2.89\,Hz$ (Keil, 2012) and that the first mode of vibration is the vertical mode. Since the loading was applied to coincide with the fundamental natural frequency it was important to ensure that the FEM had the same fundamental frequency and mode of vibration.

For this FEM, manual "fine-tuning" was done by adjusting the boundary conditions of the spring support until the fundamental natural frequency was equal to $2.89\,Hz$. Figure 6.5 shows a plot from COMSOL Multiphysics showing the fundamental natural frequency of the bridge.

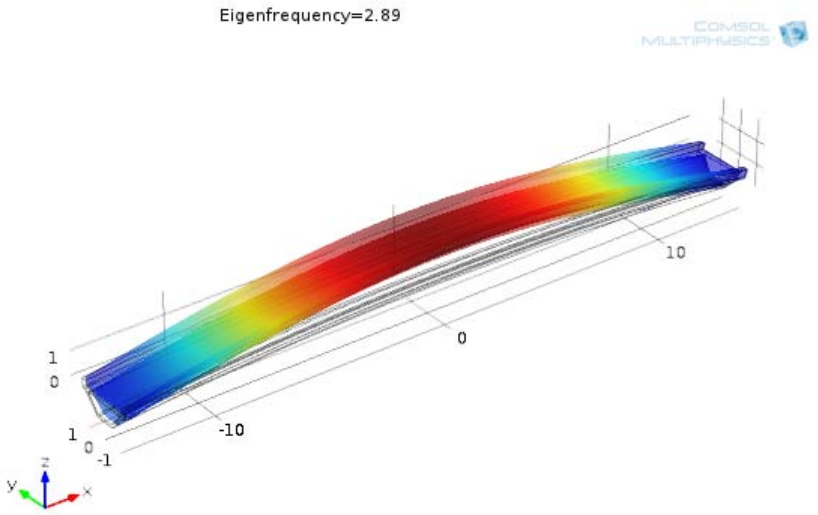

Figure 6.5.: *Fundamental Natural Frequency of Modelled Bridge*

6.4. Step 4 - Applying the Jogging Load Models

The jogging load models were applied to the bridge in a similar manner as in the simulations, however in this case the lateral and longitudinal load models were also used and the loads were applied over an area of $0.2\,m\,x\,0.2\,m$. For this exercise the following assumptions were made:

- Weight of the joggers is $700\,N$
- Step length of the joggers is $1.19\,m$ based on the average stride length determined by Barreira *et al.* (2010).

- Running frequency of $2.89\,Hz$ to coincide with the natural frequency of the bridge
- The jogging loads were applied at $1.19\,m\,c/c$ along a curved line which runs down the centre of the bridge deck. This coincides with the loading that would occur if one person were to jog across the bridge with a stride length of $1.19\,m$. Figure 6.6 shows the position of the load along the curved centre line of the bridge. The load plots for one to seven people for each of the jogging load models are given in Appendix C.

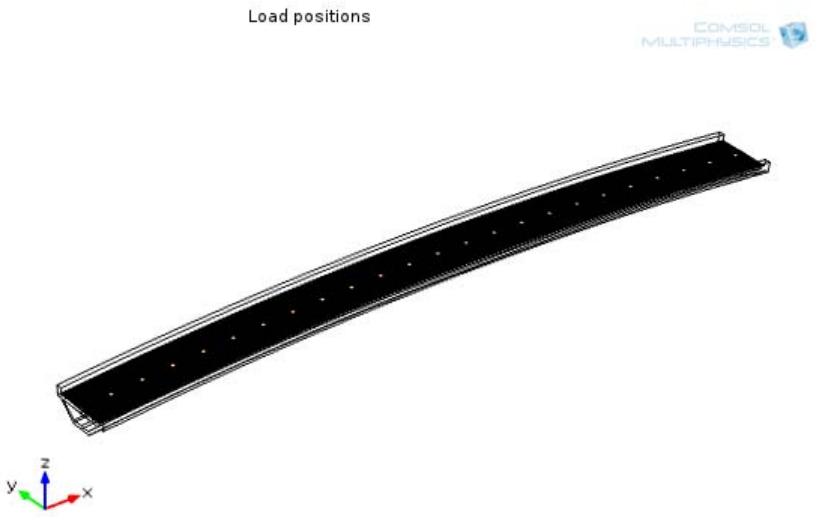

Figure 6.6.: *Position of line upon which Jogging Loads will be applied.*

A study using the above loading was conducted in COMSOL Multiphysics with the following time steps:

- Start time = $0\,s$
- Time steps = $0.01\,s$
- End time = $20\,s$

Figure 6.7 gives a graphical representation of how the jogging loads were applied to the FEM of the Rhodes Memorial Bridge. From this the accelerations for the bridge with groups of up to seven people jogging across it were determined. Figure 6.10 gives a plot of the first attempt to obtain the accelerations from COMSOL Multiphysics for one person using the Semi-Sinusoidal Model. This plot shows that the acceleration results obtained for the FEM of the Rhodes Memorial Bridge were not as smooth as those obtained during the simulations. The reason for this is related to the mesh refinement. When the FEM was run using a normal mesh some of the applied loads were not picked up and hence not accounted for which resulted

in the acceleration plot shown in Figure 6.10. Due to computer hardware limitations it was not possible to have a fine enough mesh across the whole FEM of the bridge to pick up every load from the jogging model. Therefore, the mesh was refined as shown in Figure 6.9, with a maximum mesh size of 0.1 *m* at the position of the loads and a normal mesh over the rest of the bridge.

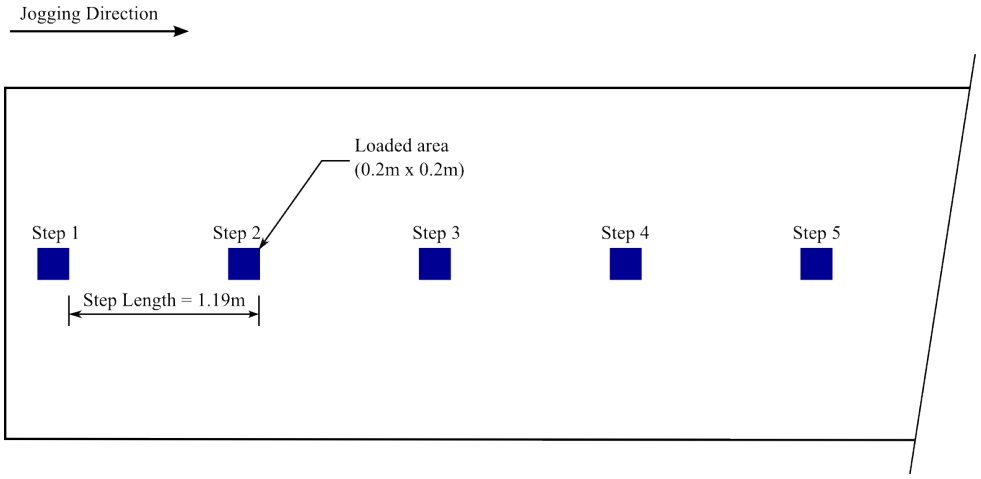

Figure 6.7.: *Graphical representation of how the Jogging Loads were applied.*

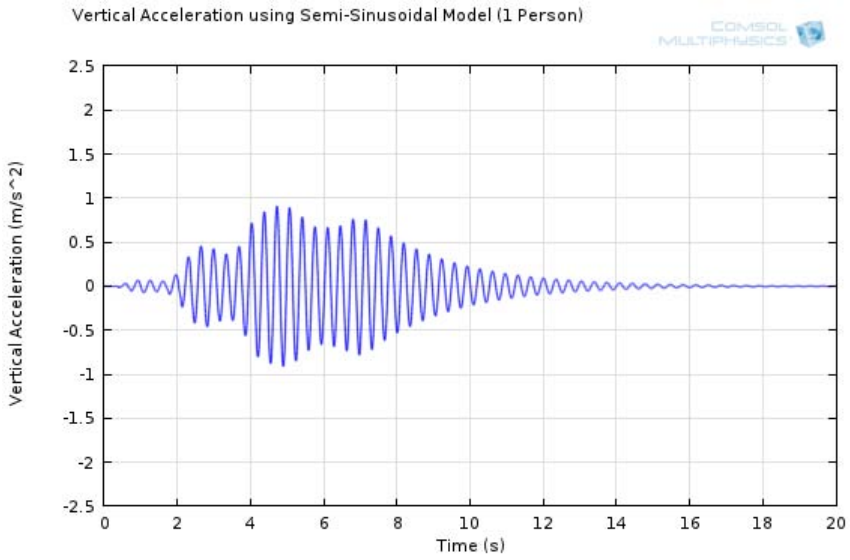

Figure 6.8.: *Semi-Sinusoidal Model Accelerations due to One Person - Normal Mesh*

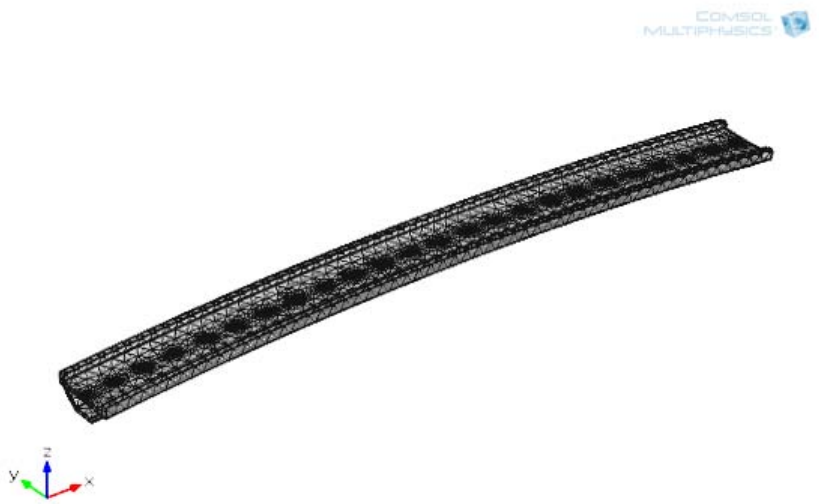

Figure 6.9.: *Final Mesh for the FEM of the Rhodes Memorial Bridge*

Using this mesh refinement it was possible to obtain a smooth acceleration plot for the various jogging load models shown in Figure 6.10. Refer to Appendix C for all the plots generated in COMSOL Multiphysics for the maximum accelerations with respect to time at a point in the middle of the bridge deck.

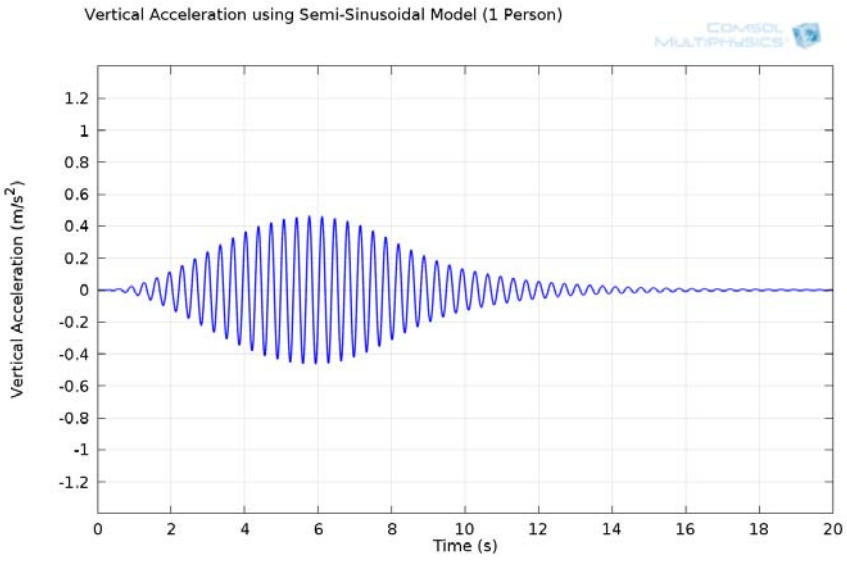

Figure 6.10.: *Semi-Sinusoidal Model Accelerations due to One Person - Refined Mesh*

Furthermore, it should be noted that because of the manner in which the longitudinal force has been applied to the FEM model as a single pulse force in one direction only, it has been

assumed that the force pulse in the other direction is of equal magnitude and symmetrical to the applied force.

Table 6.1 gives a summary of the maximum predicted accelerations in the bridge from the three jogging load models as calculated using COMSOL Multiphysics. Section 6.7 gives a comparison between these accelerations and the actual accelerations measured on the bridge. As can be seen, the three jogging models give similar results for the vertical acceleration. The longitudinal acceleration is about 0.1 of the vertical acceleration and the lateral acceleration just over 0.1 of the longitudinal acceleration.

Table 6.1.: *Maximum accelerations determined in COMSOL Multiphysics*

Number of	Max Vertical Acceleration (m/s^2)			Max Lateral	Max Longitudinal
People	Semi-Sinusoidal	Fourier	Analytical	Acceleration (m/s^2)	Acceleration (m/s^2)
1	0.464	0.487	0.483	0.006	0.045
2	0.656	0.689	0.682	0.008	0.064
3	0.803	0.844	0.836	0.010	0.078
4	0.928	0.975	0.965	0.012	0.090
5	1.037	1.090	1.079	0.013	0.101
6	1.136	1.194	1.182	0.015	0.111
7	1.227	1.289	1.277	0.016	0.119

6.5. Step 5 - Simplified Methods of Determining Accelerations

The literature review describes seven simple methods for calculating the acceleration of a footbridge. Table 6.2 gives the calculated accelerations for the Rhodes Memorial Bridge using each of these methods. The actual calculations for these methods can be found in Appendix C.

As can be seen, the results from the simplified methods differ greatly from $0.042\,m/s^2$ to $165\,m/s^2$ for a single person. Furthermore, these simple methods are generally only applicable for a single person walking across a bridge and not for someone jogging. This shows that these methods are not suitable for determining the acceleration due to jogging loads. Furthermore, the Eurocode which does include a method for calculating the acceleration for jogging loads is for a timber bridge and can not be used on a concrete bridge.

Table 6.2.: *Calculated accelerations for Simple Beam Structure*

Name	Maximum Acceleration (m/s^2)	Number of People
TMH7	$a_{vert,walk} = 112$	1
Eurocode	$a_{vert,walk} = 0.041$	1
	$a_{hor,walk} = 0.021$	1
	$a_{vert,walk} = 0.11$	4
	$a_{hor,walk} = 0.039$	4
	$a_{vert,run} = 0.25$	1
Rainier	$a = 0.23$	1
Allen and Murray	$a = 2.4$	1
Grundmann	$a_{vert,walk} = 0.045$	1
	$a_{lat,walk} = 0.011$	1
Young	$a_n = 0.19\mu_i\mu_j$	1
Pimentel and Frenandes	$a_{max} = 165$	1

6.6. Step 6 - Summary of the Testing

Philip Keil (2012) tested the Rhodes Memorial Footbridge on the 2 October 2012 with 1 to 7 people jogging across it as part of his undergraduate thesis at the University of Cape Town. This section gives a brief summary of the testing he conducted and the results thereof. For more detailed results from this testing refer to Appendix D.

The following equipment was used by Philip Keil (2012) to obtain the measurements:

- 6 Honey QA700 Accelerometers placed at midspan to record the vertical and lateral accelerations
- 2 x 4 Channel Drums
- 1 x 24 Channel Input Station
- 1 x 24 Channel Input Data Card
- 1 Electronic Metronome set to 2.89 Hz
- LabView (Signal Express) Version Software to record and translate the captured data
- ME'scope VES to analyse the raw data

Using the electronic metronome, groups of up to 7 people jogged across the bridge at a running frequency equal to that of the beats given by the metronome, and the accelerations were recorded. For the first test only the vertical accelerations were recorded and for the second test both the vertical and lateral accelerations were recorded. After each group of runners crossed the bridge the bridge was allowed to return to its neutral state before the next group ran across. Table 6.3 gives the resulting maximum accelerations for both tests and the root-mean-square (RMS) accelerations for the second test.

Table 6.3.: *Accelerations Recording during Testing.*
(Keil, 2012)

No. of Pedestrians	Maximum Measured Accelerations (m/s^2)			RMS Accelerations (m/s^2)	
	Vertical*	Vertical	Lateral	Vertical	Lateral
1	0.80	0.70	0.048	0.35	0.012
2	1.37	1.07	0.048	0.53	0.016
3	2.50	0.91	0.061	0.39	0.015
4	3.32	1.60	0.156	0.72	0.034
5	3.50	0.74	0.148	0.20	0.024
6	1.84	1.03	0.074	0.34	0.016
7	1.67	1.40	0.018	0.54	0.024

* The first test where only vertical accelerations were recorded.

As can be seen, the maximum vertical and lateral accelerations occurred when 5 or 4 pedestrians jogged across the bridge for the first and second test respectively. Thereafter there is a decrease in the acceleration most likely owing to the fact that once there are more than 4 joggers they tend to become unsynchronised. This shows that with more people jogging across the bridge it is difficult to predict the response of the bridge as people are never perfectly synchronised. However, if one compares the measured vertical accelerations for one person of $0.80\,m/s^2$ and $0.70\,m/s^2$ it is clear that the measured accelerations of one person are reproducible with minor difference most like due to the weight of the person jogging across the bridge.

Figure 6.11 and Figure 6.12 give the respective vertical and lateral time-history response of the bridge for the second test when 4 pedestrians jogged across it. Refer to Appendix D for the rest of the time-history responses for the second test.

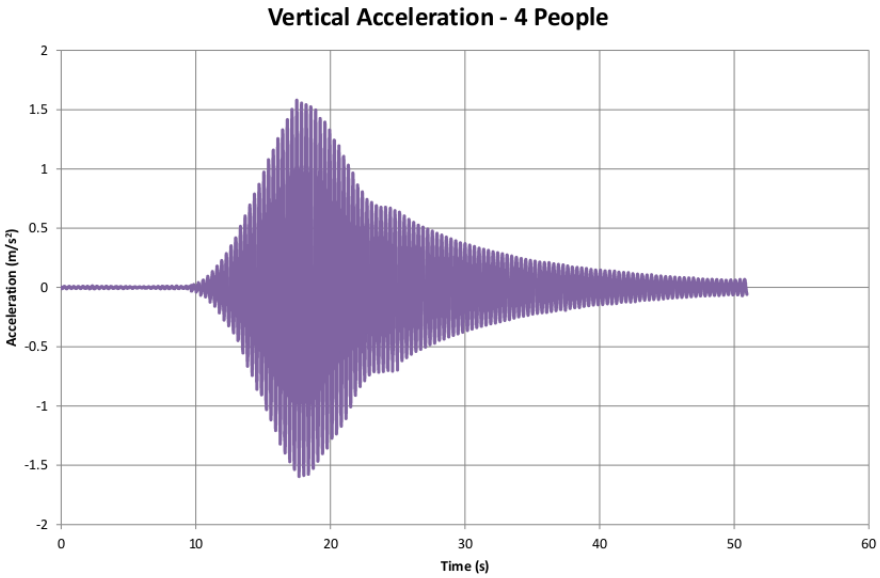

Figure 6.11.: *Vertical Time-History Response due to 4 Joggers (Re-plotted from raw data obtained by Keil (2012))*

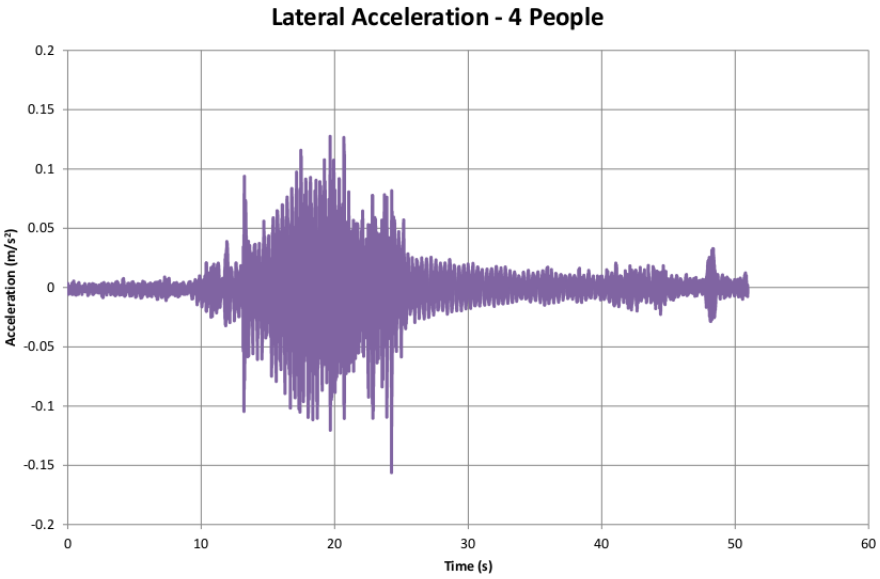

Figure 6.12.: *Lateral Time-History Response due to 4 Joggers (Re-plotted from raw data obtained by Keil (2012))*

6.7. Step 7 - Comparison of Results

In this section the various accelerations, both calculated and measured, for the Rhodes Memorial Bridge are compared. Thereafter, the measured results are reviewed with respect to the relevant Codes of Practice described in the literature review.

6.7.1. Comparison of Accelerations

Tables 6.4 and 6.5 show a summary of all the measured accelerations for the Rhodes Memorial Bridge and those obtained from the FEM in COMSOL Multiphysics. The accelerations determined using the simplified methods (see Section 6.5) are not shown in this table due to their inaccuracy in predicting the accelerations due to jogging loads.

Table 6.4.: *Comparison of Vertical Accelerations*

Number	Measured Accelerations (m/s^2)			COMSOL Multiphysics Accelerations(m/s^2)		
of People	Maximum		RMS	Semi-Sinusoidal	Fourier	Analytical
1	0.80	0.704	0.349	0.464	0.487	0.483
2	1.37	1.065	0.527	0.656	0.689	0.682
3	2.50	0.905	0.388	0.803	0.844	0.836
4	3.32	1.595	0.720	0.928	0.975	0.965
5	3.50	0.743	0.196	1.037	1.090	1.079
6	1.84	1.027	0.341	1.136	1.194	1.182
7	1.67	1.404	0.543	1.227	1.289	1.277

Table 6.5.: *Comparison of Lateral and Longitudinal Accelerations*

Number	Measured Lateral Accelerations (m/s^2)		COMSOL Multiphysics Accelerations(m/s^2)	
of People	Maximum	RMS	Lateral	Longitudinal
1	0.0475	0.0119	0.006	0.045
2	0.0484	0.0164	0.008	0.064
3	0.0605	0.0146	0.010	0.078
4	0.156	0.0342	0.012	0.090
5	0.148	0.0241	0.013	0.101
6	0.0738	0.0155	0.015	0.111
7	0.0180	0.0240	0.016	0.119

As can be seen, the vertical accelerations obtained in the FEM are just over half of the actual maximum vertical accelerations measured on the Rhodes Memorial Bridge for one person. However, the RMS of the measured vertical accelerations are similar to those obtained in the FEM for one and two people. Similarly the lateral acceleration obtained in the FEM compare more favourable with the RMS of the measured lateral accelerations than the maximum measured lateral acceleration.

With more than 4 people the measured accelerations in the second test start to decrease whereas the accelerations obtained in the FEM continue to increase. This is due to the fact that the joggers became unsynchronised when more than 4 people jogged across this bridge. Furthermore, with more than 4 joggers there was a tendency to run in time with each other instead of with the electronic metronome. Both of these situations are not accurately portrayed in the jogging load models. Figure 6.13, Figure 6.14 and Figure 6.15 give plots showing the change in acceleration due to an increase in the number of people in the vertical, lateral and longitudinal directions respectively for the FEMs and compares them with the measured accelerations.

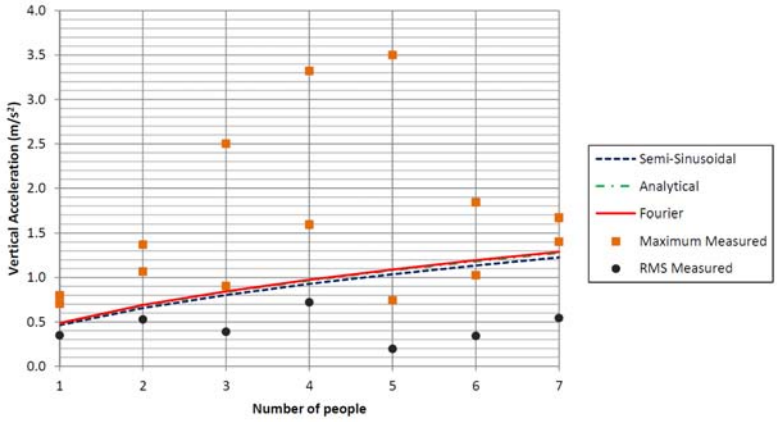

Figure 6.13.: *Vertical Acceleration versus Number of People*

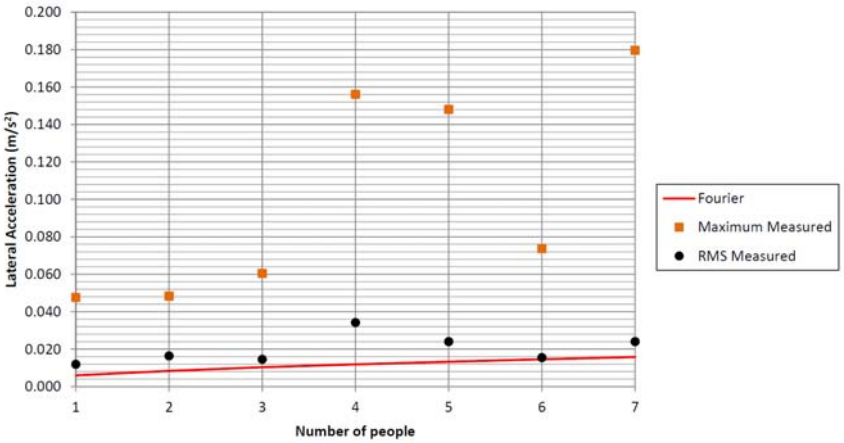

Figure 6.14.: *Lateral Acceleration versus Number of People*

Figure 6.15.: *Longitudinal Acceleration versus Number of People*

As can be seen from these plots there is a relationship between the number of people and the predicted acceleration of the bridge. The vertical and lateral accelerations obtained by applying the jogging load models to the FEM of the Rhodes Memorial Bridge correlates with the RMS values of the actual measured accelerations for one and two people and relatively well for three and four people. Thereafter, the actual measured accelerations drop because the people jogging across the bridge become unsynchronised. This suggest that there is a critical number of people to consider when designing a footbridge for synchronisation of people jogging across it. This study suggests that this value is 4 or 5 people, however this needs to be confirmed with further testing.

6.7.2. Review of relevant Codes of Practice

In this section the measured acceleration results for the Rhodes Memorial Bridge are compared with those recommended in the various Codes of Practices outlined in the literature review.

6.7.2.1. TMH7 and the Old British Standard

Since the fundamental natural frequency of the footbridge is $2.89\,Hz$ which is less than the $5\,Hz$ limit set in the codes, serviceability checks are required. These codes specify that the vertical acceleration needs to be limited to $0.5\sqrt{n_0} = 0.85\,m/s^2$. Based on this the measured maximum vertical acceleration of $3.5\,m/s^2$ when 5 people jog across the footbridge is higher than the recommended maximum and explains the vibration serviceability problems that occur on the Rhodes Memorial Bridge. Furthermore, using the simplified method to predict the maximum acceleration yields a result of $112\,m/s^2$ which is much higher than both the acceptable acceleration and the measured acceleration. This indicates that the method provided in TMH7 does not accurately predict the acceleration of a running pedestrian and may contain errors.

6.7.2.2. Sétra Guide

In this guide the comfort level of the users first needs to be determined. For the Rhodes Memorial Bridge it can be assumed that the bridge is subjected to standard traffic with the occasional large group, but that it will not have streams of pedestrians crossing it. This means that it can be classified as a Class III footbridge. For the purpose of this exercise it will be assumed that an average comfort level would be deemed acceptable for the footbridge and hence the acceptable vertical and horizontal accelerations are as follows:

- A maximum vertical acceleration of between $0.5\,m/s^2$ and $1.0\,m/s^2$
- A maximum horizontal acceleration of $0.10\,m/s^2$

The guide then states that since the natural frequency of $2.89\,Hz$ lies between $2.6\,Hz$ and $5.0\,Hz$ the footbridge has a classification of range 3 and hence dynamic load calculations are not required. However, the maximum measured vertical acceleration of $3.5\,m/s^2$ and maximum measured horizontal acceleration of $0.16\,m/s^2$ due to 5 and 4 people respectively jogging across the footbridge fall outside the acceptable acceleration limits given in the guide.

6.7.2.3. Eurocode together with the UK Annex

Eurocode 0 states that the maximum allowable vertical and horizontal accelerations that the bridge should experience are $0.7\,m/s^2$ and $0.2\,m/s^2$ respectively for normal use as its comfort criteria. Both of these values are lower than the maximum measured accelerations. Furthermore, it states that pedestrian induced activities with frequencies close to that of the natural frequency of the footbridge could lead to resonance and need to be taken into account. Since the natural frequency of the Rhodes Memorial Footbridge falls within this range, this is necessary. However, no additional information is given for designing anything other than timber bridges for vibration serviceability.

6.7.2.4. ISO Guide

The ISO guide requires that the vibration amplitude from applicable vibration sources does not exceed $0.33\,m/s^2$ in the vertical direction and $0.27\,m/s^2$ in the horizontal direction. The measured accelerations in both directions for the Rhodes Memorial Bridge exceed the maximum recommended accelerations given in the guide.

6.7.2.5. The Hong Kong Structures Design Manual for Highways and Railways

As with TMH7 and BS5400, the vertical acceleration for the Rhodes Memorial Bridge should be limited to $0.85\,m/s^2$. However, this manual also limits the lateral acceleration to $0.15\,m/s^2$. Both of these are exceeded by the Rhodes Memorial Bridge.

6.7.2.6. Swiss Standard SIA 160

This code requires that the natural frequency of the bridge is not between 2.4 to $3.5\,Hz$ if runners or joggers are likely to cross the bridge. Since the natural frequency for the Rhodes Memorial Bridge is $2.89\,Hz$, it lies within this range and hence the vibration response of the bridge needs to be checked.

6.7.2.7. The American Guide Specification

As in the Swiss Standard the American Guide recommends that any natural frequencies below $5\,Hz$ should be avoided for a footbridge which are likely to have people running across it. If the natural frequency is below the recommended value, as is the case with the Rhodes

Memorial bridge then for serviceability requirements a minimum natural frequency of $1.18\,Hz$ as calculated by Equation 6.1 shall apply. Furthermore, it suggests the installation of vibration absorbers and dampers to improve the dynamic performance of the bridge.

$$2.86 \ln \frac{8000}{0.01 \cdot (53900)(9.81)} = 1.18 \tag{6.1}$$

6.7.2.8. Summary

Table 6.6 gives a comparison of the accelerations for the various Codes of Practices outlined in the literature review. From this it can be seen that the maximum measured vertical acceleration of $3.5\,m/s^2$ for the Rhodes Memorial Bridge is higher than the recommended values in all the codes of practice. Furthermore, the maximum measured horizontal acceleration of $0.16\,m/s^2$ for the Rhodes Memorial bridge is higher than the lateral accelerations recommended in the Sétra Guide and the Hong Kong Structures Design Manual but lower than the recommended values in the Eurocode and the ISO Guide. In addition the natural frequency of $2.89\,Hz$ for the Rhodes Memorial Bridge falls within the range of frequencies which the Swiss Standard and American Guide Specification recommend should be avoided.

Table 6.6.: *Accelerations Limits from the Codes of Practice for the Rhodes Memorial Bridge when subjected to Jogging Loads*

Code of Practice	Limit for Vertical Acceleration	Limit for Lateral Acceleration
TMH7 & Old British Standard	$0.85\,m/s^2$	-
Sétra Guide	$0.5\,m/s^2$ to $1.0\,m/s^2$	$0.10\,m/s^2$
Eurocode with UK Annex	$0.7\,m/s^2$	$0.2\,m/s^2$
ISO Guide	$0.33\,m/s^2$	$0.27\,m/s^2$
Hong Kong Structures Design Manual	$0.85\,m/s^2$	$0.15\,m/s^2$
Swiss Standard SIA 160	Natural frequency may not be between 2.4 to $3.5\,Hz$	
American Guide Specification	Natural frequency should be greater than $5\,Hz$	

7. Discussion and Conclusions

The modern trend of designing slender, lightweight footbridges with longer spans and a natural frequency that is often within the normal range of frequencies for human activities such as walking, running and jogging has resulted in the design for vibration serviceability to become an important consideration when designing these bridges. As outlined in the literature review the current codes of practice and design procedures are either outdated or very limited with regards to the type of footbridge and pedestrian loading they consider. Some of the codes of practice give a simplified method for determining the maximum acceleration that could occur on a footbridge due to pedestrian loading, however these methods are only applicable to single span simply supported footbridges and they only look at the vertical acceleration due to a single pedestrian walking across the footbridge. For any more complex situation a complete dynamic analysis needs to be done. Of all the codes of practice reviewed only the Sétra Guide gives an indication of how to model the vertical component of a person running. In fact it provides the designer with two methods; the semi-sinusoidal model and the Fourier model. Another model that can be found in literature is the analytical load model which was developed by Occhiuzzi *et al.* (2008).

For all three of these jogging models one needs to make an assumption regarding the contact period during running. The Sétra Guide and Occhiuzzi *et al.* (2008) recommend using a contact period equal to half the total period. However, when comparing the jogging load model with the jogging forces obtained from the measurements taken by the University of Sheffield using an instrumented treadmill it is obvious that this assumption is incorrect and that instead the contact period is closer to 75 % of the total period. Based on this all three of the load models approximate the vertical component of the running force fairly well but none of them give any indication of how to model the horizontal forces.

The deterministic force model described in the literature review does however give an indication of how to model the lateral and longitudinal walking forces. On closer inspection of this model it is clear that the Fourier model was adapted from the vertical component of the deterministic model. By adapting the lateral and longitudinal components of the deterministic model in a similar manner it is possible to develop a Fourier jogging load model that would

produce forces in all three directions. Furthermore, by multiplying the force by the square root of the number of people crossing the bridge, as is done in many of the walking load models described in the literature review, it was possible to adapt the three jogging load models to include loading for more than one person. The adapted jogging load models are shown below.

The first model is the Semi-Sinusoidal Model given by Equation 7.1.

$$\begin{array}{cc} F_{vert}(t) = m \cdot k_p \cdot G_0 \cdot \sin\left(\frac{\pi t}{t_p}\right) & (j-1)T_m \leq t \leq (j-1)T_m + t_p \\ F_{vert}(t) = 0 & (j-1)T_m + t_p < t \leq jT_m \end{array} \tag{7.1}$$

The second model is the Fourier Transform Model which is given by Equations 7.2, 7.3 and 7.4 and gives the force in the vertical, lateral and longitudinal directions.

$$\begin{array}{cc} F_{vert}(t) = m \cdot G_0 + \sum_{i=1}^{N} m \cdot G_0 \cdot \alpha_{i,vert} \cdot \sin(2 \cdot \pi \cdot i \cdot f_m \cdot t) & (j-1)T_m \leq t \leq (j-1)T_m + t_p \\ F_{vert}(t) = 0 & (j-1)T_m + t_p < t \leq jT_m \end{array} \tag{7.2}$$

$$\begin{array}{cc} F_{lat}(t) = \sum_{i=1}^{N} m \cdot G_0 \cdot \alpha_{i,lat} \cdot \sin(\pi \cdot i \cdot f_m \cdot t) & (j-1)T_m \leq t \leq (j-1)T_m + t_p \\ F_{lat}(t) = 0 & (j-1)T_m + t_p < t \leq jT_m \end{array} \tag{7.3}$$

$$\begin{array}{cc} F_{long}(t) = \sum_{i=1}^{N} m \cdot G_0 \cdot \alpha_{i,long} \cdot \sin(2 \cdot \pi \cdot i \cdot f_m \cdot t) & (j-1)T_m \leq t \leq (j-1)T_m + t_p \\ F_{long}(t) = 0 & (j-1)T_m + t_p < t \leq jT_m \end{array} \tag{7.4}$$

The third model is the analytical model which is given by Equation 7.5.

$$\begin{array}{cc} F_{vert}(t) = m \cdot \left(\frac{\pi}{2 \cdot t_p}\right) \cdot G_0 \cdot \sin\left(\frac{\pi}{t_p} \cdot t\right) & (j-1)T_m \leq t \leq (j-1)T_m + t_p \\ F_{vert}(t) = 0 & (j-1)T_m + t_p < t \leq jT_m \end{array} \tag{7.5}$$

The jogging force produced by these models, with a contact period of 75 % of the total period can be represented graphically as shown in Figures 7.1, 7.2 and 7.3, assuming 1 to 3 pedestrians each weighing $700\,N$ and running in synchronisation at a frequency of $3\,Hz$.

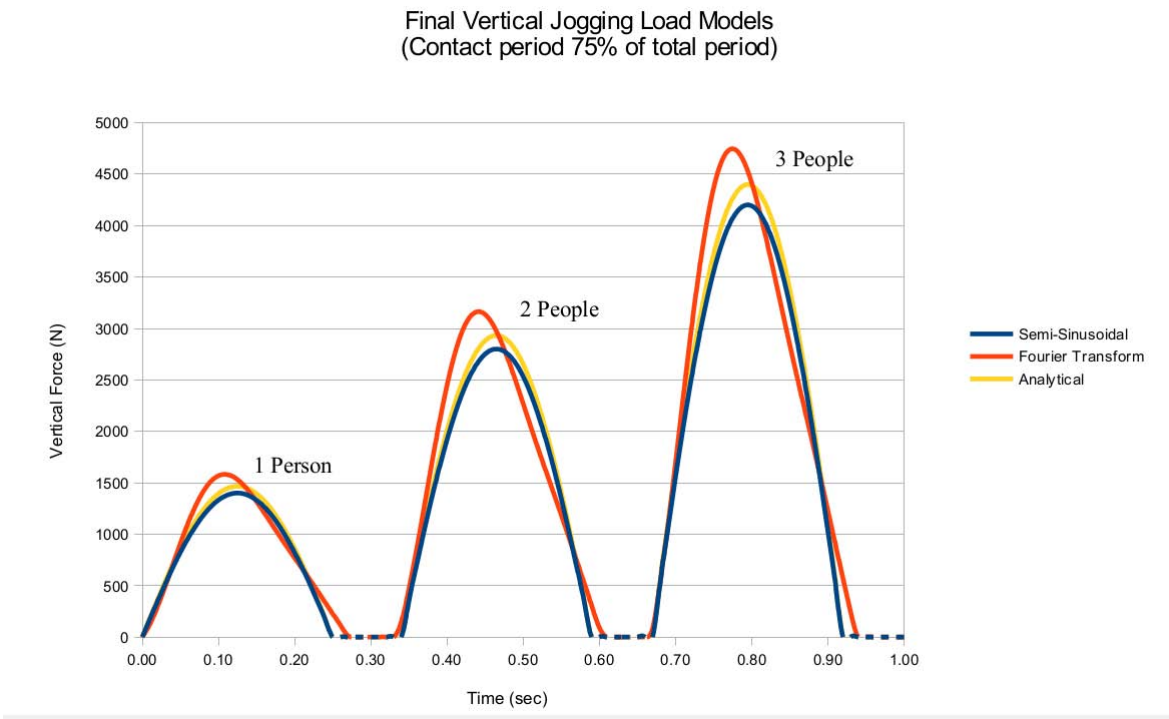

Figure 7.1.: *Final Vertical Jogging Load Models for 1 to 3 People*

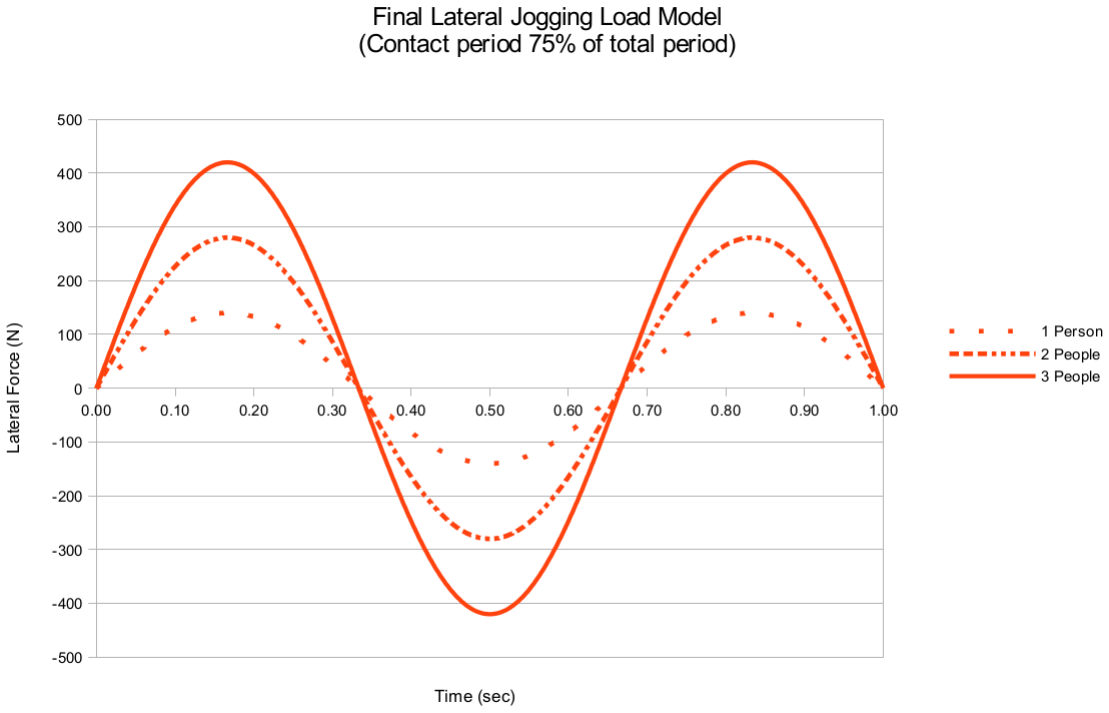

Figure 7.2.: *Final Lateral Jogging Load Model for 1 to 3 People*

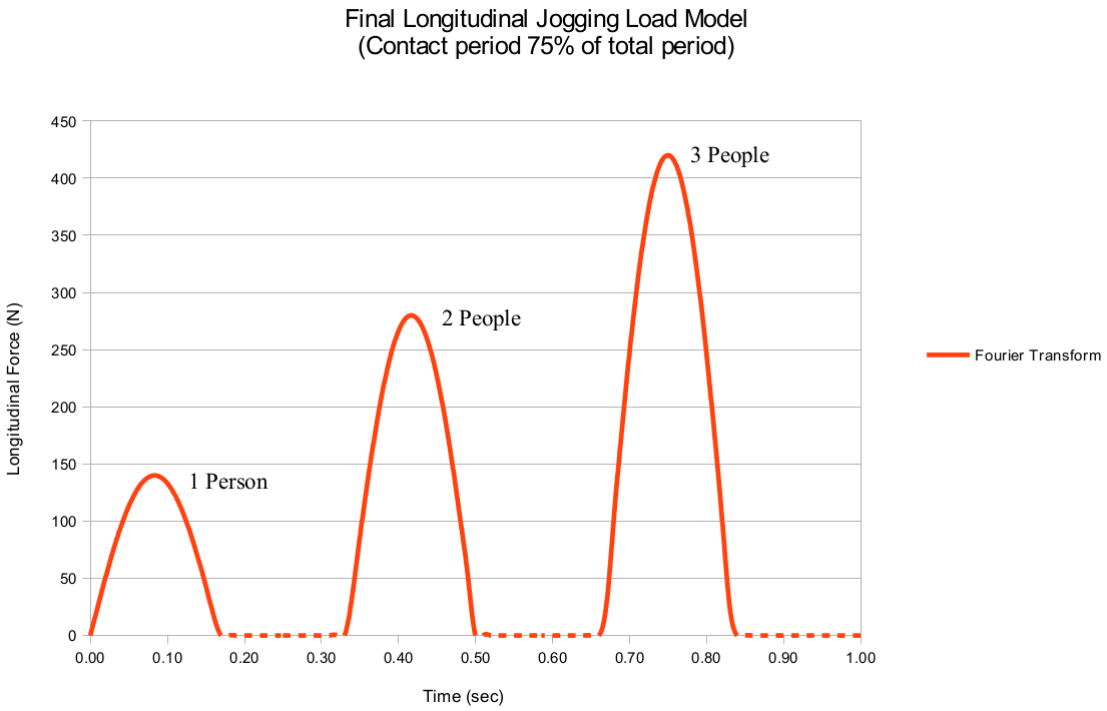

Figure 7.3.: *Final Longitudinal Jogging Load Model for 1 to 3 People*

By applying these three models to the FEM of the Rhodes Memorial Bridge as a series of forces it was possible to predict the accelerations that the bridge would experience under jogging forces. It should be noted, however, that because of the manner in which the longitudinal force has been applied to the FEM model as a single pulse force in one direction only, it has been assumed that the force pulse in the other direction is of equal magnitude and symmetrical to the applied force. The accelerations obtained in the FEM were then compared to the actual accelerations measured on the bridge under the same loading.

A comparison of these accelerations showed that the accelerations obtained by applying the jogging load models to a FEM of the bridge correlated quite well with the RMS values for the actual measured accelerations for one and two people and relatively well for three and four people. Thereafter, the actual measured accelerations drop because the people jogging across the bridge become unsynchronised. This suggest that there is a critical number of people to consider when designing a footbridge for synchronisation of people jogging. This study suggests that this value is 4 or 5 people, however this needs to be confirmed with further testing. Further research and testing are required to improve the correlation between the predicted acceleration and the actual measured acceleration.

7.1. Accuracy of the jogging load models

Based on the comparison done with the measured jogging forces obtained from the University of Sheffield it was shown that the jogging load models with a contact period of 75% of the total period give a reasonable prediction of the jogging forces. However, there is still some uncertainty regarding the accuracy of these models. This includes:

- The comparison of the forces could only be done for the 9 measured vertical forces obtained from the University of Sheffield. This is a very small sample size.
- No similar comparison was possible for the lateral and longitudinal directions and it was not possible to verify the accuracy of the lateral and longitudinal forces generated using the jogging load models.
- All of the jogging load models include a term for the weight of the pedestrian. In the codes this assumed to be $700\,N$, however during the testing of the Rhodes Memorial Bridge the weights of the people jogging across the bridge when measuring the accelerations were not recorded. Therefore it was not possible to accurately account for this in the FEM and instead the value of $700\,N$ which is given in the codes was used.
- One of the weaknesses of all of the jogging load models is that they rely on dynamic load factors which cannot be accurately determined. A lot of research has been done to determine reasonable vertical dynamic load factors for both walking and running. However, this is not the case for lateral and longitudinal dynamic load factors for jogging.
- The manner in which the number of people jogging across the bridge is accounted for is not an accurate depiction of what occurred during the testing of the Rhodes Memorial Bridge.

7.2. Accuracy of the FEM

Due to the limited information available it was not possible to fully update the FEM of the Rhodes Memorial Bridge and the natural frequency for only the first mode of vibration was confirmed. Further areas of concern with the FEM include:

- The reinforcement and post tensioning cables were not modelled and this could have an effect on the displacement and hence the accelerations predicted by the FEM.
- The accuracy of the other modes of vibration was not checked.
- The results of a FEM are sensitive to the meshing technique used and the level of refinement.

7.3. Conclusions

The following conclusions were made based on the original objectives of this thesis:

1. TMH7 and some of the other older codes are outdated and only consider a single pedestrian walking across a bridge. Furthermore, the majority of the current codes of practice in use are based on a deterministic force model which can not be used to accurately predict jogging loads. With the exception of the Sétra Guide none of the codes of practice reviewed give a method to determine the forces produced by people jogging across a footbridge. This is a serious problem, especially if one considers the research done by Keller *et al.* (1996) that showed that slow jogging can cause vertical forces up to 1.6 times greater than these caused by walking at the same speed or running at higher speeds.
2. Three vertical jogging load models discussed in the literature review. Testing found that the assumption made by all of these models that the contact period is equal to 50 % of the total period was incorrect and it is in fact closer to 75 % of the total period.
3. The models discussed in the literature review were adapted for a contact period of 75 % of the total period and to include lateral and longitudinal forces. They were also adapted to include the effect of multiple people by using information obtained from human induced force models for walking that were discussed in the literature review.
4. Regardless of the issues with the jogging load models and FEM of the Rhodes Memorial Bridge it was possible to determine the response of the Rhodes Memorial Bridge to jogging forces and compare it to a FEM of the same footbridge when subjected to the jogging load models that were described in this thesis.

8. Recommendations

On the basis of the conclusions in Chapter 7, the following recommendations are made:

- Further measurements need to be done using an instrumented treadmill to obtain the vertical, lateral and longitudinal jogging forces for a much larger sample size in order to do a more comprehensive comparison of the forces produced using the jogging load models with the actual measured forces.
- Further research is required to determine the dynamic load factors in the lateral and longitudinal directions due to jogging.
- Further testing of real footbridges and a comparison of the measured accelerations to those obtained in fully updated FEMs of the same bridges are required to further test and refine the jogging load models. During these tests the weights of the people participating in the tests should be recorded. It is also recommended that more than one reading be taken for each group of people jogging across the bridges to provide statistically relevant data.
- The manner in which the number of people jogging across the bridge is accounted for needs to be updated to more accurately depict what occurred during the testing of the Rhodes Memorial Bridge when more than four people jogged across it.
- The acceptable acceleration limits given in the codes of practice need to be confirmed.
- The way in which the dynamic properties of a bridge change due to human-structure synchronisation need to be determined.
- Probabilistic and frequency domain jogging force models need to be developed to see whether they give a more accurate representation of randomness of the jogging force and multi-pedestrian loads.

References

A view on cities, 2014. Millennium Bridge - London Millennium Footbridge [Online]. Available: http://www.aviewoncities.com/london/millenniumbridge.htm [2014, April 21].

Adao da Fonseca, A., 2008. Footbridges in Portugal. *Footbridges 2008: Third International Conference*. July, Portugal.

Allen, D. and Murray, T., 1993. Design criterion for vibrations due to walking. *Engineering Journal*, 30(4), pp. 117–129.

Andriacchi, T., Ogle, J., and Galante, J., 1977. Walking speed as a basis for normal and abnormal gait measurements. *Journal of Biomechanics*, 10, pp. 261–268.

Bachmann, H., 1995. Vibration Problems in Structures. *Practical Guidelines, Birkhauser Verlag, Basel, Boston, Berlin*.

Bachmann, H. and Ammann, W., 1987. Vibrations in Structures Induced by Man and Machines. *International Association of Bridge and Structural Engineering, Zurich, Switzerland*.

Bachmann, H., Pretlove, A., and Rainer, H., 1995. *Dynamic forces from rhythmical human body motions, in: Vibration Problems in Structures: Practical Guidelines*. Birkhäuser, Basel. Appendix G.

Barreira, T., Rowe, D., and Kang, M., 2010. Parameters of Walking and Jogging in Healthy Young Adults. *International Journal of Exercise Science*, 3(1), pp. 4–13 [Online]. Available: http://digitalcommons.wku.edu/cgi/viewcontent.cgi?article=1183\&context=ijes [2013, August 27].

Blanchard, J., Davies, B., and Smith, J., 1977. Design criteria and analysis for dynamic loading of footbridges. *Proceedings of the DOE and DOT TRRL Symposium on Dynamic Behaviour of Bridges*. Crowthorne, UK.

Brownjohn, J., Pavic, A., and Omenzetter, P., 2004. A spectral density approach for modelling continuous vertical forces on pedestrian structures due to walking. *Canadian Journal of Civil Engineering*, 31, pp. 65–77.

BSI, 2010. *Eurocode 1: Actions on structures - Part 2: Traffic loads on bridges*. BS EN 1991-2.

Butz, C., 2008. Codes of Practice for Lively Footbridges: State-of-the-Art and Required Measures. *Footbridges 2008: Third International Conference*. July, Portugal.

COMSOL, 1998-2013. *COMSOL Documentation*. North America.

CSIR, 1981. *TMH7: Parts 1 and 2 - Code of Practice for the Design of Highway Bridges and Culverts in South Africa*. PO Box 395, Pretoria, 0001. National Institute for Transport and Road Research of the Council for Scientific and Industrial Research.

Ellis, B., 2003. The influence of crowd size on floor vibrations induced by walking. *The Structural Engineer*, 81, pp. 20–27.

Eriksson, P., 1994. *Vibration of Low-Frequency Floors - Dynamic Forces and Response Prediction*. Ph.D. thesis, Chalmers University of Technology, Goteborg, Sweden.

Faber, M., 2009. Lecture 9: Finites Elements Procedure, Klaus-Jurgen Bathe. Swiss Federal Institute of Technology Zurich [Online]. Available: http://www.ibk.ethz.ch/emeritus/fa/education/FE_II/Lecture_9_Schauwecker.pdf [2013, August 10].

Faisca, R. G., Coutinho, D. P., Maglita, C., and Roitman, N., 2008. Exploratory Data Analysis of Human Induced Dynamic Load in Structures. *Footbridges 2008: Third International Conference*. July, Portugal.

Feichtinger, D., 2008. Bridge Design. *Footbridges 2008: Third International Conference*. July, Portugal.

Google Maps, 2013. Rhodes Memorial Footbridge [Online]. Available: https://maps.google.com [2013, July 23].

Grundmann, H., Kreuzinger, H., and Schneider, M., 1993. Dynamic calculations of footbridges. *Bauingenieur*, 68, pp. 215–225.

Hauksson, F., 2005. *Dynamic Behaviour of Footbridges Subject to Pedestrian-Induced Vibrations*. Master's thesis, Lund Universtiy, Division of Structural Mechanics, LTH, Lund University, Box 118, SE-221 00 Lund, Sweden [Online]. Available: http://www.byggmek.lth.se/fileadmin/byggnadsmekanik/publications/tvsm5000/web5133.pdf [2010, September 21].

ISO, 2004. *Bases for design of structures - Serviceability of buildings and pedestrian walkways against vibration*. International Organisation for Standardization.

Keil, A., 2008. Design of Footbridges - Are There Limits? *Footbridges 2008: Third International Conference*. July, Portugal.

Keil, P., 2012. Evaluation of the Vibration Serviceability of Footbridges with regards to Jogging. University of Cape Town.

Keller, T., Weisberger, A., Ray, J., Hasan, S., Shiavi, R., and Spengler, D., 1996. Relationship between vertical ground reaction force and speed during walking, slow jogging, and running. *Clinical Biomechanics*, 11, pp. 253–259.

Kerr, S., 1998. *Human Induced Loading on Staircases*. Ph.D. thesis, University College London, Mechanical Engineering Department, London, UK.

Kubota, Y. and Kishimoto, T., 2008. Structural Continuity and Relativity for Footbridge Design. *Footbridges 2008: Third International Conference*. July, Portugal.

Matsumoto, Y., Nishioka, T., Shiojiri, H., and Matsuzaki, K., 1978. Dynamic design of footbridges. **P-17/78**, ed., *IABSE Proceedings*, pp. 1–15.

Matsumoto, Y., Sato, S., Nishioka, T., and Shiojiri, H., 1972. A study on design of pedestrian over-bridges. *Transactions of JSCE 4*, pp. 50–51.

Matsuo Bridge Co. Ltd, 1999. The Basic Bridge Types [Online]. Available: http://www.matsuo-bridge.co.jp/english/bridges/index.shtm [2009, February 09].

McMahon, T. and Greene, P., 1979. The influence of track compliance on running. *Journal of Biomechanics*, 12, pp. 893–904.

Mouring, S. and Ellingwood, B., 1994. Guidelines to minimize floor vibrations from building occupants. *Journal of Structural Engineering*, 120(2), pp. 507–526.

Moyo, P., 2008. Advanced Structural Dynamics with Applications - Dynamics Module. (Unpublished).

Newland, D. E., 2002. Vibration of the London Millennium Footbridge: Part 1 - Cause. Department of Engineering, University of Cambridge [Online]. Available: http://www2.eng.cam.ac.uk/\~den/ICSV9_06.htm [2010, September 05].

Occhiuzzi, A. and Spizzuoco, M., 2008. A Running Pedestrian Dynamic Load Model for Footbridges. *Footbridges 2008: Third International Conference*. July, Portugal.

Occhiuzzi, A., Spizzuoco, M., and Ricciardelli, F., 2008. Loading models and response control of footbridges excited by running pedestrians. *Structural Control and Health Monitoring*, 15, pp. 349–368 [Online]. Available: www.interscience.wiley.com [2010, September 30].

Ohlsson, S., 1982. *Floor Vibrations and Human Discomfort*. Ph.D. thesis, Chalmers University of Technology, Goteborg, Sweden.

Pachi, A. and Ji, T., 2005. Frequency and velocity of people walking. *The Structural Engineer*, 83, pp. 36–40.

Pavic, A. and Brownjohn, J., 2008. Vibration Serviceability of Civil Structures: Design and Assessment of Structures for Vibration. (Unpublished).

Pavic, A., Hung Yu, C., Brownjohn, J., and Reynolds, P., 2005. Verification of the Existence of Human-Induced Horizontal Forces due to Vertical Jumping [Online]. Available: vibration.shef.ac.uk/pdfs/IMAC_XX_2.pdf [2010, Septemebr 29].

Pernica, G., 1990. Dynamic load factors for pedestrian movements and rhythmic exercises. *Canadian Acoustics*, 18, pp. 3–18.

Pimentel, R., 1997. *Vibrational Performance of Pedestrian Bridges Due to Human-Induced Loads*. Ph.D. thesis, University of Sheffield, Sheffield, UK.

Pimentel, R. and Frenandes, H., 2002. A simplified formulation for vibration serviceability of footbridges. *International Conference on the Design and Dynamic Behaviour of Footbridges*. Paris, France.

Pimentel, R., Pavic, A., and Waldron, P., 2001. Evaluation of design requirements for footbridges excited by vertical forces from walking. *Canadian Journal of Civil Engineering*, 28(5), pp. 769–777 [Online]. Available: http://www.ingentaconnect.com/content/nrc/cjce/2001/00000028/00000005/art00002;jsessionid=27n5qtlfe29cc.alice [2008, August 11].

Pirner, M. and Urushadze, S., 2008. Pedestrian Dynamics and Footbridges. *Footbridge 2008: Third International Conference*. July, Portugal.

Pizzimenti, A. and Ricciardelli, F., 2005. Experimental evaluation of the dynamic lateral loading of footbridges by walking pedestrians. *Sixth European Conference on Structural Dynamics EURODYN*. September, Paris, France.

Project for Public Spaces. Millennium and Jubliee Pedestrian Bridges [Online]. Available: http://www.pps.org/great_public_spaces/one?public_place_id=658# [2010, September 05].

Racic, V., Brownjohn, J., and Pavic, A., 2007. *Human Walking and Running Forces: Novel Experimental Characterization and Application in Civil Engineering Dynamics*. Ph.D. thesis, The University of Sheffield, Vibration Engineering Section, Department of Civil and Structural Engineering [Online]. Available: http://sem-proceedings.com/26i/sem.org-IMAC-XXVI-Conf-s38p04-Human-Walking-Running-Forces-Novel-Experimental-Characterization.pdf [2013, May 18].

Racic, V., Brownjohn, J., and Pavic, A., 2010. Reproduction and application of human bouncing and jumping forces from visual marker data. *Journal of Sound and Vibration* [Online]. Available: http://www.sciencedirect.com [2010, September 30].

Racic, V., Pavic, A., and Brownjohn, J., 2009. Experimental identification and analytical modelling of human walking forces: Literature review. *Journal of Sound and Vibration* [Online]. Available: http://www.sciencedirect.com [2010, September 30].

Rainer, J., Pernica, G., and Allen, D., 1988. Dynamic loading and response of footbridges. *Canadian Journal of Civil Engineering*, 15, pp. 66–71.

Romanov, N., 2006. Pose Tech [Online]. Available: http://www.posetech.com/pose_method/pose-logo.html [2010, September 29].

Ronnquist, A., 2005. Pedestrian Induced Lateral Vibrations of Slender Footbridges. Tech. rep., Norwegian University of Science and Technology, Trondheim, Norway.

Sahnaci, C. and Kasperski, 2005. Random loads induced by walking. *Sixth European Conference on Structural Dynamics, EURODYN*. September, Paris.

Sétra, 2006. *Technical Guideline: Footbridges - Assessment of Vibrational Behaviour of Footbridges under Pedestrian Loading (English Translation)*. 28 rue des Saints-Peres, 75007 Paris, France.

Standards Policy and Strategy Committee, 2006. *Steel, Concrete and Composite Bridges - Part 2: Specification for Loads*.

Stevenson, R., 1821. Description of bridges of suspension. *Edinburgh Philosophical Journal*, 5(10), pp. 237–256.

Sun, L. and Yuan, X., 2008. Study on Pedestrian-Induced Vibration of Footbridge. *Footbridges 2008: Third International Conference*. July, Portugal.

Sun, L. M. and Yan, X. F., 2004. Human walking induced footbridge vibration and its serviceability design. *Journal of Tongji University (Natural Science)*, 32(8), pp. 996–999.

Switek, B., 2010. Evo. Anthro. Study Suggests You Might Be Running Wrong [Online]. Available: http://scienceblogs.com/laelaps/2010/01/humans_that_had_to_escape.php [2010, September 29].

The Concrete Centre, 2004. Eurocode [Online]. Available: http://www.concretecentre.com [2010, September 27].

The Institution of Structural Engineers, 2007. Eurocodes Experts [Online]. Available: http://www.eurocodes.co.uk/ [2010, September 23].

Wheeler, J., 1982. Prediction and control of pedestrian induced vibration in footbridges. *ASCE Journal of the Structural Division*, 108(ST9), pp. 2045–2065.

Yamasaki, M., Sasaki, T., and Torii, M., 1991. Sex difference in the pattern of lower limb movement during treadmill walking. *European Journal of Applied Physiology*, 62, p. 103.

Yao, S., Wright, J., Pavic, A., and Reynolds, P., 2006. Experimental study of human-induced dynamic forces due to jumping on a perceptibly moving structure. *Journal of Sound and Vibration*, 296, pp. 150–165.

Yao, S., Wright, J. R., Pavic, A., and Reynolds, P., 2002. Forces generated when bouncing or jumping on a flexible structure [Online]. Available: vibration.shef.ac.uk/pdfs/ISMA_2002_1.pdf [2010, September 29].

Young, P., 2001. Improved floor vibration prediction methodologies. *Proceedings of Arup Vibration Seminar on Engineering for Structural Vibration—Current Developments in Research and Practice*. London, UK.

Živanović, S., 2006. *Probability-Based Estimation of Vibration for Pedestrian Structures due to Walking*. Ph.D. thesis, University of Sheffield, UK.

Zivanovic, S., Brownjohn, J., and Pavic, A., 2008. Vibration Performance of Footbridges under Pedestrian Traffic. *Footbridge 2008: Third International Conference*. July, Portugal.

Živanović, S., Pavić, A., and Reynolds, P., 2005. Vibration Serviceability of Footbridges Under Human-Induced Excitation: A Literature Review. *Journal of Sound and Vibration*, 279(1-2), pp. 1–74 [Online]. Available: http://www.sciencedirect.com [2010, September 27].

Živanović, S., Pavić, A., and Reynolds, P., 2007. Probability-based prediction of multi-mode vibration response to walking excitation. *Engineering Structures*, 29, pp. 942–954.

Appendix A. Jogging Models

A.1. Introduction

This Appendix shows the Matlab plots for the comparison of the Semi-Sinusoidal, Fourier and Analytical running load models with the actual running forces measured by the University of Sheffield.

A.2. Comparison with Contact Period at Half Running Period

These plots from Matlab show the comparison with the assumption that the contact period is equal to the half the running period in each of the running load models.

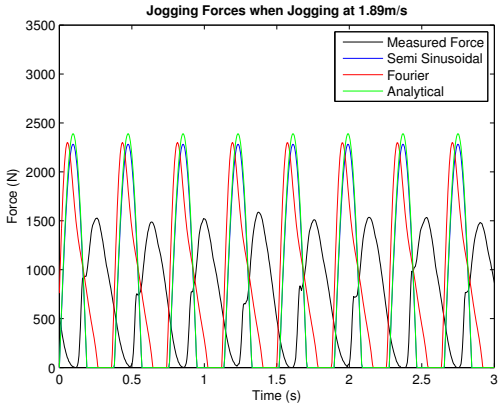

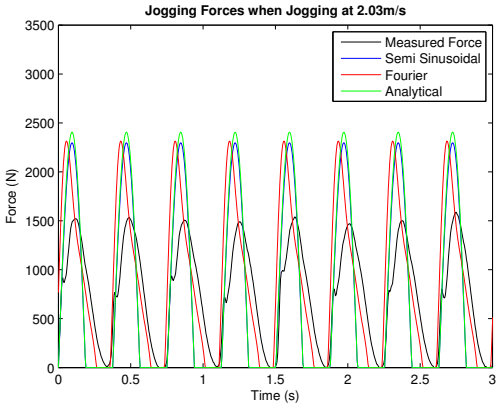

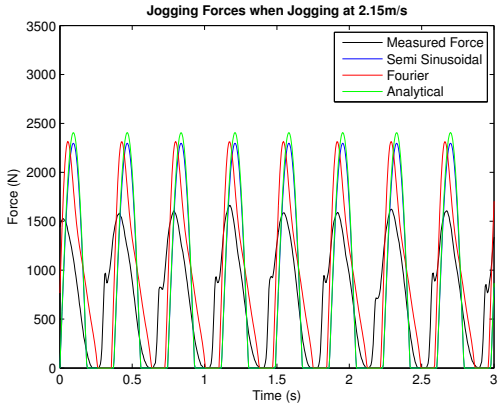
Jogging Forces when Jogging at 2.15m/s
Measured Force
Semi Sinusoidal
Fourier
Analytical
Force (N)
Time (s)

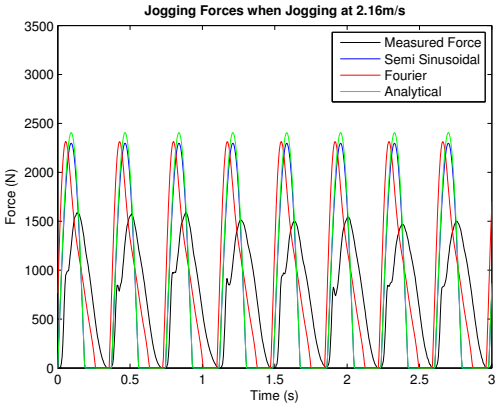
Jogging Forces when Jogging at 2.16m/s
Measured Force
Semi Sinusoidal
Fourier
Analytical
Force (N)
Time (s)

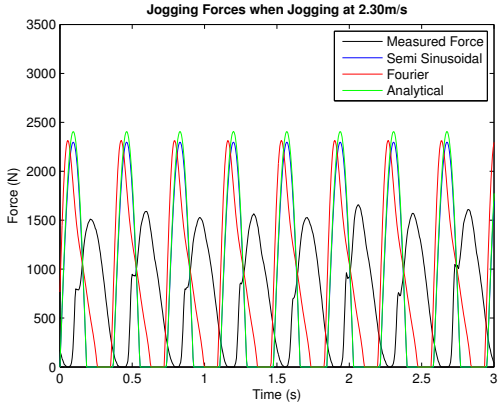
Jogging Forces when Jogging at 2.30m/s
Measured Force
Semi Sinusoidal
Fourier
Analytical
Force (N)
Time (s)

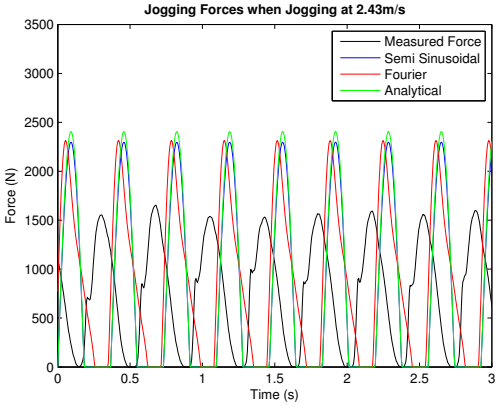
Jogging Forces when Jogging at 2.43m/s
Measured Force
Semi Sinusoidal
Fourier
Analytical
Force (N)
Time (s)

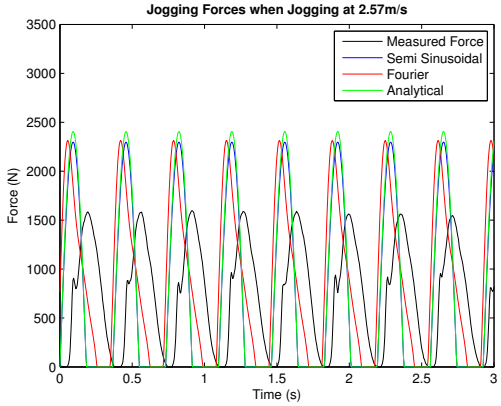
Jogging Forces when Jogging at 2.57m/s
Measured Force
Semi Sinusoidal
Fourier
Analytical
Force (N)
Time (s)

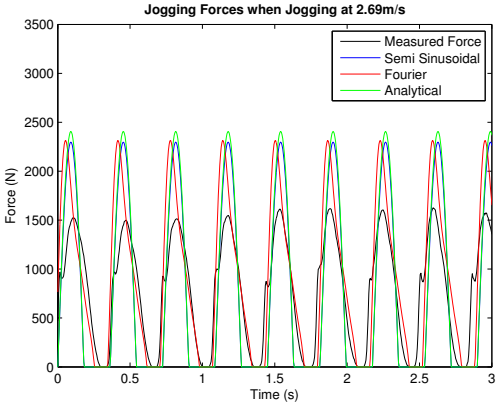
Jogging Forces when Jogging at 2.69m/s
Measured Force
Semi Sinusoidal
Fourier
Analytical
Force (N)
Time (s)

A.3. Comparison with Longer Contact Period

These plots from Matlab show the comparison with the assumption that the contact period is equal to the $\frac{3}{4}$ of the running period in each of the running load models.

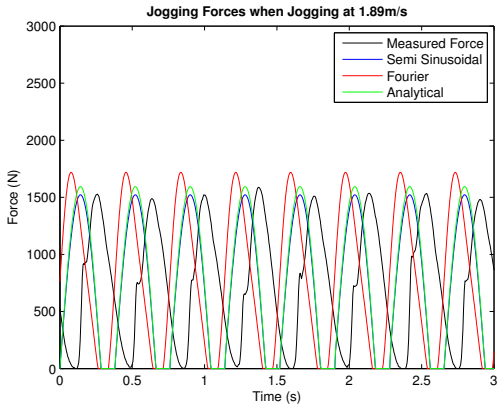

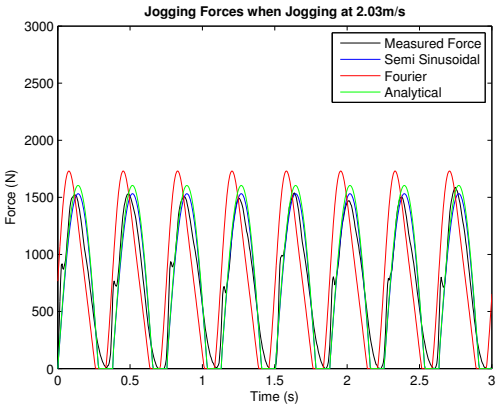

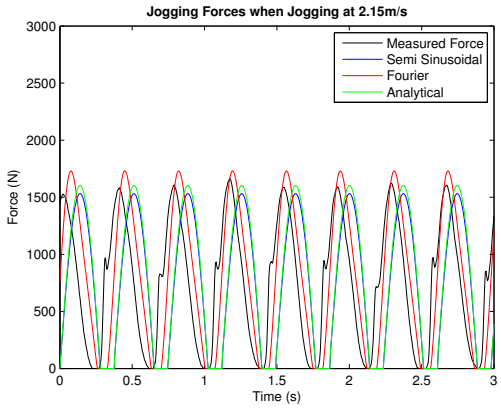

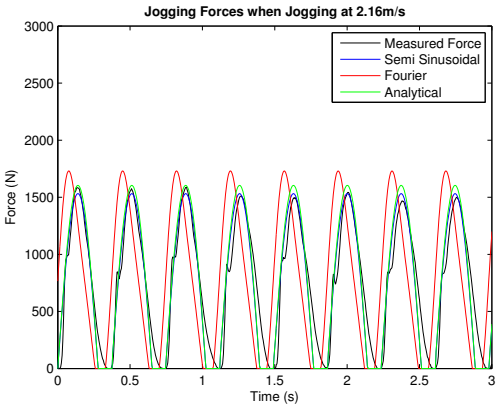

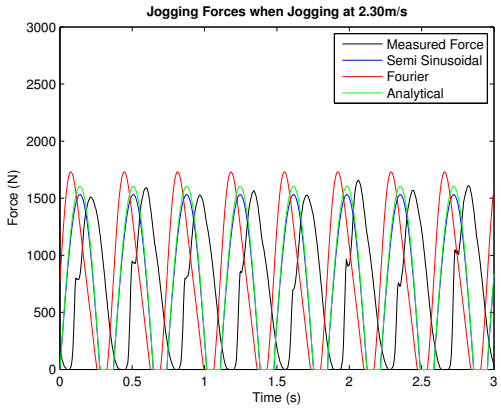

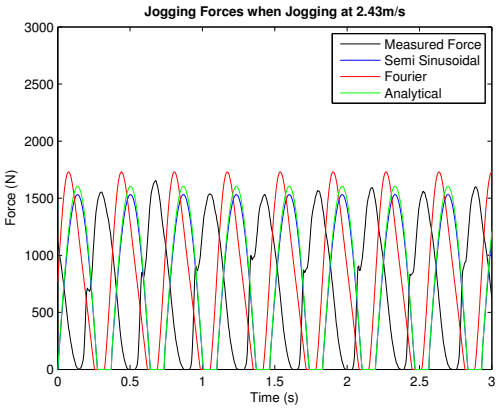

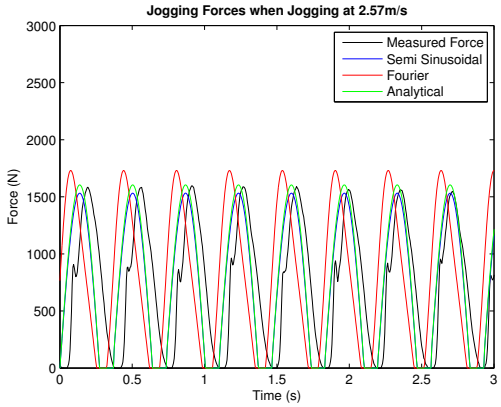
Jogging Forces when Jogging at 2.57m/s
Measured Force
Semi Sinusoidal
Fourier
Analytical
Force (N)
Time (s)
0
500
1000
1500
2000
2500
3000
0.5
1
1.5
2
2.5
3

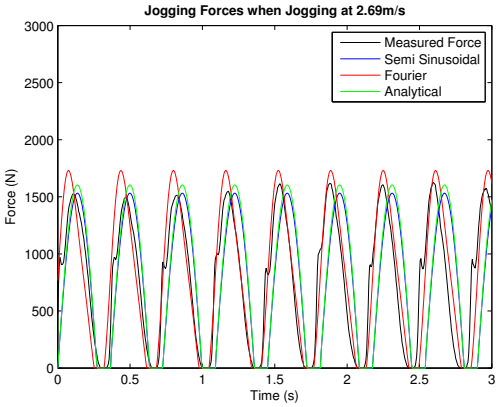
Jogging Forces when Jogging at 2.69m/s
Measured Force
Semi Sinusoidal
Fourier
Analytical
Force (N)
Time (s)
0
500
1000
1500
2000
2500
3000
0.5
1
1.5
2
2.5
3

Appendix B. Simulations Results

B.1. Introduction

This Appendix shows the COMSOL Multiphysics plots for the simulations done to determine the ease in which the jogging load models can be applied to a simple beam structure in order to determine the accelerations in the vertical direction due to one person running across the structure.

B.2. Acceleration Results

The resulting vertical accelerations at each time step for the 3 jogging load models obtained in the middle of the beam are summarised in the plots below.

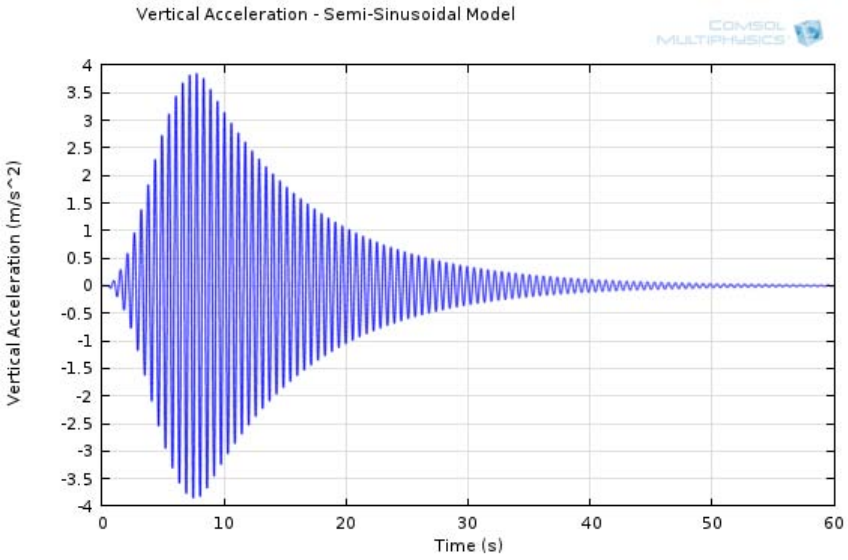

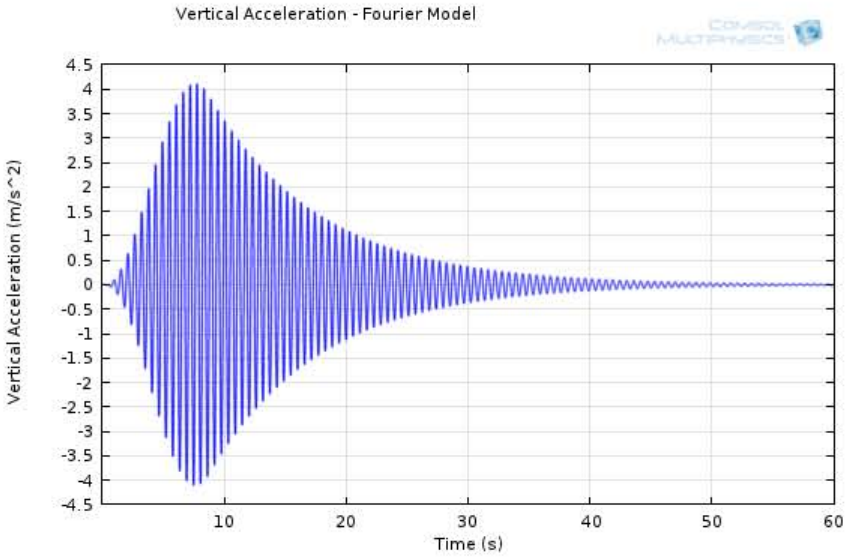
Vertical Acceleration - Fourier Model
Vertical Acceleration (m/s^2)
Time (s)

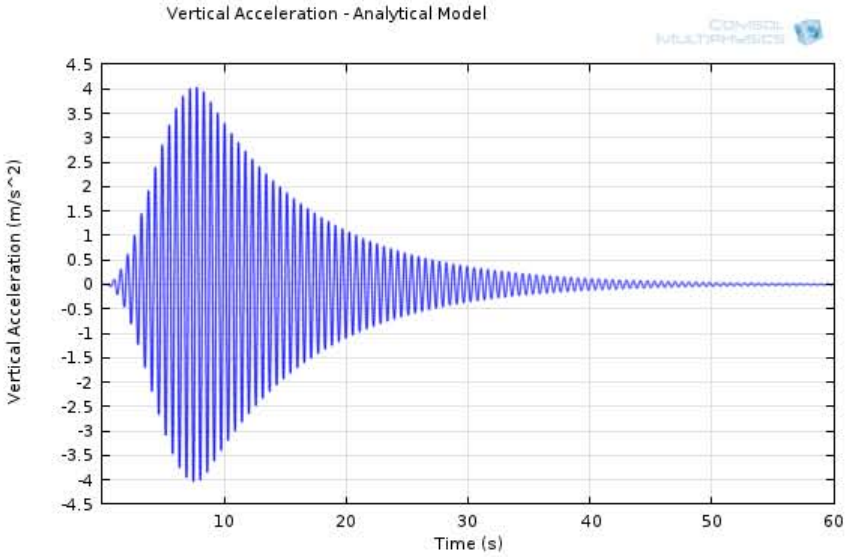
Vertical Acceleration - Analytical Model
Vertical Acceleration (m/s^2)
Time (s)

Appendix C. Verification Results

C.1. Introduction

This Appendix shows the data obtained for the Rhodes Memorial Bridge, the COMSOL Multiphysics plots for the bridge and the predicted accelerations for the bridge calculated using the simple methods described in literature.

C.2. Rhodes Memorial Bridge Data

This section outlines the data obtained for the Rhodes Memorial Bridge.

C.2.1. Drawings

The following two drawings were obtained from the City of Cape Town for the footbridge. The first drawing shows the general layout of the bridge and the second drawing gives the reinforcement and prestressing details for the bridge. The originals obtained were A0 size.

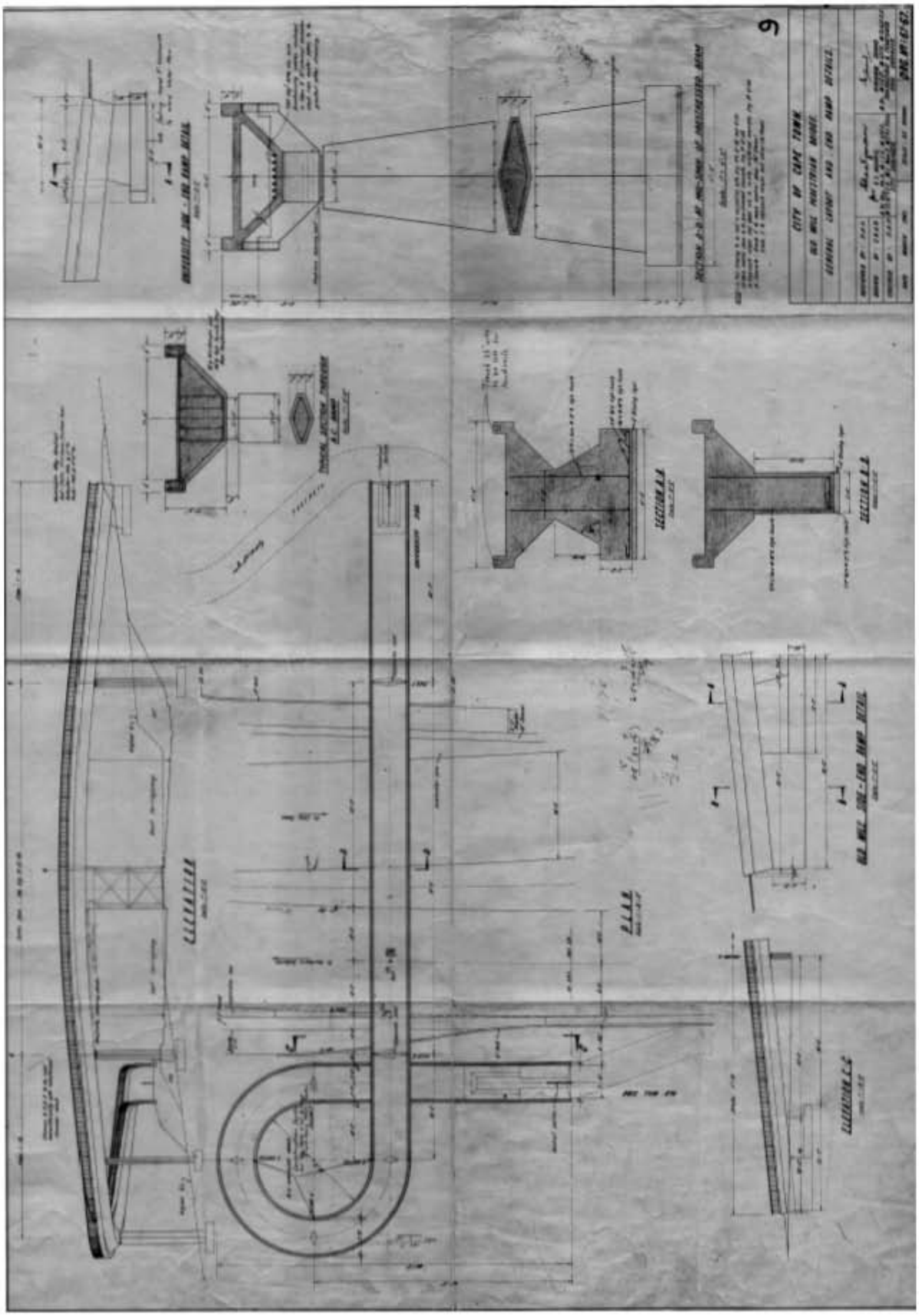

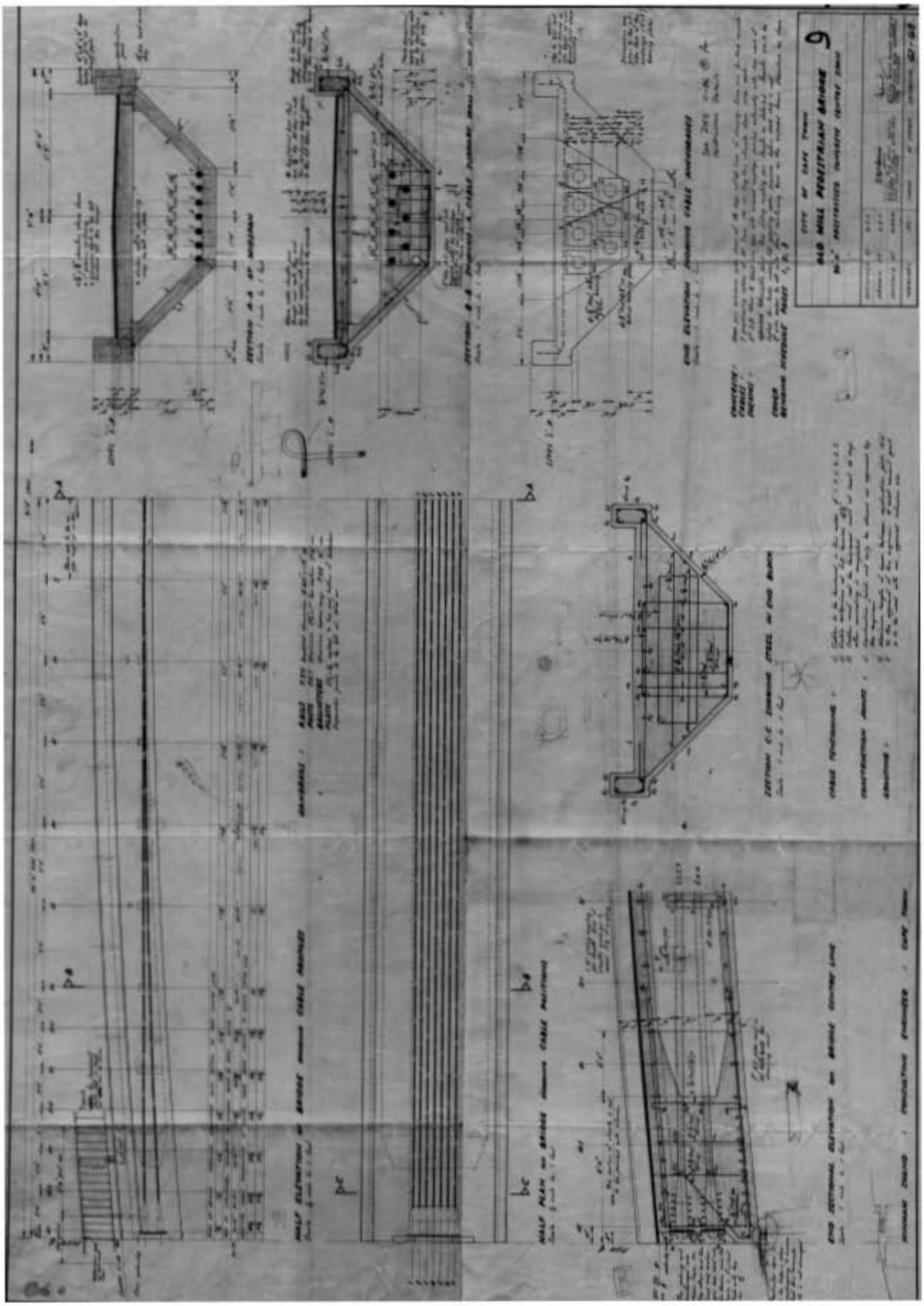

C.2.2. Site Measurements

The following measurements were taken during the site visit conducted on the 23 July 2013.

- Arc length of bridge deck $= 27.750\,m$
- Width of bridge deck $= 2.240\,m$
- Inside height of edge upstand $= 0.200\,m$
- Top width of edge upstand $= 0.250\,m$
- Outside height of edge upstand $= 0.375\,m$
- Bottom width of edge upstand $= 0.150\,m$
- Width of bottom of bridge $= 0.910\,m$
- Skew length of side of bridge $= 1.080\,m$

C.3. COMSOL Multiphysics

C.3.1. Input Data - Jogging Load Models Applied

This section gives the plots of the forces that were applied to the FEM of the Rhodes Memorial Bridge for the various jogging load models for multiple people running. Each load plot only gives the load for the first period and they are based on the assumption that the contact period is 75% of the total period.

Vertical Load Plots for Multiple People

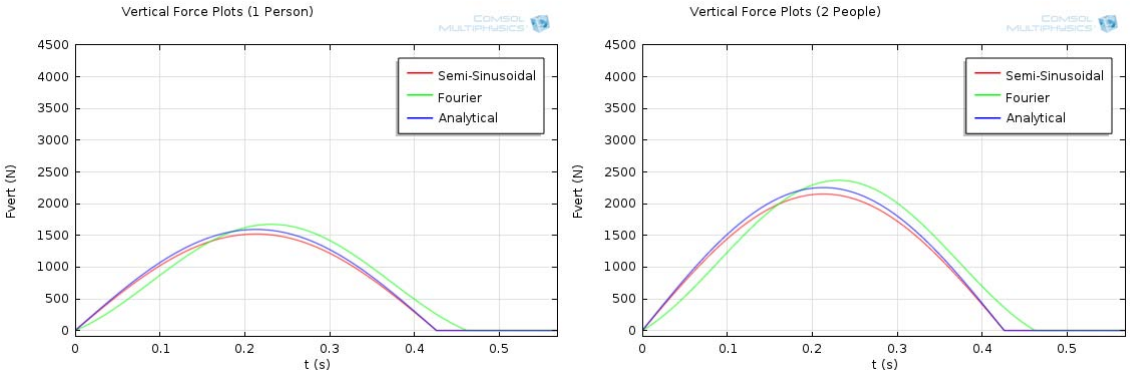

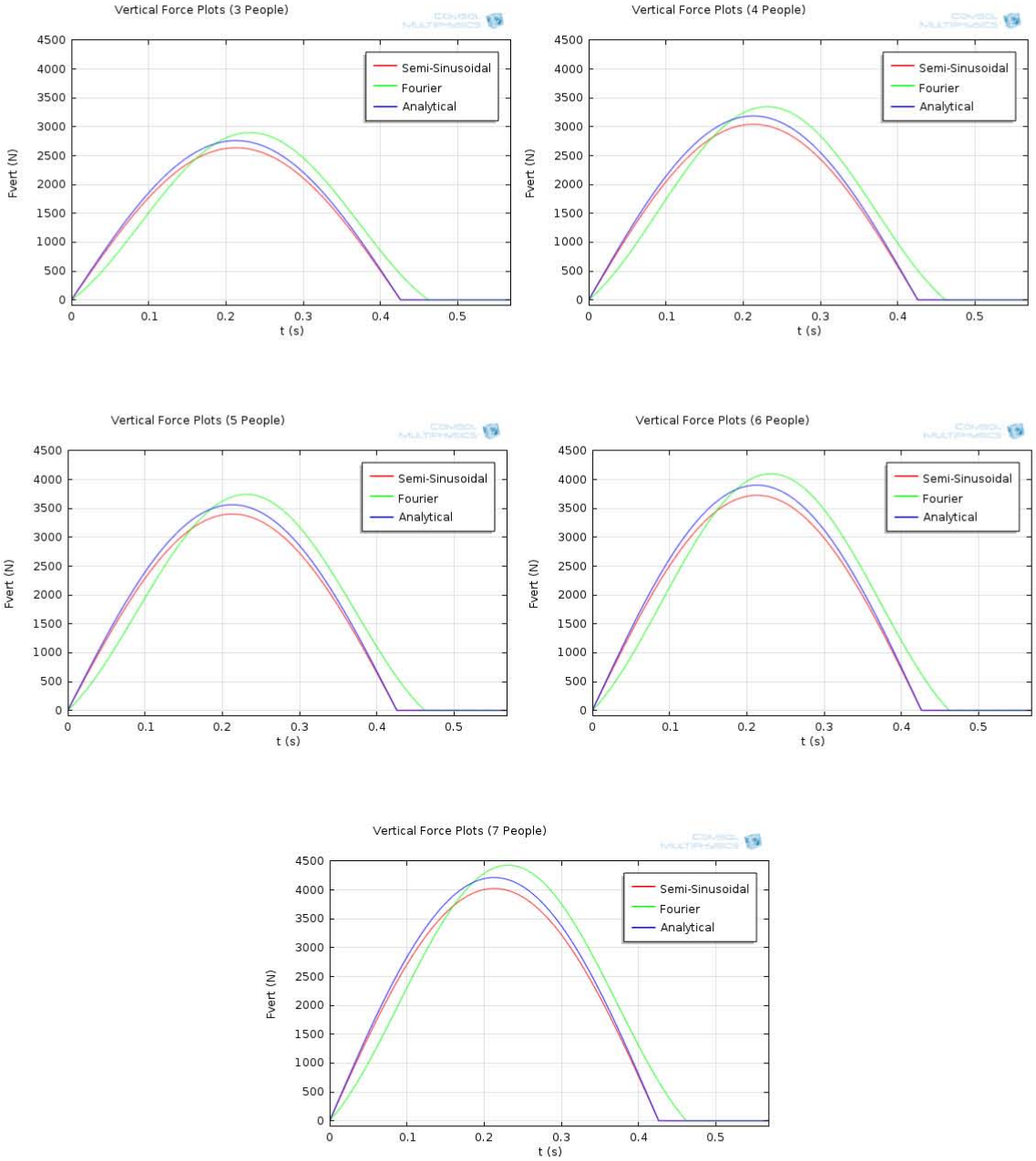
Vertical Force Plots (3 People)
Vertical Force Plots (4 People)
Vertical Force Plots (5 People)
Vertical Force Plots (6 People)
Vertical Force Plots (7 People)
Semi-Sinusoidal
Fourier
Analytical
Fvert (N)
t (s)

Lateral Load Plots for Multiple People

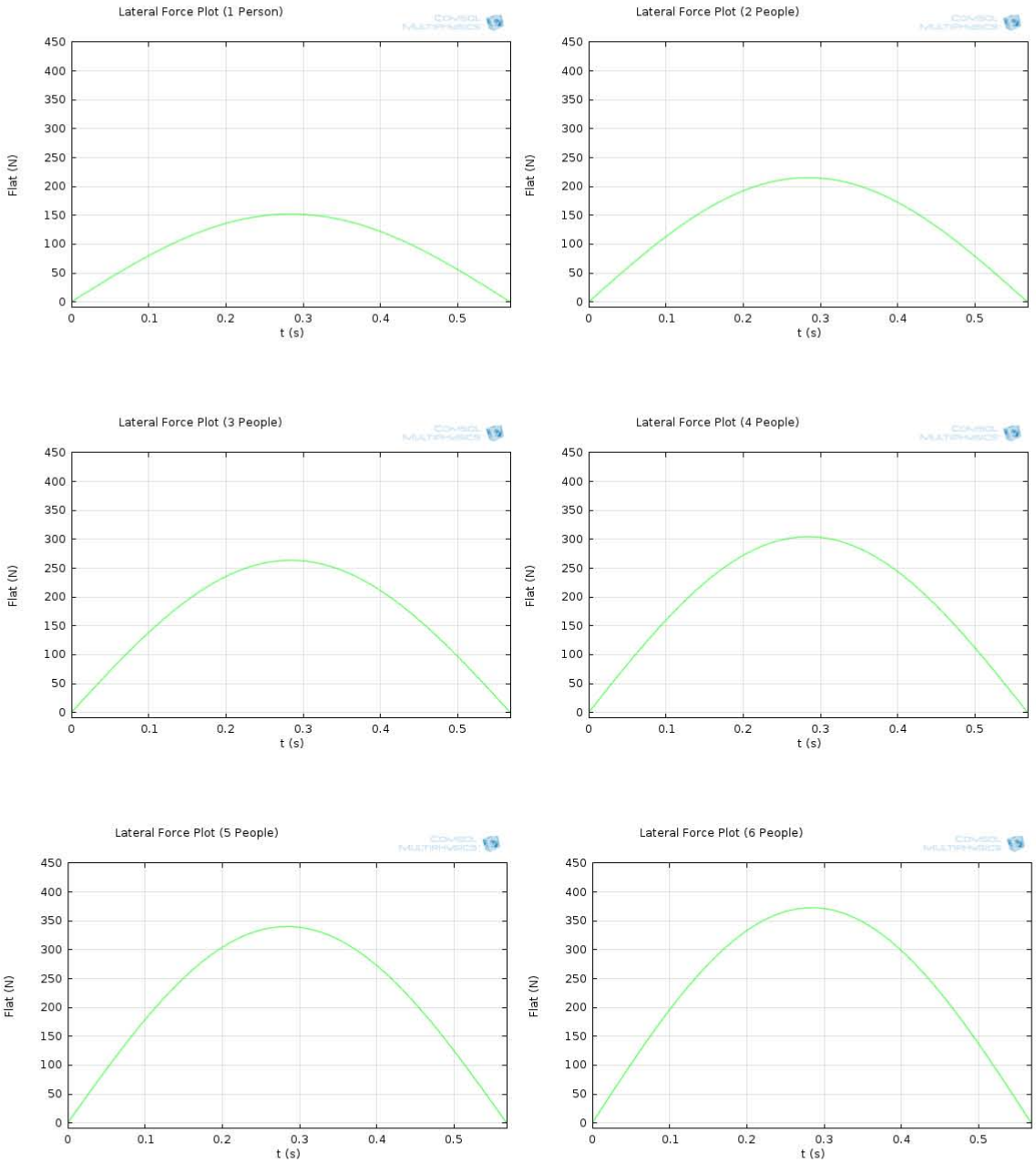

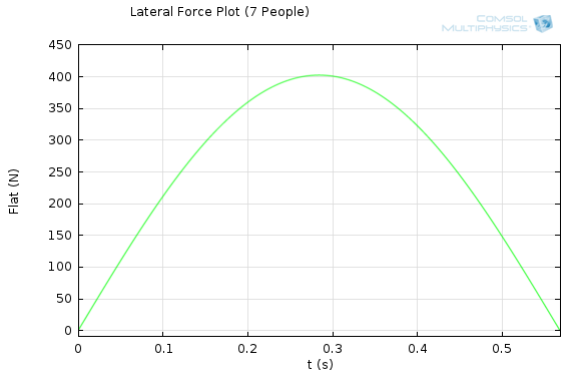

Longitudinal Load Plots for Multiple People

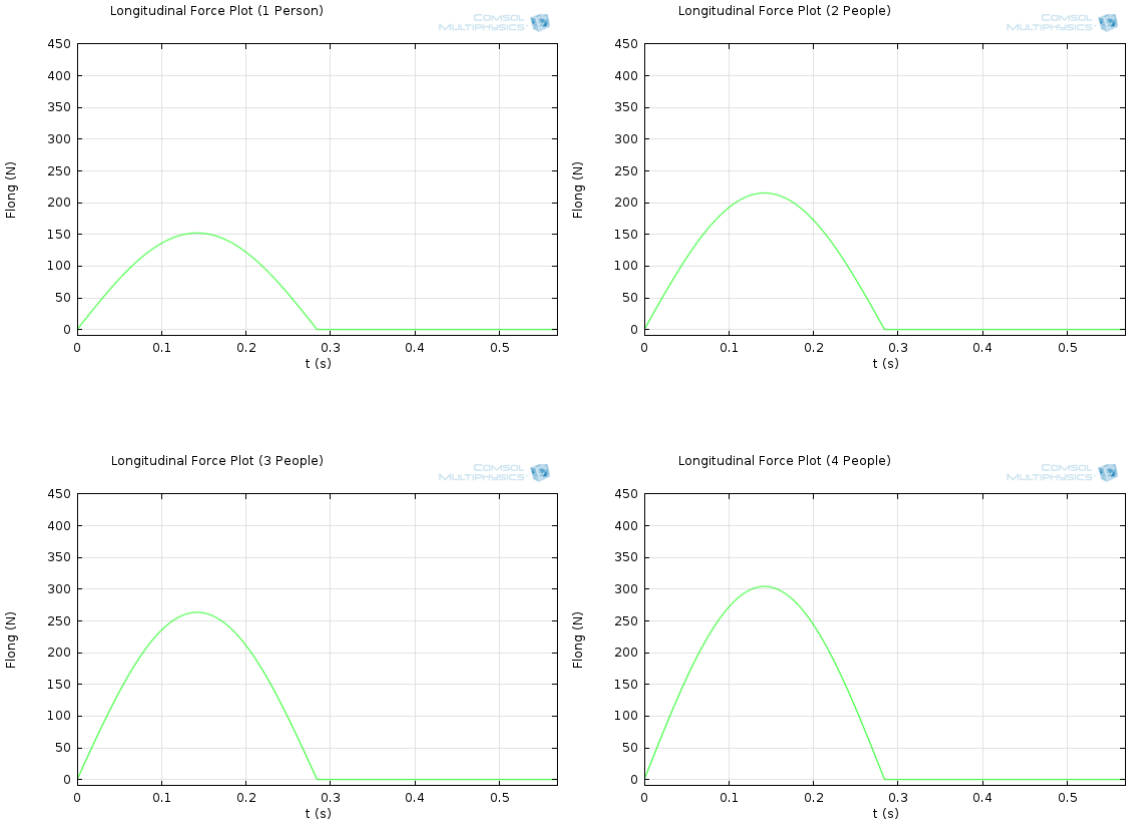

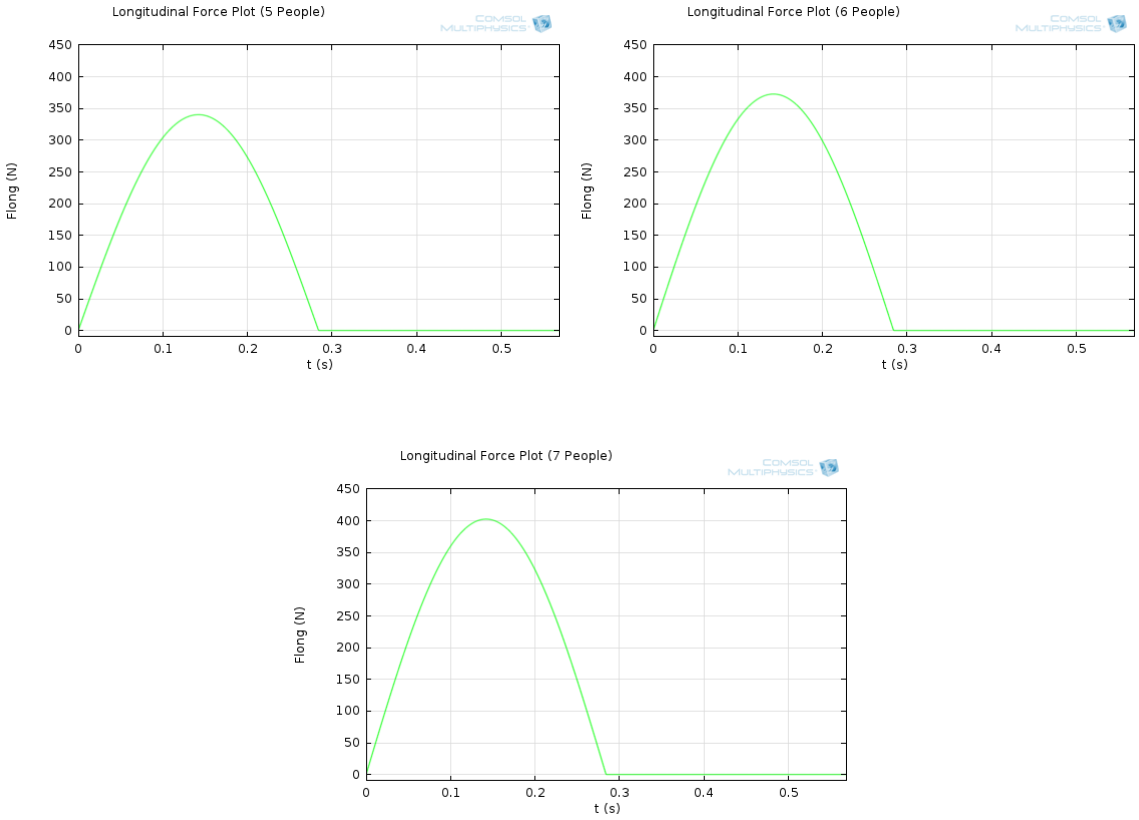

C.3.2. Output Data

This section gives the accelerations determined in COMSOL Multiphysics at a point in the middle of the bridge deck for each of the jogging load models calculated for groups of up to 7 people.

Semi-Sinusoidal Load Plots

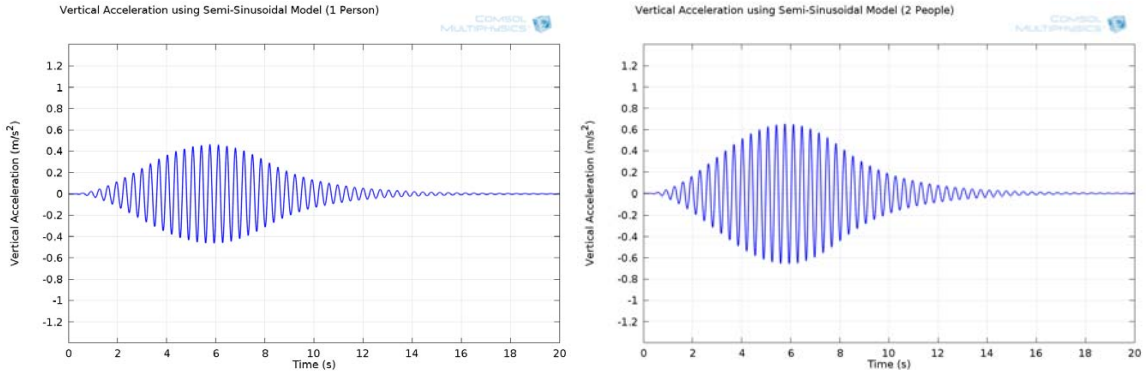

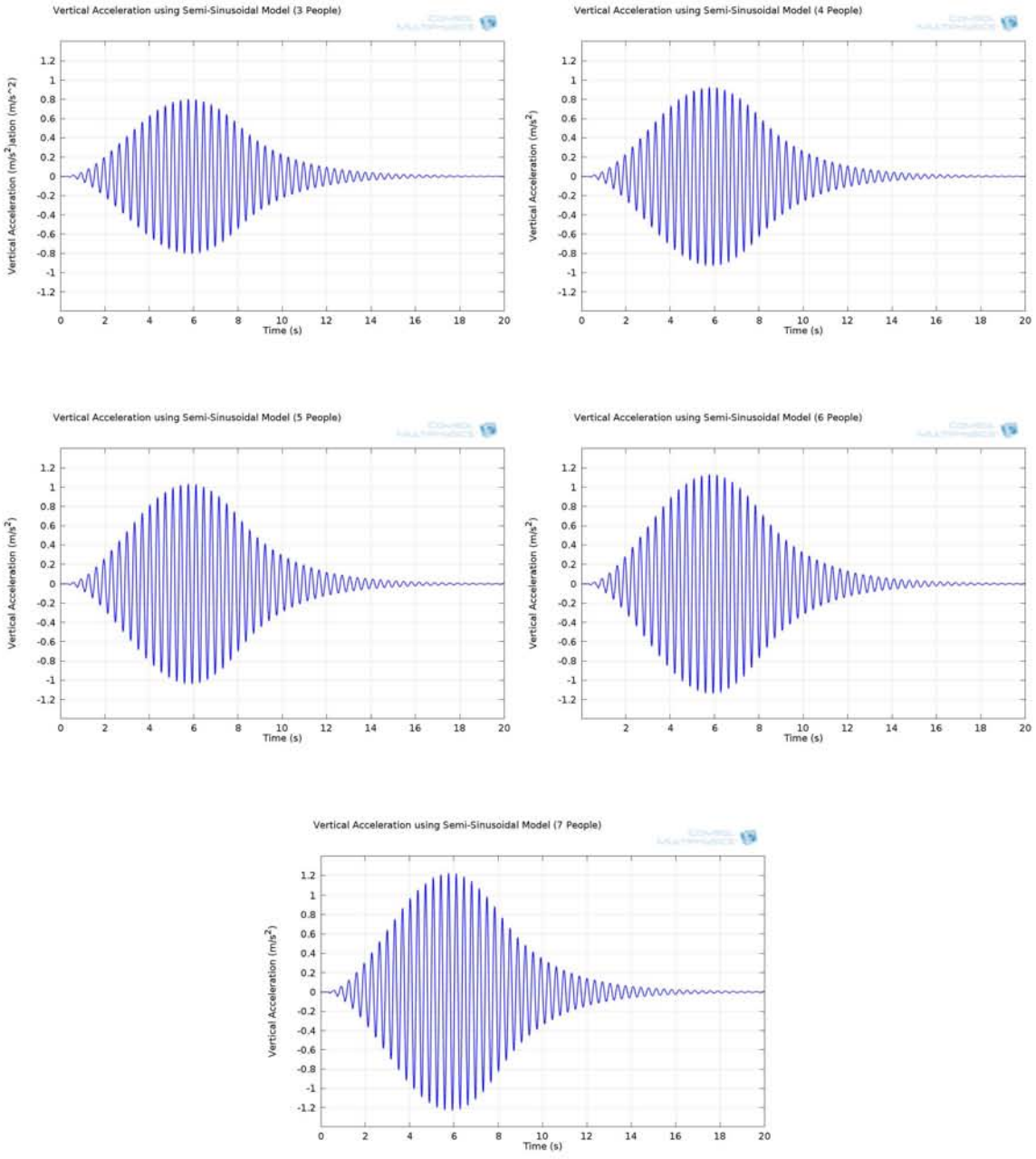
Vertical Acceleration using Semi-Sinusoidal Model (3 People)
Vertical Acceleration using Semi-Sinusoidal Model (4 People)
Vertical Acceleration using Semi-Sinusoidal Model (5 People)
Vertical Acceleration using Semi-Sinusoidal Model (6 People)
Vertical Acceleration using Semi-Sinusoidal Model (7 People)
Vertical Acceleration (m/s^2)
Time (s)

Vertical Fourier Load Plots

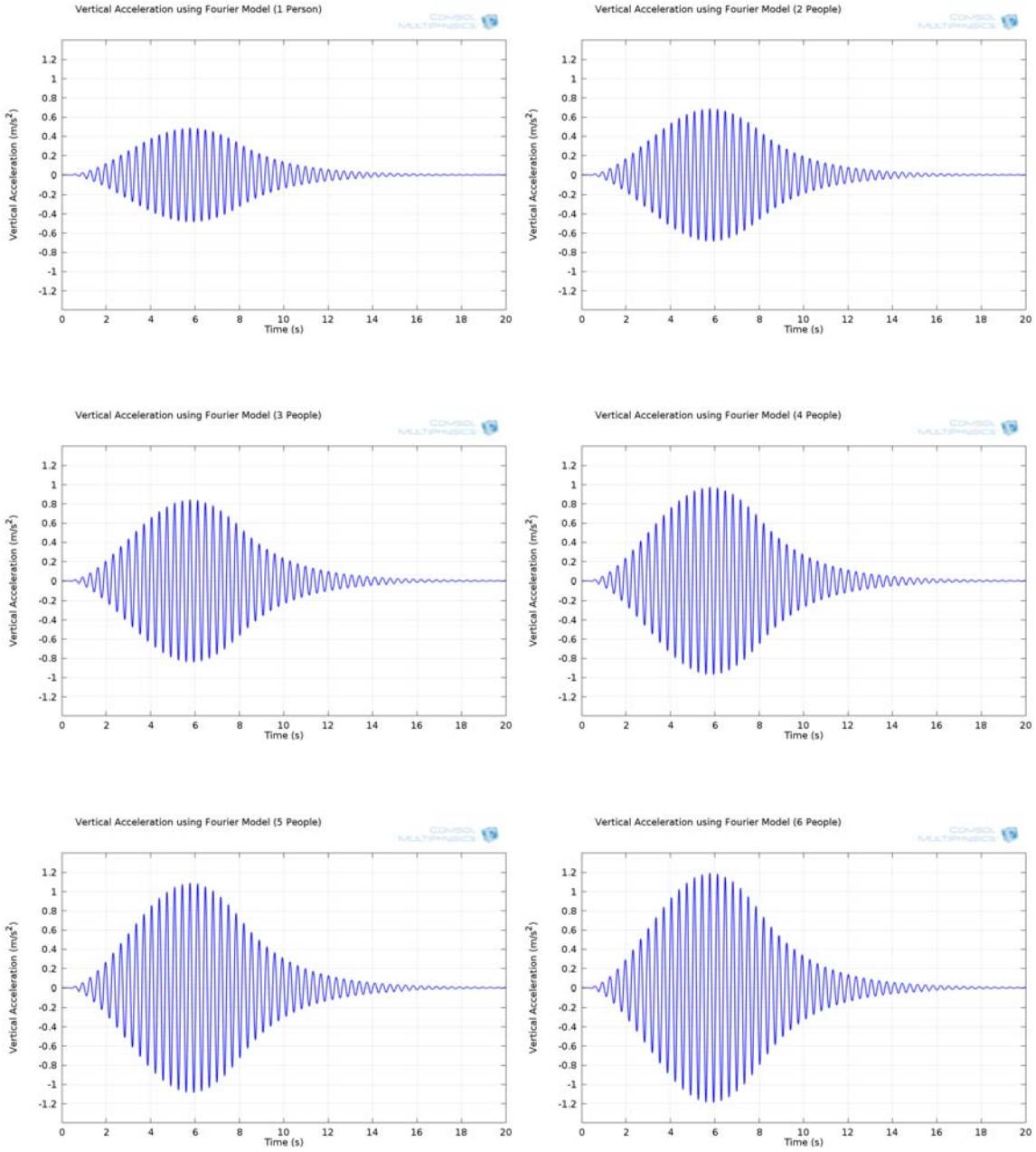

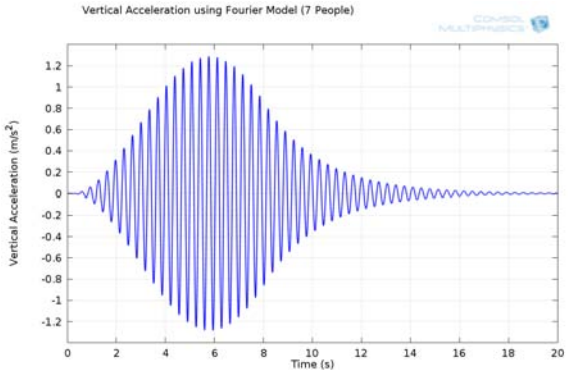

Lateral Fourier Load Plots

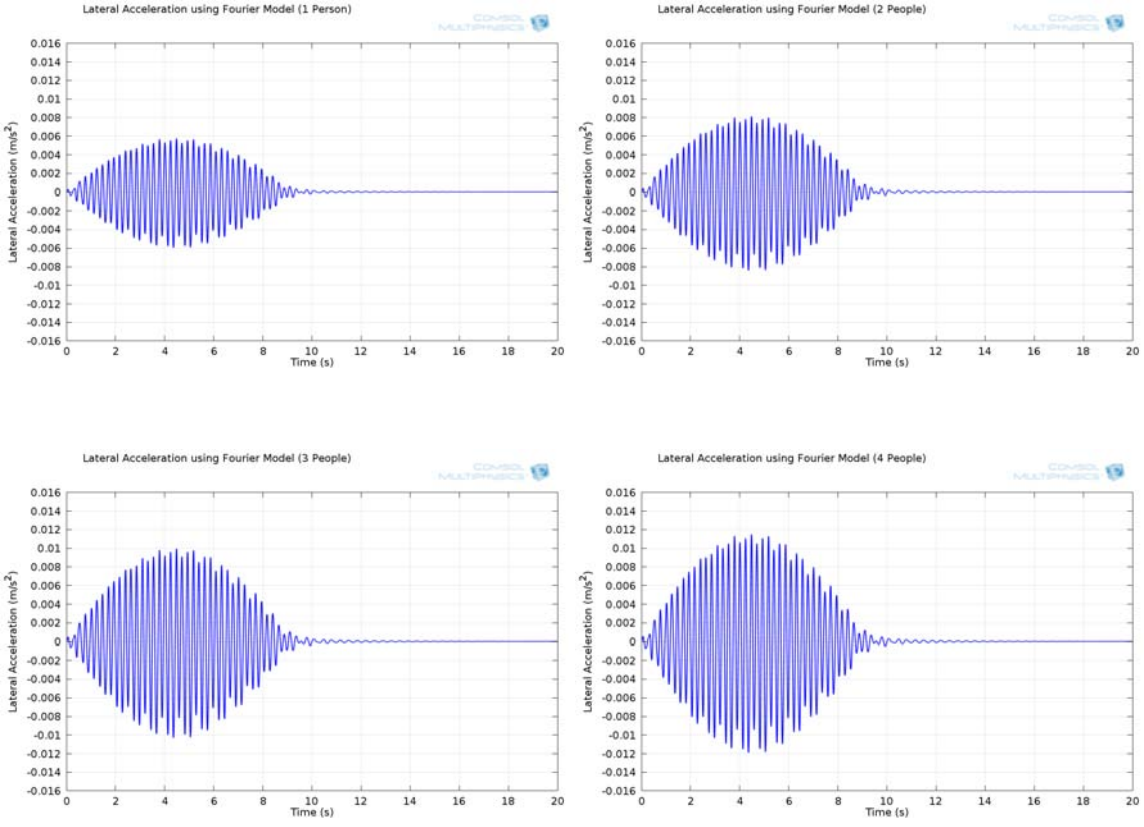

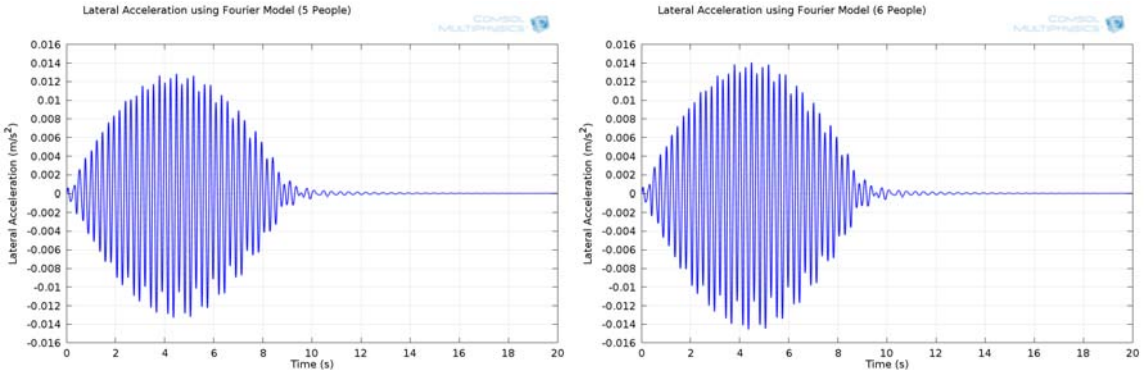

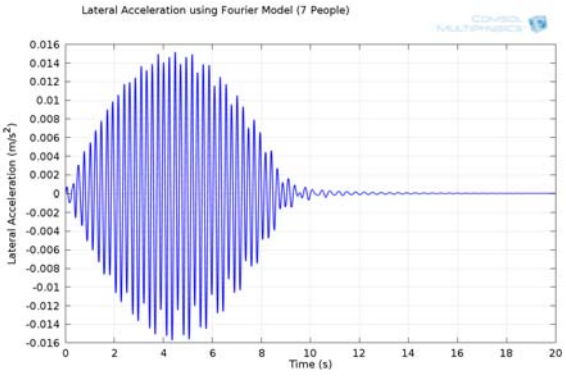

Longitudinal Fourier Load Plots

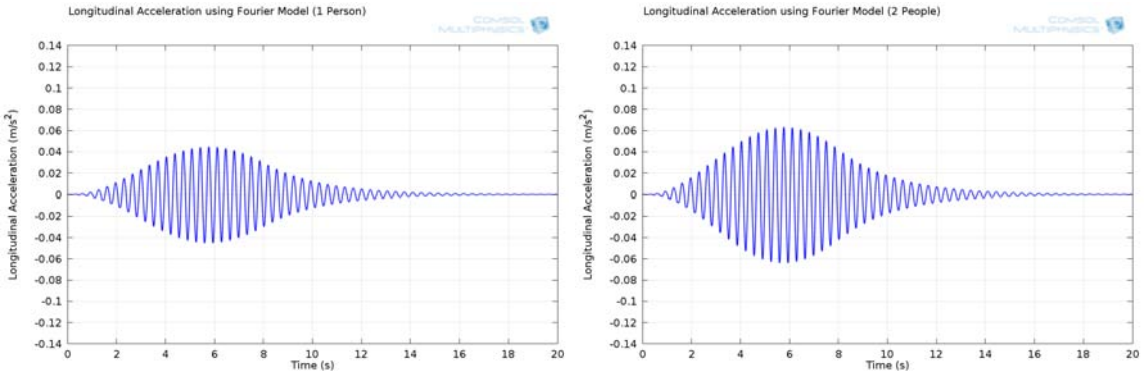

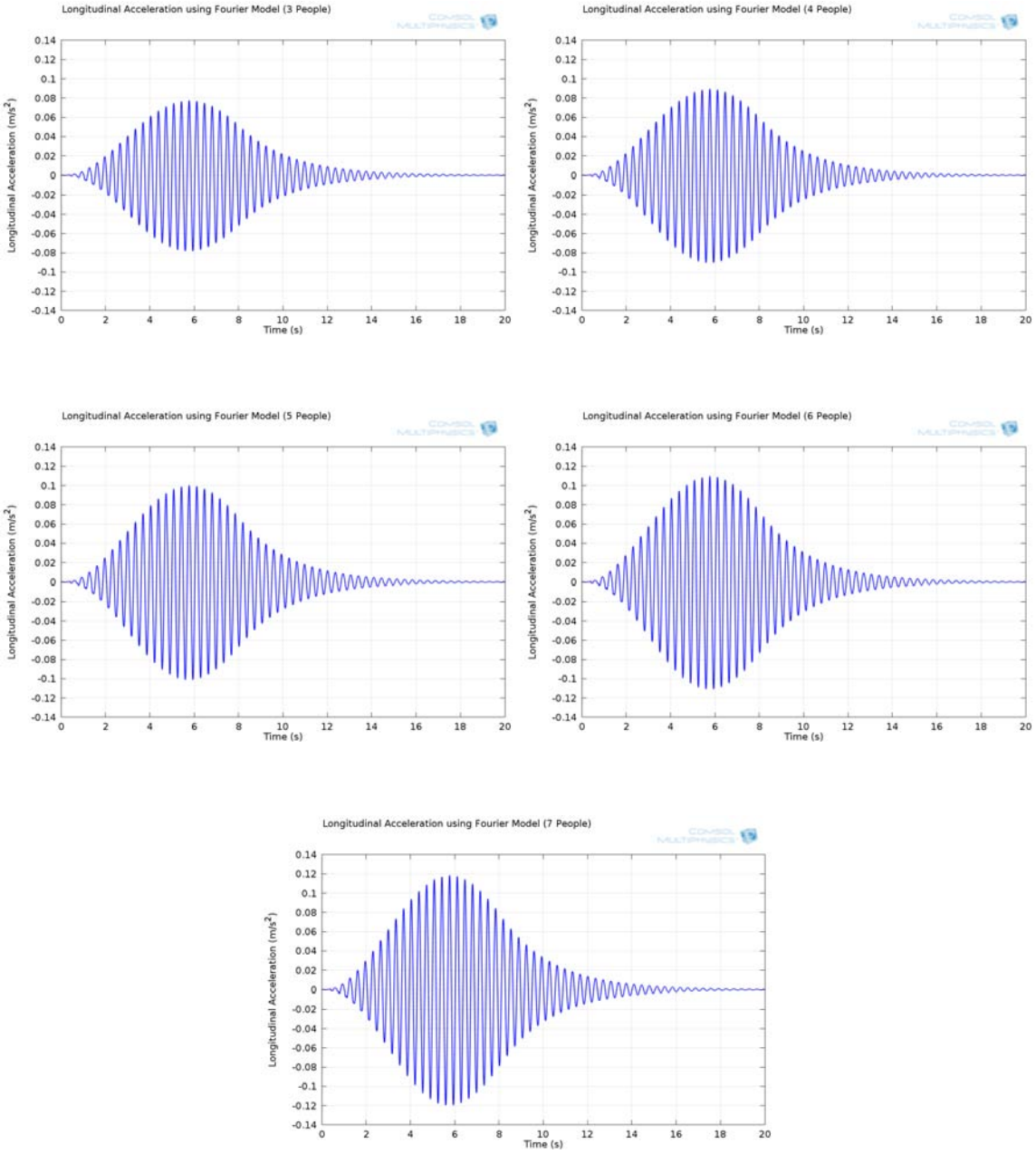
Longitudinal Acceleration using Fourier Model (3 People)
Longitudinal Acceleration using Fourier Model (4 People)
Longitudinal Acceleration using Fourier Model (5 People)
Longitudinal Acceleration using Fourier Model (6 People)
Longitudinal Acceleration using Fourier Model (7 People)
Longitudinal Acceleration (m/s²)
Time (s)

Analytical Load Plots

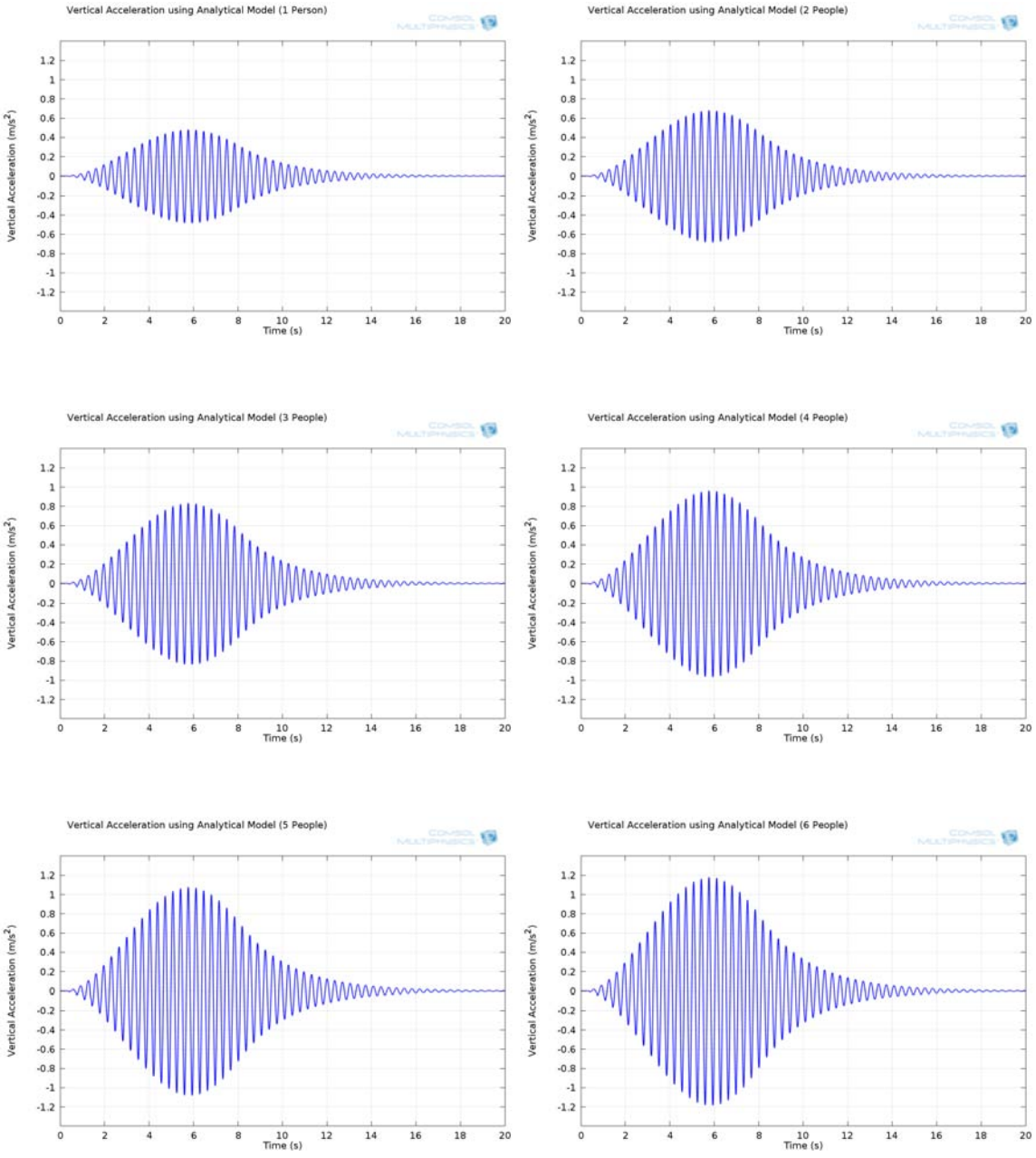

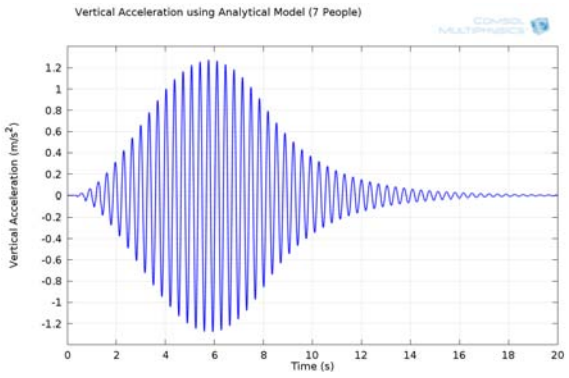

C.4. Calculated Accelerations using Simple Methods

C.4.1. TMH7 - Simplified Method

The maximum vertical accelerations due to a single pedestrian can be determined using the simplified method in TMH7 provided the bridge has less than 3 spans, is simply supported and has a constant cross section. Since the simple beam structure which was used to do the simulations meets all three of these criteria the maximum vertical acceleration can be calculated using this method as shown below, using a fundamental natural frequency of $n_0 = 2.89\,c/s$, a static deflection of $Y_s = 0.0376\,m$, a configuration factor of $K = 1$ for a single span bridge and a dynamic response factor of $\Psi = 9$ for reinforced concrete structure with a corresponding logarithmic decrement of decay of vibration of $\delta = 0.05$ and a total bridge length of $27.737\,m$.

$$\begin{aligned} a &= 4\pi^2 n_0^2 Y_s K \Psi \\ &= 4\pi^2 (2.89)^2 (0.0376)(1)(9) \\ &= 112\,m/s^2 \end{aligned}$$

C.4.2. Eurocode - Method for Timber Footbridges

The maximum vertical and horizontal accelerations for a single person or multiple people walking across a timber bridge can be determined using Appendix B of EN 1995-2. Since the simple beam structure used in the simulations is a concrete structure this method is not applicable. However, it would be interesting to determine the maximum accelerations using this method to compare its results with the other methods. Since the fundamental natural frequency of the bridge is $2.89\,Hz$ which is between $2.5\,Hz$ and $5.0\,Hz$, this acceleration can be calculated as shown below for 1 person, where the a total mass of the bridge is $53900\,kg$ and the damping ratio is $\zeta = 0.045$.

$$\begin{aligned} a_{vert,1} &= \left(\frac{100}{M\zeta}\right) \\ &= \frac{100}{(53900)\,(0.045)} \\ &= 0.041\,m/s^2 \end{aligned}$$

$$\begin{aligned} a_{hor,1} &= \left(\frac{50}{M\zeta}\right) \\ &= \frac{50}{(53900)\,(0.045)} \\ &= 0.021\,m/s^2 \end{aligned}$$

Similarly the acceleration for a distinct group of pedestrians can be calculated as shown below, using $n = 13$ and vertical and horizontal coefficients of 0.9 and 0.8 respectively.

$$\begin{aligned} a_{vert,5} &= 0.23\left(\frac{100}{M\zeta}\right) nk_{vert} \\ &= 0.23\left(\frac{100}{(53900)\,(0.045)}\right)(13)\,(0.9) \\ &= 0.11\,m/s^2 \end{aligned}$$

$$\begin{aligned} a_{hor,5} &= 0.18\left(\frac{50}{M\zeta}\right)nk_{hor} \\ &= 0.18\left(\frac{50}{(53900)(0.045)}\right)(13)(0.8) \\ &= 0.039\,m/s^2 \end{aligned}$$

However, the above accelerations are based on people walking across a bridge. The vertical acceleration of a person running across a timber bridge can be calculated in a similar manner as shown below, provided the fundamental natural frequency of the bridge is between $2.5\,Hz$ and $3.5\,Hz$.

$$\begin{aligned} a_{vert,1} &= \left(\frac{600}{M\zeta}\right) \\ &= \frac{600}{(53900)(0.045)} \\ &= 0.25\,m/s^2 \end{aligned}$$

C.4.3. Rainier et al's Method

The maximum vertical acceleration can also be calculated using Rainer et al's method as shown below with a modal mass of $m = 41300\,kg$ for the first mode of vibration (taken from the FEM of the bridge), a pedestrian weight of $P = 700\,kg$, a dynamic load factor of $\alpha = 1.2$ and a dynamic amplification factor of $\Phi = \frac{1}{(2\cdot\zeta)} = \frac{1}{(2\cdot 0.045)} = 11.1$ since the running load frequency is equal to the natural frequency of the bridge and resonance occurs (Moyo, 2008).

$$\begin{aligned} a &= \frac{\alpha P}{m}\Phi \\ &= \frac{(1.2)(700)}{41300}\cdot(11.1) \\ &= 0.23\,m/s^2 \end{aligned}$$

C.4.4. Allen and Murray's Method

The maximum vertical acceleration can also be calculated using Allen and Murray's method as shown below with a dynamic load factor of $\alpha_i = 1.2$, a pedestrian weight of $P = 700\,kg$, total bridge weight of $W = 53900\,kg$, a reduction factor of $R = 0.7$ and a damping ratio of $\beta = 0.045$. In this method the peak acceleration will occur when $t = 0$.

$$\begin{aligned}
\frac{a}{g} &= \frac{R\alpha_i P}{\beta W}\cos(2\pi i f t) \\
a &= \frac{R\alpha_i P g}{\beta W}\cos(2\pi i f t) \\
&= \frac{(0.7)(1.2)(700)(9.81)}{(0.045)(53900)}\cos(2\pi(1)(2.89)(0)) \\
&= 2.4\,m/s^2
\end{aligned}$$

C.4.5. Grundmann et al's Method

The maximum vertical acceleration can also be calculated using Grundmann et al's method as shown below with a pedestrian weight of $G = 700\,kg$, a modal mass of the structure of $M = 41300\,kg$, a logarithmic decrement of $\delta \approx 2\pi\zeta = 2\pi \cdot 0.045 = 0.283$ (Moyo, 2008) and a $n = 24$ the number of steps required to cross the structure.

$$\begin{aligned}
a_{vert,1rz} &= 0.6\left(\frac{0.4G}{M}\right)\left(\frac{\pi}{\delta}\right)(1-e^{-n\delta}) \\
&= 0.6\left(\frac{0.4(700)}{41300}\right)\left(\frac{\pi}{0.283}\right)(1-e^{-(24)(0.283)}) \\
&= 0.045\,m/s^2
\end{aligned}$$

$$\begin{aligned}
a_{vert,1rz} &= 0.6\left(\frac{0.1G}{M}\right)\left(\frac{\pi}{\delta}\right)(1-e^{-n\delta}) \\
&= 0.6\left(\frac{0.1(700)}{41300}\right)\left(\frac{\pi}{0.283}\right)(1-e^{-(24)(0.283)}) \\
&= 0.011\,m/s^2
\end{aligned}$$

C.4.6. Young's Method

The maximum vertical acceleration can also be calculated using Young's method as shown below with a harmonic force frequency of $f = 2.89\,Hz$, a harmonic force amplitude of $P = 700\,kg$, a natural frequency of $f_n = 2.89\,Hz$, a modal mass of the structure of $M = 41300\,kg$ and a damping ratio of $\zeta_n = 0.045$.

$$\begin{aligned}
a_n &= \mu_i\mu_j \left(\frac{f}{f_n}\right)^2 \left(\frac{P}{M}\right)(DMF) \\
&= \mu_i\mu_j \left(\frac{f}{f_n}\right)^2 \left(\frac{P}{M}\right) \left(\frac{1}{\sqrt{\left(1-\left(\frac{f}{f_n}\right)^2\right)^2 + \left(2\zeta_n\left(\frac{f}{f_n}\right)\right)^2}}\right) \\
&= \mu_i\mu_j \left(\frac{2.89}{2.89}\right)^2 \left(\frac{700}{41300}\right) \left(\frac{1}{\sqrt{\left(1-\left(\frac{2.89}{2.89}\right)^2\right)^2 + \left(2\,(0.045)\left(\frac{2.89}{2.89}\right)\right)^2}}\right) \\
&= \mu_i\mu_j \left(\frac{700}{41300}\right) \left(\frac{1}{(2\,(0.045))}\right) \\
&= 0.19\mu_i\mu_j\, m/s^2
\end{aligned}$$

C.4.7. Pimentel and Frenandes' Method

Finally the maximum vertical acceleration can also be calculated using Pimentel and Frenandes' method as shown below with a fundamental circular bridge frequency of $\omega_0 = 18.16\,Hz$ (Keil, 2012), a static deflection due to the weight of a pedestrian of $Ys = 0.0376\,m$, a dynamic load factor of $\alpha_i = 1.2$, a dynamic amplification factor of $\Omega_d = 11.1$ and a geometry factor for the number of spans of $k_a = 1$.

$$\begin{aligned}
a_{max} &= \omega_0^2 y_s \alpha_i \Omega_d k_a \\
&= (18.16)^2\,(0.0376)\,(1.2)\,(11.1)\,(1) \\
&= 165\,m/s^2
\end{aligned}$$

Appendix D. Measured Accelerations

D.1. Introduction

This Appendix shows the data obtained from Philip Keil (2012) for the testing done on the Rhodes Memorial Bridge as part of his undergraduate thesis for the University of Cape Town. The plots shown below have all been re-plotted based on the raw data obtained by Keil (2012).

D.2. Vertical Time-History Responses

The following plots show the vertical time-history responses of the Rhodes Memorial Bridge for 1, 2, 3, 4, 6 and 7 joggers.

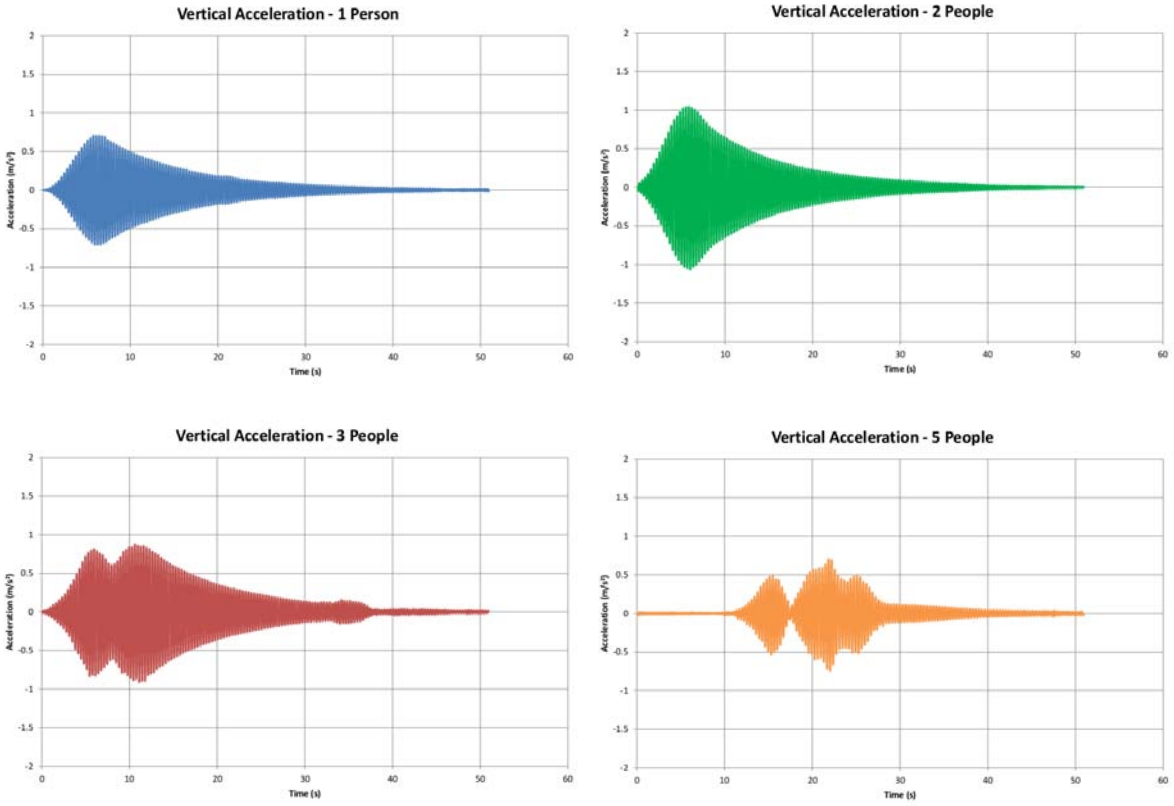

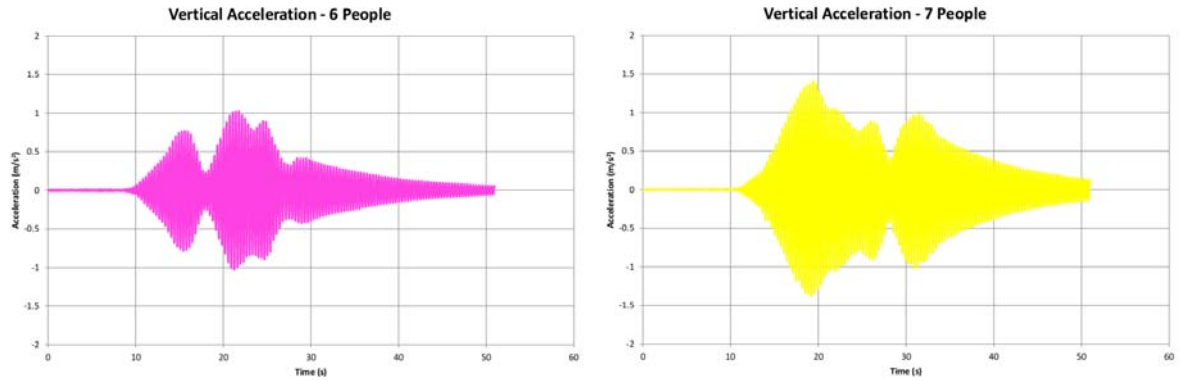

D.3. Lateral Time-History Responses

The following plots show the lateral time-history responses of the Rhodes Memorial Bridge for 1, 2, 3, 4, 6 and 7 joggers.

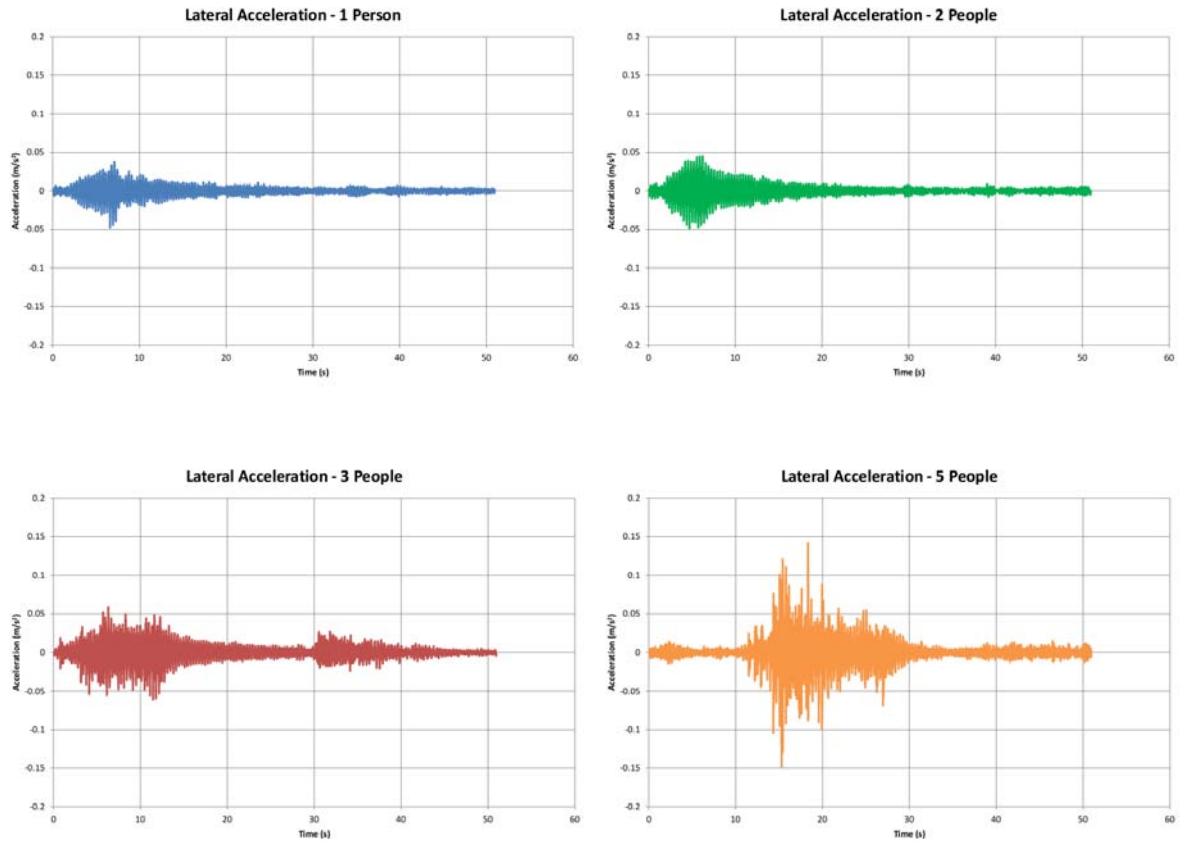

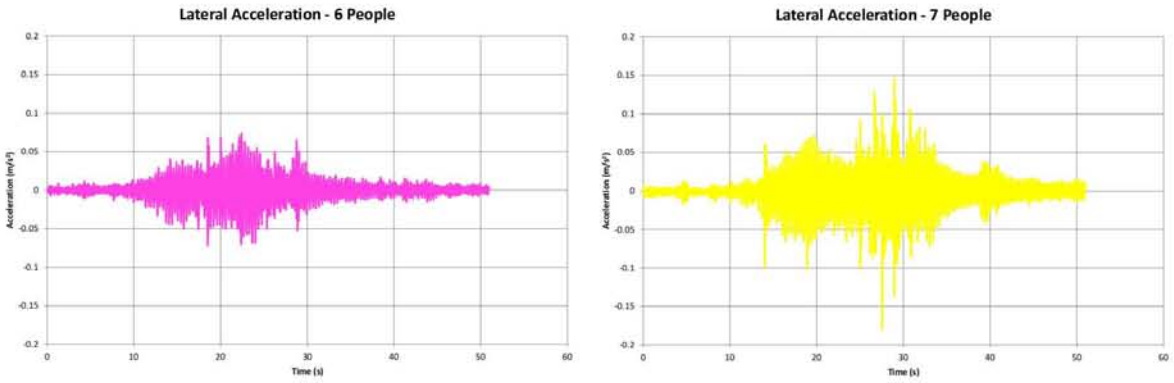
Lateral Acceleration - 6 People
Acceleration (m/s²)
Time (s)
Lateral Acceleration - 7 People
Acceleration (m/s²)
Time (s)